A corticothalamic circuit for refining tactile encoding: a switch between feature detection and discrimination

by

François Philippe Pauzin

A thesis submitted in partial fulfilment of the requirements for the degree of

Philosophiae Doctoris (PhD) in Neuroscience

From the International Graduate School of Neuroscience

Ruhr-Universität Bochum

July 18th 2018

This research was conducted at the Department of systems Neuroscience, within the Faculty of Medicine at the Ruhr-Universität Bochum under the supervision of Prof. Dr. Patrik Krieger.

Printed with the permission of the International School of Neuroscience, Ruhr-Universität Bochum

Statement

I certify herewith that the dissertation included here was completed and written independently by me and without outside assistance. References to the work and theories of others have been cited and acknowledged completely and correctly. The "Guidelines for Good Scientific Practice" according to § 9, Sec. 3 of the PhD regulations of the International Graduate School of Neuroscience were adhered to. This work has never been submitted in this, or a similar form, at this or any other domestic or foreign institution of higher learning as a dissertation.

The abovementioned statement was made as a solemn declaration. I conscientiously believe and state it to be true and declare that it is of the same legal significance and value as if it were made under oath.

François Philippe Pauzin

Bochum, 18.07.2018

PhD Commission

Chair:

1st Internal Examiner:

2nd Internal Examiner:

External Examiner:

Non-Specialist:

Date of Final Examination:

PhD Grade Assigned:

TABLE OF CONTENT

I. List of Figures and tables

Figures

Tables:

II. List of Abbreviations

AMPAR: α-amino-3-hydroxy-5-methyl-4-isoxazolepropionic acid receptor

BC: Barrel Cortex

CC: Corticocortical

CT: Corticothalamic

EPSP: Excitatory post-synaptic potential

FS: fast spiking

GABA: *gamma*-Aminobutyric acid

L1, L2/3, L4, L5, L6: Layers of cortex

mGluR: N-methyl-D-aspartate receptor

NMDAR: *N*-methyl-D-aspartate receptor

nRT: Reticular Thalamic nucleus. It is the inhibitory part of the sensory thalamus

OD: Opposite direction = PD + π

PD: principal direction = direction of the whisker deflection that elicit the greatest number of spike

POm: Postero-medial nucleus of the thalamus

PrV: Principal trigeminal nucleus

S1: Primary Somatosensory Cortex

S2: Secondary Somatosensory Cortex

TC: Thalamocortical

VPM: Ventro Postero Medial nucleus of the thalamus (VPMvl: Ventral lateral part of the VPM and VPMdm: the dorso medial part of VPM)

WD: whisker deflection

WER: whisker-evoked response

III. Abstract

A fundamental task for the brain is to determine which aspects of the continuous flow of information is the most relevant in a given behavioral situation. The information flow is regulated via dynamic interactions between feedforward and feedback pathways. One such pathway is via corticothalamic feedback. Layer 6 corticothalamic cells (L6 CT) make both cortical and thalamic connections, and as such are key modulators of activity in both areas. The functional properties of L6 CT cells in somatosensory processing were investigated in the mouse whisker system. Optogenetic activation of L6 CT neurons decreased cortical spontaneous spiking, with the net effect that a whisker-evoked response was more accurately detected (larger evoked-to-spontaneous spiking ratio), at the expense, however, of reducing the response probability. In addition, L6 CT activation switches barrel cortex to an adapted mode where cortical processing of high frequency inputs do not adapt anymore and where direction selectivity disappear. L6 CT activity can thus tune the tactile system depending on the behaviorally relevant tactile input. In somatosensory processing, the concept of detection and discrimination are often in opposition. In the present thesis, I will expose evidence that a subpopulation of L6 CT cells is useful while the animal is performing a discrimination task.

Key findings of the thesis

- L6 CTs depress spontaneous activity in most of the excitatory cortical cells
- L6 CTs decrease whisker evoked responses by a decrease in the response probability
- L6 CTs increase the evoked-to-spontaneous spiking ratio
- L6 CTs switch cortex to an adapted mode where responses from persistent inputs no longer adapt
- L6 CTs abolish direction selectivity information in L4 and L5
- L6 CTs do not affect direction selectivity in the VPM thalamus

1 Introduction

1.1 A few words from the author

We have five senses! Almost everybody knows this saying and can cite the five commonly used approaches of perception: smell, taste, sight, sound and touch. One of the main goals in in neuroscience is to decipher how these different sensations are transformed from their physical and/or chemical properties (e.g. light wavelengths for sight) into electrical information that will reach the brain, and how this electrical processing will reach our consciousness (or not) to modulate our mental activity and motor behavior. In mammals, these five senses are developed to different degrees depending on the strategy used by the animals to survive in their environment. The correct development of these senses is indispensable to investigate and understand our surroundings properly. In wildness, the correct development of these senses is of importance for survival. Interestingly, most of our sensory experiences are gained by exploration of the world, requiring active movements of sensory organs (Kleinfeld and Deschenes, 2011). In this procedure, motor components and sensory perceptions are tightly connected; it is called sensorimotor integration, the process by which the sensory and motor systems communicate and coordinate with each other. In other words, senses are tools to investigate the world, but we must experience the world to develop our senses.

By using our sensory organs, we see what our brain has extracted from reality but not the reality itself. We see what we expect, and unconsciously dismiss the abnormalities. I illustrate this by referring back to lines 2 and 3 where the word “in” is written two times, but those of you who have been fitted with efficient suppressors may not have seen it (Asher, 1960). Deciphering how the brain processes this sensory information in order to create our own reality is of fundamental importance in neuroscience.

1.2 Somatosensation and experimental model

In the present thesis, I will focus on the sense of touch. To efficiently investigate tactile processing in a sensorimotor integration context, it is favorable to use an experimental model where the sensory stimuli can be well-defined and where certain motor outputs can be precisely measured. The rodent whisker-related tactile system with its striking modular cortical representation fulfils these criteria and is thus ideal as an experimental system (Lubke and Feldmeyer, 2007, Schubert et al., 2007, Fox, 2008, Kanold and Luhmann, 2010, Krieger and Groh, 2015). Furthermore, transgenic approaches are available in mice and allow experimenters to target specific neuronal populations with high precision. The facial whiskers (also called vibrissae) are the main tactile organs for rodents and serve as arrays of highly sensitive detectors to identify and locate objects. The whisker surface is not smooth, indeed the vibration of the rough structure of the tactile organ are mandatory to discriminate fine structures of objects (Swift, 1991, Adineh et al., 2015). The role is analogous to the function of fingertips in humans. Rodents (including mice) rhythmically move their whiskers to explore and discriminate objects in their immediate environment (Diamond and Arabzadeh, 2013, Feldmeyer et al., 2013, Krieger and Groh, 2015). Since mice are nocturnal animals, the whisker system is likely to have evolved to compensate for the poverty of visual information during much of these rodent's life (Petersen, 2007).

Since the 1970s, a detailed description of the anatomical pathways of the vibrissae system has evolved in the literature. One characteristic of the whisker system is the noteworthy one-to-one correspondence between the peripheral whisker pad and corresponding brain areas in the brainstem, thalamus and the primary somatosensory cortex (S1). Tactile information via the whisker system is mediated by an array of parallel and nested motor-sensory loops (Hill et al., 2011), and is transmitted to the neocortex by trigemino-thalamic pathways, where the thalamus is the main gateway to the cerebral cortex (Bosman et al., 2011). A common principle (Bale and Petersen, 2009) for the organization of sensory systems is a massive expansion in neuronal numbers from the periphery to the cerebral cortex. In the rat whisker system, for example, ~150 mechanoreceptors innervate each whisker follicle (Lee and Woolsey, 1975), each thalamic barreloid contains ~250-300 neurons (Land et al., 1995), but each cortical barrel column contains ~15,000 neurons (Welker and Van der Loos, 1986). S1 is also called barrel cortex (BC) where each whisker is represented by a discrete and well-defined structure in layer 4 : the barrels (Woolsey and Van der Loos, 1970). These cortical structures are somatotopically arranged in an almost identical fashion to the layout of the whiskers on the

snout. Each L4 barrel is contained in a barrel column (100-500μm in diameter), formed by a group of interconnected neurons that share common properties and extend vertically through the cortical layers to form the column (Lorente De Nó, 1938, Mountcastle, 1957, Mountcastle, 1997, Fox et al., 2003, Mountcastle, 2003). These large columns are formed by interconnected smaller units called "minicolumns" (20–60 μm in diameter) (Favorov and Whitsel, 1988a, Favorov and Whitsel, 1988b, McCasland and Woolsey, 1988, Favorov and Diamond, 1990, Tommerdahl et al., 1993, Kohn et al., 1997, Bruno et al., 2003, Krieger et al., 2007). The underlying anatomical substrate for a minicolumn has been proposed to be a columnar organization of pyramidal cells with bundled apical dendrites originating from layer 5 pyramidal neurons as the core element (Fleischhauer et al., 1972, Peters and Walsh, 1972, Escobar et al., 1986, White and Peters, 1993, Casanova, 2005, Krieger et al., 2007). Examples of other repeating anatomical structures that could be components of minicolumns include dendrite bundles formed by layer 6 pyramidal cells, which in mouse neocortex are separate from layer 5 dendrite bundles (Escobar et al., 1986, Lev and White, 1997). But intrinsic electrical excitability and the properties of synaptic connections between this subtypes of L5B pyramidal cells are independent of the cell clusters defined by bundling of their apical dendrites (Krieger et al., 2007). A defined architecture is also described in layer 6 with the term of infrabarrels (de Kock et al., 2007, Meyer et al., 2010, Wimmer et al., 2010, Oberlaender et al., 2012, Constantinople and Bruno, 2013, Crandall et al., 2017) representing a cluster of cells aligned vertically within the same cortical column to the layer 4 barrel. I thus decided to study somatosensory processing in the context of sensorimotor integration in the *in vivo* model of the mouse. I performed all electrophysiology recordings in the anesthetized state, all pro-and-cons of *in vivo* anesthetized for brain recording experiments are further discussed in regards of the literature and results.

1.3 Different pathways from the periphery to reach cortex

Somatosensory information processing of the whisker system is conveyed from periphery to cortex along three different parallel pathways which differ by their passage through thalamus. Whisking kinematics information is relayed through the postero-medial nucleus of the somatosensory thalamus (POm) by the paralemniscal pathway. The exact role of this pathway in sensing vibrissa motion is controversial (Ahissar et al., 2000, Golomb et al., 2006, Yu et al., 2006, Urbain and Deschenes, 2007, Ahissar et al., 2008, Masri et al., 2008, Moore et al., 2015). POm sensory neurons are involved in the temporal processing of whisker movement (Ahissar et al., 2000, Ahissar and Arieli, 2001, Ahissar and Zacksenhouse, 2001). POm respond weakly to vibrissa deflections but rather adjusts a time and intensity dependent regulation on somatosensory cortical processing (Lavallee et al., 2005, Castejon et al., 2016). POm is a higher-order nucleus that is reciprocally connected with multiple cortical areas (S1, secondary somatosensory cortex (S2), etc) and it is involved in the transfer of sensory and perhaps other types of information (Diamond et al., 2008, Groh et al., 2014, Yamawaki and Shepherd, 2015, Sherman, 2016). Given its direct anatomical connections emanating from the motor cortex, the POm has indeed been proposed to be involved in the pre-cortical encoding of whisker motion (Yu et al., 2006, Yu et al., 2015). The functions of POm are not entirely clear; it is however known that POm conveys complex multivibrissa signals (Diamond et al., 1992, Ahissar et al., 2000, Yu et al., 2006, Diamond et al., 2008). Touch information is conducted through the VPMvl (ventrolateral part of the ventro-postero-medial nucleus of the thalamus (VPM)) by the extralemniscal pathway. Both POm and VPMvl are involved in temporal processing of object location. Kinematic and touch information are transmitted through the dorsomedial part of the VPM (VPMdm) by the lemniscal pathway. It is not a combination of signals transmitted by the POm and VPMvl but represent the highest level of control so far. Indeed, VPMdm sensory neurons are conveying information related to the object characterization.

But why would sensory information be transmitted in parallel pathways (Perl, 1963, Diamond et al., 1992, Casagrande, 1994, Kim and Ebner, 1999, Ahissar et al., 2000, Diamond, 2000, He and Hu, 2002, Jones, 2003)? In 1959, Bishop proposed that parallel sensory pathways evolved in successive steps, incorporating successively higher brain areas to implement novel functions (Bishop, 1959). Indeed, the three pathways described here, may have evolved sequentially, by adding contact detection to movement control, and identification process to contact detection (Yu et al., 2006, Petersen, 2007). The anatomical segregation of the parallel pathway does not imply functional separation; these parallel circuits are interacting between each other to form the most complete and precise representation of the surrounding. For example, in an object

localization task, contact timing (extralemniscal) must interact with whisking information (paralemniscal) to extract object location. Sensory neurons in these three different tracks are not spiking synchronously (Yu et al., 2006), VPMdm firing is of the shortest latency and the lemniscal pathway is considered to be the major sensory pathway for whisker-related somatosensory information in the context of sensorimotor integration (Yu et al., 2006). The present thesis will therefore mainly focus on the lemniscal pathway. Furthermore, my study concentrates on somatosensory processing in the anesthetized *in vivo* mouse model and the paralemniscal pathway is unlikely to contribute strongly to sensory processing since a rapid GABAergic inhibition from zona incerta silences the POm nucleus (Trageser and Keller, 2004, Lavallee et al., 2005). However, this inhibition depends upon brain state (Trageser et al., 2006) and in addition POm receives strong cortical excitatory input (Diamond et al., 1992, Mease et al., 2016a, Mease et al., 2016b). The paralemniscal pathway may therefore play important roles during awake active exploration, probably contributing to sensorimotor coordination (Petersen, 2007).

1.4 Focus on the lemniscal pathway

Clear anatomical pathways separate individual neighboring whiskers in the lemniscal pathway. This partition of kinematic information strongly suggests a unique single-whisker signaling pathway from the periphery to the barrel cortex.

Physical information (e.g., vibration of whiskers following a touch event) is conveyed to the whisker follicle (Yan et al., 2013, Whiteley et al., 2015) and is transformed into an electrical signal by mechanoreceptors in the nerve endings of sensory neurons (Hartmann et al., 2003, Neimark et al., 2003, Andermann et al., 2004, Ritt et al., 2008, Jadhav and Feldman, 2010). This will lead to a depolarization that can trigger action potentials in sensory neurons of the infraorbital part of the trigeminal nerve (Jacquin et al., 1986). Noteworthy, a single sensory neuron carries information (action potentials) from one specific whisker. The innervation of the hair follicle shows a diversity of nerve endings (Fundin et al., 1997a, Fundin et al., 1997b, Fundin et al., 1997c, Ebara et al., 2002), which may be specialized for detecting different types of sensory input (Szwed et al., 2003), e.g., the direction in which the whisker was moved. The sensory neurons form excitatory glutamatergic synapses in the trigeminal nuclei of the brain stem (Petersen, 2007). They project to somatotopically arranged structures called “barrelettes” formed by trigeminothalamic neurons in the principalis trigeminal nucleus (PrV) that are all dedicated to the processing of the same single whisker (Veinante and Deschenes, 1999). These

neurons project to the VPM thalamic nucleus where neurons also form a somatotopically arranged structure called “barreloids” (Minnery et al., 2003). Sensory neurons of the VPM respond with short and sharp latencies to whisker movement, the principal whisker evoking the strongest response compared to all the other whiskers (Simons and Carvell, 1989, Steriade et al., 1997, Friedberg et al., 1999, Brecht and Sakmann, 2002). The VPM thalamic neurons send axons to the primary somatosensory cortex where they form, in their primary target area, the emblematic layer 4, discrete clusters named “barrels” that can be seen in both living and stained brain slices (Woolsey and Van der Loos, 1970, Welker and Woolsey, 1974, Pasternak and Woolsey, 1975, Woolsey et al., 1975, Petersen and Sakmann, 2000). A weaker anatomical innervation of upper layer 6 is also observed (de Kock et al., 2007, Meyer et al., 2010, Wimmer et al., 2010, Oberlaender et al., 2012, Constantinople and Bruno, 2013) and has been recently described that preferentially L6 corticocortical cells (L6 CC cells) are targeted, so mostly in between the infrabarrels so in between the cortical columns (Crandall et al., 2017). Primary sensory areas in the cerebral cortex are composed of a stack of six neuronal layers (Callaway, 1998, Dantzker and Callaway, 2000, Thomson and Bannister, 2003, Douglas and Martin, 2004, Lefort et al., 2009). Anatomical and physiological data indicate that these layers are interconnected via vertical excitatory axons suggesting that sensory processing in any given layer may be modulated by activity in several other layers (Callaway, 1998, Dantzker and Callaway, 2000, Douglas and Martin, 2004, Lefort et al., 2009, Thomson, 2010, Feldmeyer, 2012, Qi et al., 2015, Qi and Feldmeyer, 2016, Feldmeyer et al., 2018). To date, however, the exact contribution of each layer to cortical processing is still under investigation. Sensory processing is further distributed to other cortical areas through corticocortical horizontal synaptic connections from primary to secondary somatosensory cortex and from somatosensory to motor cortex (White and DeAmicis, 1977, Welker et al., 1988, Chakrabarti and Alloway, 2006).

Despite the fact that the lemniscal pathway is dedicated for processing a unique whisker from periphery to cortex, there are however, two striking characteristics. At the beginning of the processing path, sensory information in the trigeminal ganglion is encoded with striking reliability (Jones et al., 2004a, Jones et al., 2004b, Arabzadeh et al., 2005) whereas neocortex responds with larger variability to identical well-controlled stimuli. This discrepancy is driven predominantly by interactions with ongoing spontaneous cortical activity (Petersen et al., 2003, Sachdev et al., 2004). There is a gradient for which, the more information gets away anatomically from the whisker follicle, the more the information is shared by a large number

of neurons. Furthermore, the single-whisker receptive fields found in the trigeminal ganglion contrast with the broad receptive fields in the neocortex (Simons, 1978, Moore and Nelson, 1998, Zhu and Connors, 1999, Brecht et al., 2003, Higley and Contreras, 2003). These observations suggest that a primary function of the neocortex is to generate associations of different sensory inputs which are processed in a highly context-dependent manner (Petersen, 2007). The increasing complexity of sensory processing in higher brain areas is likely to be mediated, in part, through interactions of parallel ascending pathways for processing whisker-related information. The lemniscal pathway where information pass through VPMdm is still likely to be the major sensory pathway for whisker-related information (Yu et al., 2006, Bale and Petersen, 2009).

1.5 Focus on VPMdm nucleus

Sensory signals "en route" to the cortex undergo signal transformations in the thalamus. VPMdm neurons can operate in two firing modes which determine how sensory inputs are transmitted to the cortex (Sherman, 2001, Sherman, 2005, Yu et al., 2006, Mease et al., 2014). In tonic mode cells respond to sensory input by firing single action potentials, while in burst mode, cells fire high-frequency action potentials separated by relatively long intervals of silence. While these distinct transmitting modes are associated with behavioral states, the influence of cortical activity on these firing modes *in vivo* is still under investigation. Both tonic and burst modes have been described during anesthesia/sleep and wakefulness/behavior, with a pronounced shift toward the tonic mode during alertness (Guido and Weyand, 1995, Ramcharan et al., 2000, Fanselow et al., 2001, Aguilar and Castro-Alamancos, 2005, Halassa et al., 2011). The transition from burst to tonic mode is mediated by the voltage-dependent availability of the transient low-threshold calcium current. At hyperpolarized membrane potentials, the low-threshold calcium current is de-inactivated and gives rise to bursts, whereas depolarization inactivates the low-threshold calcium current and promotes tonic firing (Llinas and Jahnsen, 1982, Mease et al., 2014). These firing modes determine the input/output properties of thalamic neurons: in tonic firing mode, firing rate codes linearly for stimulus strength, as EPSPs are directly linked to action potentials (Sherman, 2001). In contrast, in burst mode, stimuli are encoded nonlinearly, as EPSPs are indirectly linked to action potentials via the all-or-none low-threshold calcium current conductance. Both the intrinsic properties of thalamic neurons and the reciprocal synaptic connectivity between excitatory cells in thalamic relay nuclei and inhibitory neurons in the thalamic reticular nucleus (nRT) are modulating the VPM sensory neurons firing modes (Warren et al., 1994, Cox et al., 1997, Mease et al., 2014).

This fundamental biophysical property has been firmly established for single sensory thalamic neurons; however, it is less clear how this affects the relay of sensory signals in the intact *in vivo* brain and will be of investigation in the present thesis. One issue hampering the interpretation of burst/tonic responses is that cortex itself is involved in the rapid changes in firing modes seen in the awake and anesthetized animal (McCormick and von Krosigk, 1992, Landisman and Connors, 2007, Mease et al., 2014, Mease et al., 2016a, Mease et al., 2017).

Another important thalamic transformation is sensory adaptation (Whitmire and Stanley, 2016, Liu et al., 2017). Adaptation is a common characteristic of sensory systems in which neural output adjusts to the statistics and dynamics of past stimuli, thereby better encoding small stimulus changes across a wide range of scales despite the limited range of possible neural outputs (Fairhall et al., 2001, Wark et al., 2007, Mease et al., 2014). Thalamic sensory adaptation is characterized by a steep decrease in action potential activity during sustained sensory stimulation (Simons and Carvell, 1989, Diamond et al., 1992, Castro-Alamancos, 2002a, Castro-Alamancos, 2002b, Mease et al., 2014), decreasing the efficacy at which subsequent sensory stimuli are transmitted to the cortex.

1.6 Feedback processing

The transfer of tactile whisker signals from the periphery to the cortex is not simply a one-to-one relay but a dynamic process involving reciprocal communications, such as the feedback pathway between cortex and thalamus (Alitto and Usrey, 2003, Crandall et al., 2015). This organization shows that cortex has a strong influence on thalamic activity, and thereby, on its own tactile whisker processing input (Temereanca and Simons, 2004, Groh et al., 2014, Mease et al., 2014). Indeed, most sensory information enters the mammalian cortex via sensory thalamic nuclei, mostly via VPM nucleus for the rodent whisker system.

Corticothalamic fibers originate in cells located in layers 5 and 6, and produce distinct synapses in VPM and POm nuclei. Upper L6 CT cells of barrel cortex leave a fiber collateral in the inhibitory part of the sensory thalamus, the nRT and also project mostly to VPM where they form rod-like terminal fields in a thalamic barreloid. Thus, thalamocortical cells in VPM and corticothalamic cells in layer 6 form closed-loops for the flow of information between a thalamic barreloid and a cortical barrel column (Bourassa et al., 1995), with nRT inputs modulating this loop. In contrast, lower L6 CT cells innervate large sectors of POm and intralaminar thalamic nuclei (Deschenes et al., 1998, Hoerder-Suabedissen et al., 2018). L5-CT cells leave fiber collaterals in POm as they continue to midbrain and brainstem. There are

potentially at least three different types of corticothalamic synapses: upper L6 to VPM, lower L6 to POm, and L5 to POm. Corticothalamic synapses in VPM release glutamate and trigger EPSPs in thalamocortical and nRT cells by activating AMPA, NMDA and mGLU receptors (Golshani et al., 2001). The amplitude of EPSPs evoked in nRT neurons by stimulating single corticothalamic fibers is several times larger than EPSPs evoked in thalamocortical neurons, and the number of Glu4-receptor subunits at these synapses may provide a basis for the differential synaptic strength (Golshani et al., 2001). The stronger corticothalamic EPSPs on nRT cells assure that low-frequency corticothalamic activity drives these inhibitory cells and triggers robust feedforward inhibition in VPM thalamocortical cells. Corticothalamic synapses in POm can produce two different types of responses, which have been ascribed to corticothalamic cells originating in layers 5 and 6. POm responses for cells originating in layer 6 are similar to the responses evoked in VPM by layer 6 cells, while POm responses originating in layer 5 are similar to trigeminothalamic synapses (Reichova and Sherman, 2004). Consequently, corticothalamic synapses originating in layer 5 have been assigned the role of drivers of POm cells (Hoogland et al., 1991, Sherman and Guillery, 1996). The present thesis will focus on the anatomical dissection and on the electrophysiological investigation of the L6 corticothalamic feedback in the context of sensorimotor integration.

1.7 Cortical layer 6

The neocortical L6 is an input/output layer that has an essential role in modulating both cortical and thalamic activities (Temereanca and Simons, 2004, Li and Ebner, 2007, Lam and Sherman, 2010, Olsen et al., 2012, Kim et al., 2014, Mease et al., 2014, Crandall et al., 2015, Denman and Contreras, 2015, Guo et al., 2017, Pauzin and Krieger, 2018). For L6, heterogeneity would be the key word and is perhaps the most enigmatic cortical layer (Briggs, 2010, Thomson, 2010). Among all the cortical layers, L6 contains also the richest diversity of morphologically and physiologically distinct neurons (Zhang and Deschenes, 1997, Kumar and Ohana, 2008, Chen et al., 2009, Briggs, 2010, Thomson, 2010, Briggs et al., 2016). Indeed, some cells, putative CC-cells, (Crandall et al., 2017) receive direct thalamocortical input, placing layer 6 with layer 4 as a sensory input layer and implying that L6 may play a strategic role in early thalamocortical processing (Beierlein and Connors, 2002, Cruikshank et al., 2010, Oberlaender et al., 2012, Constantinople and Bruno, 2013, Yang et al., 2014). L6 CC cells form a large group of pyramidal cells that send long horizontal axons which form connections across cortical columns and cortical areas (e.g. somatosensory and motor cortices). Another class of

pyramidal cells in layer 6 projects to the claustrum in addition to sending long horizontal axons through the deep cortical layers. Layer 6 contains also inhibitory interneurons.

As presented previously, layer 6 is an important input layer but it is also a major output layer, from which large descending projections to many thalamic nuclei arise. The several subclasses of CT neurons constitute around 30–50% of the pyramidal cells in layer 6 (Thomson, 2010) and would represent more than 50% for L6a (Kim et al., 2014, Crandall et al., 2017). L6 CT neurons feature both a long-range feedback projection to the thalamus and dense local connectivity with inhibitory neurons and to a lesser extend to excitatory neurons within the cortical column (Bourassa and Deschenes, 1995, Zhang and Deschenes, 1997, Winer et al., 2001, West et al., 2006, Binzegger et al., 2007, Jones, 2007, Llano and Sherman, 2008, Lefort et al., 2009, Thomson, 2010, Bortone et al., 2014, Briggs et al., 2016). L6 CT cells may thus influence cortical sensory responses directly via intra-cortical projections and indirectly via corticothalamic projections. It can be noticed that L6 CT and CC cells participate in distinct subcircuits within the infragranular network (Kumar and Ohana, 2008, Velez-Fort et al., 2014). L6 CT neurons are thought to shape the neural response to incoming sensory information in a context-dependent manner, modulating receptive-field properties to enhance behaviorally relevant information (Sherman, 2005, Sillito et al., 2006, Briggs and Usrey, 2008, Thomson, 2010, Harris and Mrsic-Flogel, 2013). In addition to providing feedback to the sensory thalamus, these neurons are thought to influence the cortical response to sensory input through their intracortical axonal projections to the major thalamorecipient layer, layer 4 (Ahmed et al., 1994, Stratford et al., 1996, Guillery and Sherman, 2002, Binzegger et al., 2004, Sherman, 2005, Sillito et al., 2006, Briggs and Usrey, 2008, Thomson, 2010, Harris and Mrsic-Flogel, 2013). Although the standard view of the corticothalamic system is that the primary intracortical target of L6 CT neurons is L4, anatomical reconstructions of individual L6 CT neurons include examples of neurons with axonal processes ramifying within layer 5, the principal output layer of the cortex (Katz, 1987, Zhang and Deschenes, 1997, Thomson, 2010, Feldmeyer, 2012). Although quantitative studies using electron microscopy initially suggested that L6 CT neurons preferentially target inhibitory neurons within L4, other studies indicate that they synapse onto both excitatory and inhibitory neurons (McGuire et al., 1984, White and Keller, 1987, Ahmed et al., 1994, Anderson et al., 1994, Staiger et al., 1996, Binzegger et al., 2004). However, the relative anatomical and functional input of L6 CT cells to L4 and L5 is not known. The identity of the cell types targeted by the intracortical axons of L6 CT neurons are also not completely clear and will be of investigation in the present thesis.

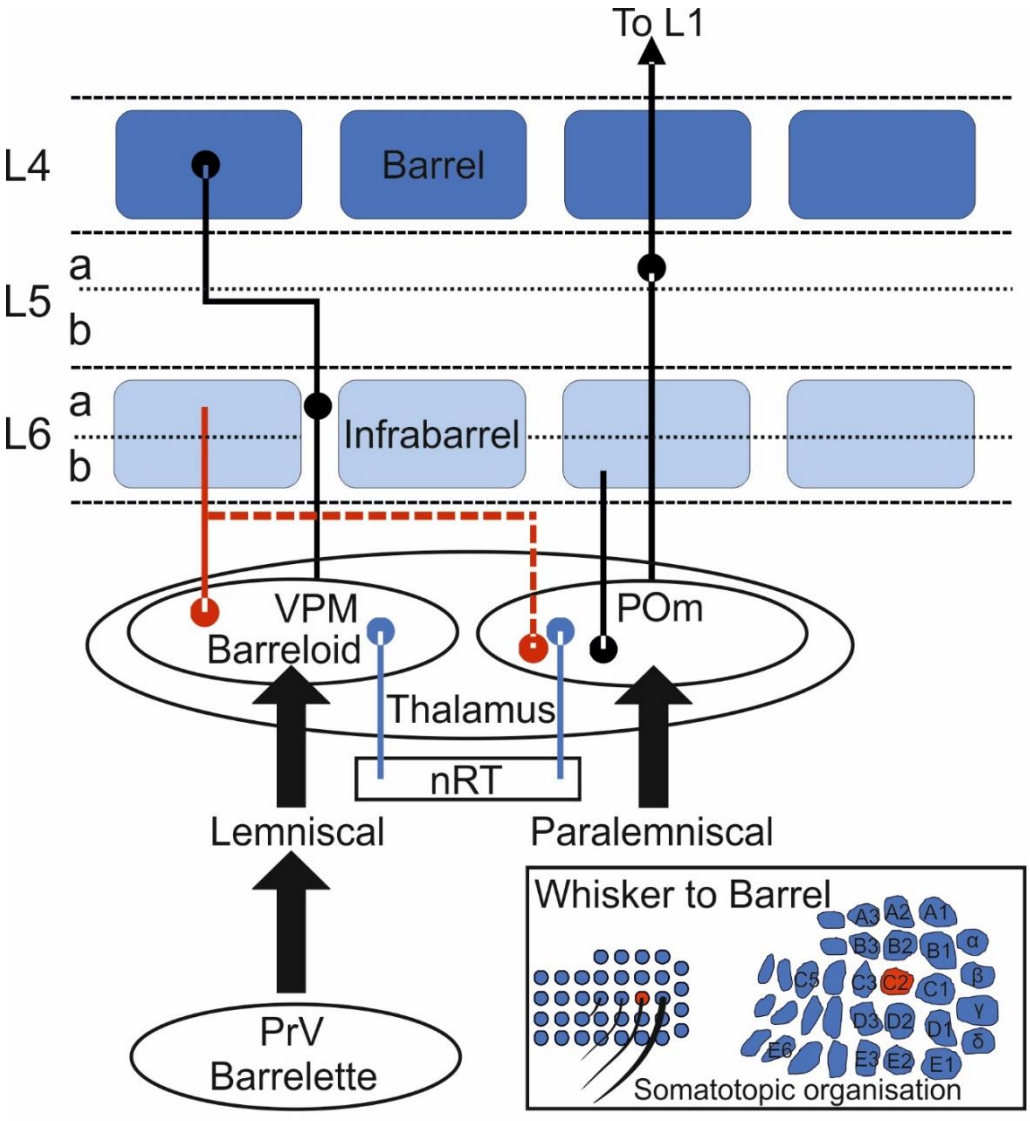

FIGURE 1: AN OVERVIEW, FROM WHISKER TO CORTEX.

Box: Representation of the noteworthy one-to-one correspondence between the peripheral whisker pad and corresponding brain areas in the layer four of the primary somatosensory cortex, the well-defined structure called "barrel". Modified from Figure 1 of Peterson et al., 2007.

Main figure: Scheme of the two main parallel pathways (Paralemniscal and lemniscal) with the layer 6 corticothalamic feedback. Paralemniscal: Carry whisking kinematics information through POm, involved mainly in the temporal processing of whisker movement. POm projects mostly to L5a and L1. It can be noticed that lower L6 CT cells project back to POm. Lemniscal: Carry information about kinematics and touch. Clear anatomical pathways are separating individual neighboring whiskers creating a unique single-whisker signaling pathway from the whisker follicle to barrelettes in PrV to barreloid in VPM to barrel (and inter-infrabarrel) in S1. It can be noticed in red, that upper L6 CT cells (Ntsr1 cells) project back to VPM mainly and to a lesser extend to POm. L6-Ntsr1 cells project all to VPM, a subset of them project also to POm (Chevee et al., 2018). Furthermore, inhibitory projections from nRT regulate the somatosensory thalamus.

1.8 Experimental transgenic model for L6 CT investigation

In order to study the L6 CT circuit, we choose the GN220 Ntsr1-Cre mouse line where a sub-population of layer 6 corticothalamic cells with both cortical and thalamic connections are labelled (Zhang and Deschenes, 1997, Lefort et al., 2009, Thomson, 2010, Olsen et al., 2012, Bortone et al., 2014, Kim et al., 2014, Mease et al., 2014, Crandall et al., 2015, Pauzin and Krieger, 2018). The organization of these cells revealed a cortical circuit module, the L6 infrabarrels (see paragraphs above and (Crandall et al., 2017)). These L6 CT neurons appear to be key modulators of activity in both cortical and thalamic areas. Indeed, optogenetics has been used to study these cells *in vitro* in the somatosensory system (Kim et al., 2014). These L6-Ntsr1 cells were also studied *in vivo* in the visual (Olsen et al., 2012, Denman and Contreras, 2015) and auditory system (Guo et al., 2017), and in somatosensory thalamus (Mease et al., 2014). L6 CT Ntsr1 cells are mostly in the upper part of L6, projecting to two different areas of the somatosensory thalamus (Figure 1: projections represented in red): The VPM and the POm nuclei. Indeed, all Ntsr1 cells project to the VPM while a subset of them also project to the POm (Chevee et al., 2018). L6-Ntsr1 cells also project to the nRT, a modulator of the sensory thalamus.

In all of these studied sensory systems, L6-Ntsr1 cells are identified as glutamatergic pyramidal neurons. In the visual and auditory systems, experimental *in vivo* investigations have shown so far that their targeted activation via optogenetic strategies primarily induces a net suppression of spontaneous and sensory-evoked activity in the cortex via direct connections onto local fast-spiking (FS) inhibitory GABAergic interneurons that modulates sensory gain in all layers of the cortical column (Olsen et al., 2012, Bortone et al., 2014, Guo et al., 2017). So far, only in-vitro experiments have shown the same effect in the somatosensory system (Kim et al., 2014). In this study, Kim et al., demonstrated that axonal projections of L6 CT neurons to L5a strongly activates both the excitatory pyramidal cells and inhibitory FS cells of this output layer of the cortex. Whereas activating L6 CT neurons scales down sensory-evoked responses in most layers, these CT neuron's effect on thalamic responses is a mixture of modest facilitation and suppression (Temereanca and Simons, 2004, Olsen et al., 2012, Mease et al., 2014, Denman and Contreras, 2015). In auditory system, L6 CT activation induces a weaker additive increase in spiking in the thalamus with no demonstrable effect on sound detection or discrimination (Guo et al., 2017). In the somatosensory system, it was shown that L6-Ntsr1 activation reduced the adaptation of thalamic responses to repetitive whisker stimulation, thereby presumably allowing thalamic neurons to relay higher frequencies of sensory input (Mease et al., 2014).

CT projections were reported to be both suppressive and facilitatory on thalamic activity, depending on the precise alignment between L6 and thalamic neurons (Guillery and Sherman, 2002, Sillito and Jones, 2002, Cudeiro and Sillito, 2006, Sillito et al., 2006, Briggs and Usrey, 2008). In this scheme, brief activation of L6 may guarantee burst firing via recruitment of the reticular nucleus (Halassa et al., 2011), resulting in the cortex of a "wake up call from the thalamus". In contrast, longer periods of L6 activity, for example, as a result of motion may promote the tonic mode of operation through the direct L6 corticothalamic depolarization that (Mease et al., 2014) have described. In the visual system, no significant effect of targeted L6 CT activation on thalamic (dLGN) response mode was found (Olsen et al., 2012), whereas earlier studies showed alternately no effect after general inhibition of the visual cortical column (Andolina et al., 2007), or a change of response modes in both directions after hyperactivation of L6 (Sillito and Jones, 2002). These discrepancies could indicate that in addition to anatomical alignment, the direction of the mode shift is determined by the relative timing of L6 activity and sensory input. Indeed, most recently, some studies have shown that L6-Ntsr1 cells modulation depends entirely on timing: L6 CT neurons can dynamically mediate either synaptic suppression or enhancement, depending on the frequency and time course of their activation (Crandall et al., 2015, Guo et al., 2017) and would favor either an enhanced detection or an enhanced discrimination of sensory inputs (Lakatos et al., 2008, Guo et al., 2017).

In conclusion, previous studies of the L6 corticothalamic pathway do not create an entirely cohesive picture of its network functions. Furthermore, how somatosensory responses in cortex are affected by L6 activity has remained largely unexplored *in vivo* in the somatosensory barrel cortex. Although differences are apparent between different sensory systems, it appears that the L6 CT cells in the visual, auditory and tactile system can tune the responsiveness of the system to different types of inputs but the relative contribution of intra-cortical versus cortico-thalamic projections in modulating cortical responses is currently unknown (Olsen et al., 2012).

Under normal conditions, the motion of sensory organs is adapted based on sensory processing. When this process is modified, certain features of tactile perception are impaired. How the relatively well characterized brainstem-induced modulation of thalamic neuron differs from cortical feed-back to thalamus remains to be elucidated. My working hypothesis is that whereas brainstem modulation can induce a global effect on the activity state in thalamus, cortical modulation will be important for cycle-by-cycle modulation that is necessary to improve discrimination of fine-grain textures. Brain-slice experiments have suggested only a small difference in the cortical control of different thalamic nuclei (Landisman and Connors, 2007).

Considering the rather different functions of thalamic nuclei for processing sensory information, it is likely that *in vivo* the differences will be more prominent, and also adapted to the different response characteristics in thalamus. The synaptic dynamics of corticothalamic synapses from L6 remain to be investigated and will be a specific focus of this thesis. Furthermore, I will explore L6 corticothalamic processing to clarify how changes in cortical excitability could preferentially drive different corticothalamic pathways. The general importance of this is to show how cortico-subcortical dynamics can optimize brain processing.

1.9 Layer 6 and cortical extra-features

The elementary characteristics of whisker stimulus representations continue to be a subject of great interest (Kleinfeld et al., 2006). A striking feature of neurons in the whisker-to-barrel pathway is that they respond differently depending on the direction in which the whisker is displaced (Lichtenstein et al., 1990, Bruno et al., 2003, Timofeeva et al., 2003, Lee and Simons, 2004, Temereanca and Simons, 2004, Puccini et al., 2006, Bale and Petersen, 2009). At each subcortical station along the afferent pathway, neurons respond to a whisker movement with transient responses composed of different numbers of spikes depending on the angular direction of the whisker's displacement and how it corresponds to the cell's preferred deflection angle (Simons, 1978, Simons, 1983, Simons and Carvell, 1989, Lichtenstein et al., 1990, Shoykhet et al., 2000, Bruno and Simons, 2002, Bruno et al., 2003, Minnery et al., 2003, Minnery and Simons, 2003, Timofeeva et al., 2003). In barrel cortex, one contribution to directional selectivity comes from latency tuning of excitatory inputs (Wilent and Contreras, 2005b). Excitatory responses to the preferred direction have shorter latencies compared to those of other directions. Other mechanisms are also involved in this direction selectivity, like amplitude tuning and changes in spike threshold (Wilent and Contreras, 2005a). In computational model, directional selectivity is strongly dependent on the mean deflection frequency: selectivity is weakened at high frequencies even when each individual deflection evokes strong directional tuning (Puccini et al., 2006). This variability of directional selectivity is due to generic properties of synaptic integration by the neuronal membrane, and is therefore likely to hold under physiological conditions. Directional selectivity depends thus on the stimulus context. It may participate in tasks involving brief whisker contact, such as detection of object position, but is likely to be weakened in tasks involving sustained whisker exploration (e.g., texture discrimination), more details will be given in the discussion part.

In the visual system, neurons in mouse primary visual cortex differentially respond to gratings of different orientations (Hubel and Wiesel, 1962, Niell and Stryker, 2008, Olsen et al., 2012). Olsen et al., 2012 investigated the effect of L6-Ntsr1 photoactivation via channelrhodopsin on orientation tuning in mouse visual cortex. Remarkably, photo-stimulation of L6 resulted in the precise scaling of the tuning curve, that is, it reduced visually evoked responses by a similar fraction irrespective of presented orientation. Photo-stimulation of L6 did not affect preferred orientation, tuning width, or the orientation selectivity index of cortical neurons throughout layers 2/3, 4 and 5 (Olsen et al., 2012).

In the somatosensory system, the L6 CT cells effect on the cortical direction selectivity is still under investigation and will be of special focus in the present thesis. Furthermore, it has been shown in many different studies, the importance of GABAergic inhibition in the modulation of responsiveness depending on input features (Sillito, 1975, Kreile et al., 2011, Li et al., 2012, Hagihara and Ohki, 2013). Therefore, since the L6 CT photoactivation is on many sensory systems modulating the activity GABAergic interneurons, its effect on direction selectivity will be scrutinized.

2 Materials and Methods

All experiments were done according to German animal welfare guidelines and were approved by the local government ethics committee (Landesamt für Natur, Umwelt und Verbraucherschutz, Nordrhein-Westfalen).

Animals

The following mouse lines were used:

- Ntsr1-cre (GENSAT strain GN220).
- Ai27(RCL-hChR2(H134R)/tdT)-D, a reporter line used to express channel rhodopsin in cre-cells. The positive offspring (male and female) "Ntsr1-ROSA-ChR2" from breeding male Ntsr1-cre with female Ai27.
- Ai14(RCL-tdT), a reporter line used to express td-Tomato in cre-cells. The positive offspring (male and female) "Ntsr1-tdTomato" from breeding male Ntsr1-cre with female Ai14.
- Gad2-IRES-cre (Stock number: 010802; Jackson Laboratory). The Gad2-IRES-cre mice were a gift from Drs Stefan Herlitze and Melanie D. Mark (Ruhr University Bochum).

Juxtacellular recordings in somatosensory cortex were performed in 43 Ntsr1-cre animals injected with AAV-Channelrhodopsin, in 5 Ntsr1-ROSA-ChR2 animals, 16 Ntsr1-cre injected with AAV-Archaerhodopsin, 6 Gad2-cre animals injected with AAV-Channelrhodopsin. Recordings in thalamus in the ventral posteromedial nucleus (VPM) were performed in six Ntsr1-cre-ChR animals, three Ntsr1-ROSA-ChR2 and five Ntsr1-cre-ArchT.

Anatomy tracing was done on 2 Ntsr1-tdTomato for cholera toxin and on 6 Ntsr1-cre animals for rabies virus injections.

One "Drd1a-tdTomato" animal was used (from breeding male Drd1a-cre with female Ai14) to compare its known POm thalamus projection (Hoerder-Suabedissen et al., 2018) with the thalamic projection of "Ntsr1-tdTomato".

Stereotaxic Viral Injections for electrophysiology

Stereotaxic injections of 1 to 10 months old male and female Ntsr1-cre mice (median age = 4.9 months; 70% between 1 to 6 months) were done using ketamine (60 mg/kg), xylazin (12 mg/kg) anesthesia plus acepromazine (0.6 mg/kg). Same procedure for the six Gad2-cre mice (median age = 2.7 months). The body temperature was kept constant (37 ºC) using a heating

pad (FHC, ME, USA). Animals were placed in a stereotaxic frame (Model 1900; David Kopf Instruments, CA, USA). After a small incision was made in the skin, a craniotomy was made over barrel cortex at coordinates 2.9 to 3.1 mm lateral and 1.6 to 1.7 mm posterior to bregma. These coordinates were approximately over the C1-C2 barrel. Then 500 (range: 400-800 nl) of Adeno-associated viral (AAV1/2-double floxed-hChR2(H134R)-mCherry-WPRE-polA) encoding for ChR2-mCherry (GeneDetect, New Zealand), or 500 (range: 400-800 nl) of Adeno-associated viral (AAV-CAG-FLEX-ArchT-GFP) encoding ArchT-GFP (UNC vector core) were injected at a depth of 0.9 mm under the dura. Mice were sutured and housed in their cages until the experiment performed 14-20 days after virus injection.

Stereotaxic Viral Injections for anatomy

Characterization of post-synaptic target areas

Stereotaxic injections of 2 months old Ntsr1-cre mice (n = 2) were done using ketamine (60 mg/kg), xylazin (12 mg/kg) anesthesia plus acepromazine (0.6 mg/kg). The body temperature was kept constant (37 ºC) using a heating pad (FHC, ME, USA). Animals were placed in a stereotaxic frame (Model 1900; David Kopf Instruments, CA, USA). After a small incision was made in the skin, a craniotomy was made and 200nL of Cholera Toxin Subunit B Recombinant (tagged with Alexa Fluor™ 647 Conjugate, Invitrogen™) were injected at coordinates 1.2 mm lateral and 1.6 mm posterior relative to bregma at the depth of 3.0 mm for targeting POm thalamus. 200nL of Cholera Toxin Subunit B Recombinant (tagged with Alexa Fluor™ 488 Conjugate, Invitrogen™) were also injected at coordinates 1.8 mm lateral and 1.6 mm posterior relative to bregma at the depth of 3.5 mm for targeting VPM thalamus. Mice were sutured and housed in their cages for four days before perfusion and brain removal.

Characterization of pre-synaptic cells

A modified floxed rabies virus is used for is capacity to specifically target cre-cells and is ability to jump synapses retrogradely. The used trans-synaptic tracing viruses were a gift from Dr. M.K. Schwarz.

Stereotaxic injections of 4 to 7 months old Ntsr1-cre mice (n = 6) were done using ketamine (60 mg/kg), xylazin (12 mg/kg) anesthesia plus acepromazine (0.6 mg/kg). The body temperature was kept constant (37 ºC) using a heating pad (FHC, ME, USA). Animals were placed in a stereotaxic frame (Model 1900; David Kopf Instruments, CA, USA). After a small incision was made in the skin, a craniotomy was made over barrel cortex at coordinates 2.9 mm lateral and 1.5 mm posterior to bregma. These coordinates were made to target the center

of barrel cortex (approximately over C3 barrel) in order to infect only somatosensory cortical cells. Injections were made at a depth of 0.9 mm.

This injection protocol is executed in two steps. First an injection of 600nL of a mix of two rAAVs is injected (300nL of each AAV). One AAV is encoding for the tumor virus A receptor (TVA receptor), necessary for the initial rabies virus infection (during the second step), this AAV is floxed and coupled with tdTomato, allowing the specific visualization of the cre-cells (A132 pAAV-double floxed mCherry WPrepA). The other AAV is encoding for the rabies virus glycoprotein, allowing transsynaptic transport of the modified rabies virus (A147 AAVEFRGiresT800d.floxed). Mice were sutured and housed in their cages until the second step, 6 days after the first injection. Same protocol, same anesthesia, same coordinates. 500nL of an EnvA pseudotyped, glycoprotein-gene deleted rabies virus expressing EGFP (RABVΔG-EGFP (EnvA)) was injected at the depth of 0.9 mm. Mice were sutured and housed in their cages for 14 days before perfusion and brain removal.

Animal Preparation and Electrophysiology

To immobilize the animal, anesthesia was first induced by isoflurane 5% (vol/vol) in O_2 via a vaporizer (EZ-7000; E-Z Anesthesia, PA, USA) at 1L/min. For animal surgery and electrophysiology recordings, animals were anesthetized with an intraperitoneal injection of urethane (1-1.5 g/kg animal weight; Sigma-Aldrich, USA) with acepromazine (0.5 mg/kg) dissolved in in saline (NaCl 0.9 %). When necessary 1-3 more injections of urethane (0.05 g to 0.1 g/kg animal weight) were done during the experiment to ensure that the animal was not spontaneously whisking. To ensure a stable depth of anesthesia the breathing cycle (350-500 ms from peak to peak) was monitored using a pressure sensitive piezo element (Zehendner et al., 2013). The craniotomy made 2 to 3 weeks before, during the virus injection, was still visible facilitating the appropriate placement of the recording electrode after re-drilling the skull carefully. The animal's head was fixed on a metal plate allowing stable and long-time juxtacellular recordings of single units. Cells were filled with biocytin via electroporation at the completion of the recording in order to identify the cell depth relative to pia. All electrophysiology recordings were done in the left hemisphere, and whiskers were deflected on the animals right whisker pad. Single units were found by the increase of the pipette resistance measured in current-clamp. *In vivo* juxtacellular recordings and biocytin fillings were made with 4-6 MΩ patch pipettes (1.5 mm outer diameter, 0.86 mm inner diameter, with filament) pulled from borosilicate filament glass (Hilgenberg GmbH, Germany) on a Sutter P-

1000 puller (Sutter Instruments, CA, USA). Pipettes were filled with extracellular solution: (in mM) 135 NaCl, 5.4 KCl, 1.8 $CaCl_2$, 1 $MgCl_2$, 5 HEPES and 20 mg/ml biocytin (SIGMA ALDRICH; USA), pH adjusted to 7.2 with NaOH. The bath solution on top of the animal head was saline (0.9 % NaCl). Signals were digitized between 10 and 50 kHz with a DigiData 1300 (Axon Instruments) and were acquired using pClamp 8 software (Axon Instruments). Spike sorting (threshold and template search; pClamp 8) was done to isolate single-units.

In a subset of experiments (n = 5) dual recordings from both cortex and thalamus were made. A second craniotomy was drilled for placement of the VPM thalamic recording electrode. The anesthetized animal was placed in a stereotaxic frame (Model 1900; Kopf Instruments), and a craniotomy was made 1.85-1.95 mm lateral and 1.50-1.60 mm posterior to bregma. A tungsten electrode (World Precision Instrument, Inc. TM31A50, 4.8-5.1 MΩ) was carefully implanted in the brain 2.8–3.8 mm deep, parallel to the brain mid axis. The electrophysiological criteria used to determine that recordings where from VPM thalamus was only the fact that the neuron answered distinctly to only one whisker but each time the correct recording position of the electrode was checked post mortem (Figure S7) in coronal brain slices by localizing the electrode tip that was dipped before the experiment in a fluorescent dye (DiI; D282, Life Technologies GmbH, Germany). Thalamic recordings for Ntsr1-ArchT animals (and Ntsr1-ChR for the direction selectivity experiment) were done using a glass pipette, as in the cortical recordings. The pipette tip was dipped in the fluorescent dye DiI, and in some recordings VPM cells were filled with biocytin. Both methods were used to verify the recording position (Figure S7). No dual recordings in ArchT animals.

Electrophysiology and optogenetic

The stimulation light was delivered by a LED light source (M470F1; Thorlabs, Newton, NJ, USA) while single neurons were recorded. The output power from the LED driver (DC2100, Thorlabs, NJ, USA) was regulated by voltage output from a pulse stimulator (Master-8, AMPI, Israel). The power output at the fiber (400 μm diameter; 0.39 NA) tip was measured with a power meter (PM100D; Thorlabs, NJ, USA). To activate Ntsr1 cells via channelrhodopsin, the photostimulation used for all the experiments was a 470nm blue light for a pulse width of 300 ms at a power of 2.6 mW with maximal power for the blue light of 6.4 mW. To photo-inactivate Ntsr1 cells via archaerhodopsin, 590 nm yellow light was used with pulse width of 300 ms at a power of 2.4 mW. This caused a complete silencing of Ntsr1 cells (Figure 3E).

For the direction selectivity experiment a lower light intensity was used. The intensity was of around 0.6mW but could vary depending on the strength of the effect seen on the recorded cell. Varied from 0.3mW to 1mW.

Measures of Response to Whisker stimulation

Whiskers were cut to a length of 1 cm to ensure equal movements when stimulated. A hand-held probe was used to stimulate each individual whisker to search for the whisker that evoked the strongest response (the highest number of action potentials evoked in the recorded cell), with the shortest latency. The whisker that elicited the strongest response in that particular barrel column (or in VPM thalamus) is called Principal Whisker. Dual-recordings from VPM and cortex were "aligned" meaning that the same whisker gave the strongest response in both areas. The PW tip was put into glass capillary (i.d. ~900 µm) glued to a piezo wafer (PL127.11; Physics Instruments, Germany). Stimulation was controlled with a piezo amplifier and filter (Sigmann Elektronik; Germany). Two stimulation protocols were applied: a 0.33 Hz stimulation; a 200 ms vertical (up and down) whisker deflection given every 3 seconds. An 8 Hz stimulation; eight deflections at 8 Hz evoked every 3 seconds. Whisker deflection duration for each pulse was 25 ms with a rise/fall time of around 1.5 ms, piezo-deflection amplitude of about 1.5 mm, and with 50 stimulation repeats. For the control condition only the piezo is triggered (i.e., no photostimulation). To investigate the effect of L6-Ntsr1 cell modulation, the blue light (470 nm) for activation via ChR or the yellow light (590 nm) for inhibition via ArchT were applied 100 ms before the onset of the first whisker deflection and stopped after the last whisker deflection. This delay ensures that the modified L6 activity had sufficient time to affect thalamus before the whisker input reaches it, and also that the L6 spiking activity was stable throughout the duration of the optogenetic stimulation (Figure S4).

For direction selectivity experiment: A 4 Hz stimulation protocol was applied, consisting of a train of four deflections at 4 Hz evoked every 5 seconds. Whisker deflection duration for each pulse was 25 ms with a rise/fall time of around 1.5 ms, piezo-deflection amplitude of about 1.0 mm, and with 5 stimulation repeats for each angle per turn (piezo motor: IE3-1024; Faulhaber). The starting angle is chosen randomly; after five repeats of the 4 stimulations at 4 Hz, the piezo is automatically turned by 45 degrees clockwise. A maximum of turn is executed until the cell is loose. An average of 3 turns per condition has been executed for each recorded cell (Ntsr1 data: 3.1 and Gad2: 3.3 turns). For the control condition only the piezo is triggered (i.e., no photostimulation). To investigate the effect of L6-Ntsr1 cell activation, the blue light (470 nm) for activation via ChR was applied 100 ms before the onset of the first whisker deflection and

stopped after the last whisker deflection (so 875 ms in total). This delay ensures that the modified L6 activity had sufficient time to affect thalamus and barrel cortex before the whisker input reaches it. The L6 spiking activity was stable throughout the duration of the optogenetic stimulation (Figure S4). To investigate the effect of Gad-activation, the blue light (470 nm) for activation via ChR was applied 10 ms before the onset of each whisker deflection and lasted for 80 ms (so 4 * 80 ms per sweep). Short 80 ms pulses were chosen in order to keep a stable spiking of non-specific GABAergic cells for each whisker deflection.

To compare the selectivity of spike response magnitude, I used a direction selectivity index (DSI), calculated as the percent decay in amplitude (A) from the preferred direction; that is, amplitude = (preferred direction – non-preferred direction)/preferred direction, divided by the decay constant of the fit exponential (λ). Thus, this ratio DSI is a measure of the percent decrease in response magnitude for each degree away from the preferred direction (Wilent and Contreras, 2005b).

Separating excitatory cells from interneurons

Neurons were classified as excitatory cells or inhibitory interneurons based on the shape of their action potentials using a standard classification method (Armstrong-James and Fox, 1987, Juczewski et al., 2016). Fast-spiking units (presumably interneurons) were distinguished from regular-spiking units (presumably excitatory cells) based on the spike peak-to-trough duration (the interneurons had a very short duration < 0.4 ms), a symmetrical up and down deflection (integral for the interneurons is close to zero). Based on these variables, cells were classified using the K-means clustering (n = 2 clusters) method. The “fast” waveform used as the primary criteria to differentiate excitatory from inhibitory cells, might bias the selection of putative GABAergic interneurons to be of the fast-spiking type, rather than regular-waveform GABAergic interneurons. To identify a cell as Ntsr1, all excitatory cells showing a significant increase activity with the 470 nm light were characterized based on the latency of the first spike after the onset the light emission and the standard deviation of this latency over 50 repeats.

Determining the layer specific position of each cell

Cortical layer position was based on the distance to pia determined by microdrive depth which in some cases (n = 11) was verified by histological staining (median difference in depth estimate was 6 µm (data not shown). Each cell was assigned to a respective layer based on the recording (microdrive) depth. The depth range was for L2/3: 65 – 319 µm (median depth of cells classified as L2/3 was 260 µm); L4: 320 – 539 µm (median: 436.5 µm); L5: 540 – 774

µm (median: 650 µm) and L6: >775 µm (median: 902 µm). These layer borders correspond to that determined by anatomical techniques (Groh et al., 2010).

Histology

After the experiment, the animal was perfused transcardially with 4% paraformaldehyde in 0.1 M phosphate buffer. The brain was removed and post-fixated for at least 24 h in 4% paraformaldehyde. Cell location and morphologies were determined by tissue staining with streptavidin-Alexa-Fluor 488 conjugate (Life and technologies; S11223) or DAB (3,3'-Diaminobenzidine tetrahydrochloridehydrate; D5637) as previously described (Groh and Krieger, 2013).

Statistical analysis

Data are presented as mean ± SEM except in Figure 4J which shows mean ± SD (the depth of a cell in each respective layer is not considered to be more or less close to a true population mean, rather the depth data variability is more appropriate, thus SD instead of SEM is plotted).

Spontaneous activity

For Ntsr1 data

The total number of spikes during a 300 ms control condition (the 300 ms immediately preceding the onset of the optogenetic light) and the total number of spikes during the 300 ms of photostimulation (occurring every 3 seconds) were summed over 50 sweeps and compared. To determine the effect of L6-Ntsr1 modulation on spontaneous spiking in cortex and thalamus cells, each cell was tested individually using a 95% confidence interval for Poisson count (Chi-square distribution), calculated in Excel 2010 using the function 'CHI2.INV' or in Excel 2016 using 'CHISQ.INV'. The effect was considered significant when the total number of spikes during the optogenetic light emission was not within the 95% confidence interval of that for the control condition. An index representing the photo-stimulation effect was calculated as: Opto-Index (O.I.) = (No-Nc) / (No+Nc). With Nc = number of spikes recorded in control condition during (0.3 s x 50) 15 s; No = number of spikes recorded during photo-modulation for the same duration. Index varies between -1 and 1, with -1 meaning that with modulation of L6-Ntsr1 cells the recorded cell completely stopped spiking. Cells (n = 44 for both Ntsr1-ChR and Ntsr1-ArchT; Table S1 and S2) where the spontaneous activity was too low (<5 spikes in total in a 30 s recording; 300 ms time window before and during photo-stimulation in each of 50 sweeps; 30 s = 50*2*300 ms) were not included in the analysis of spontaneous activity. The random occurrence of single spikes would, in these cases, unduly influence the result. Notably,

taken together those cells would still show a decrease in the number of spikes, on average from 1.2 to 0.5 spikes after L6 photo-activation of channelrhodopsin. Furthermore, in the total cell count L6-Ntsr1 cells are not included.

We quantified the increased activity ("rebound activity") occurring after the offset of L6 activation (i.e., after the end of the light pulse). The total number of spikes during a 300 ms control window (the 300 ms immediately preceding the onset of the optogenetic light) was compared to the total number of spikes occurring in a rebound effect window from +200 to +500 ms after the offset of the optogenetic light (time window in which the rebound effect occurred for all cortical neurons). To identify a rebound effect each cell was tested individually using a 95% confidence interval for Poisson count (Chi-square distribution), calculated in Excel 2016 (Microsoft) using the function 'CHISQ.INV'. The cell was considered to have a rebound effect if the total number of spikes during the "rebound effect" time-window was significantly higher than the control condition. For each cell displaying a significant rebound, an index was calculated as: Rebound-Index (RI) = 1 – (Nc / Nr). With Nc = number of spikes recorded in control condition during (0.3 s x 50 sweeps) 15 s; Nr = number of spikes recorded during rebound time: +200 to +500 ms after the offset of the photo-modulation. This differs from the Opto-Index because it can only be a value between 0 and 1; there is a rebound only if the rebound spike frequency is significantly higher than the spontaneous. The averaged RI per layer can be seen in Figure 4F. Cells where the number of spikes was too low (<5 spikes in total in a 30 s recording; two times 300 ms time window in each of 50 sweeps) were not included in the analysis.

The effect of L6-Ntsr1 modulation was also analyzed in a cortical layer level where the spontaneous activity (in Hz) of all cells belonging to a particular layer are compared for each condition (control and photo-modulation) by a paired t-test or Wilcoxon test depending on the normality of the data distribution (tested with Agostino-Pearson omnibus normality test).

For Gad2 data

The total number of spikes during a 320 ms control condition and the total number of spikes during the 320 ms of photostimulation (80*4 ms occurring every 5 seconds) were summed over 40 sweeps and compared. To determine the effect of Gad2 modulation on spontaneous spiking in cortex, each cell was tested individually using a 95% confidence interval for Poisson count (Chi-square distribution), calculated in Excel 2010 using the function 'CHI2.INV' or in Excel 2016 using 'CHISQ.INV'. The effect was considered significant when the total number of spikes during the optogenetic light emission was not within the 95% confidence interval of that

for the control condition. Cells (n = 4) where the spontaneous activity was too low (<5 spikes in total in a 25.6 s recording; 320 ms time window before and during photo-stimulation in each of 40 sweeps; 25.6 s = 40*2*80*4 ms) were not included in the analysis of spontaneous activity. The random occurrence of single spikes would, in these cases, unduly influence the result.

Response to low frequency whisker deflection

In the "low frequency" whisker stimulation paradigm, whiskers were deflected every 3 s with a 200 ms pulse. The whisker-evoked response was calculated during a 100 ms window following the onset of the whisker deflection. Data was analyzed with paired two-tailed t-test.

Response probability to low frequency stimulation

The "response probability", was evaluated as a measure of a neuron's "detectability" to a whisker deflection. If one or more spikes occurred in a 100 ms window following the onset of the whisker deflection, a value of one is scored, and if no spikes are detected the value is zero. The number of successful response (in %) in both condition for each cell belonging to the same layer was tested with a paired two-tailed t-test.

Response to High frequency whisker deflection

Similar to assessing the response to low frequency whisker deflection, the average number of spikes (100 ms time window) per every whisker deflection of a train of 8 stimulations given at 8 Hz in both condition for each group of cells from the same layer has been tested with two-way repeated measure ANOVA.

Thalamic recordings

The whisker evoked response is the average number of spikes per whisker deflection within the 50 ms following the deflection. In the analysis of whisker evoked responses for the dual recordings, I used repeated measure Two-way ANOVA to judge the effect of photostimulation. The protocol was a 300, 340 or 520 ms light pulse preceding the 200 ms long whisker deflection by 100, 140 or 320 ms in order to achieve various degrees of activation of VPM thalamus.

For direction selectivity experiment: A 4 Hz stimulation protocol was applied, consisting of a train of four deflections at 4 Hz evoked every 5 seconds. Five stimulation repeats for each angle per turn. The starting angle is chosen randomly; after five stimulations of 4 Hz, the piezo is automatically turned by 45 degrees clockwise. For the control condition only the piezo is triggered (i.e., no photostimulation). To investigate the effect of L6-Ntsr1 cell activation, the blue light (470 nm) for activation via ChR was applied 100 ms before the onset of the first whisker deflection and stopped after the last whisker deflection (so 875 ms in total). This delay

ensures that the modified L6 activity had sufficient time to affect thalamus before the whisker input reaches it.

In the direction selectivity experiments, the effect of L6-Ntsr1 activation on the responses (50 ms time window) was tested individually using a 95% confidence interval for Poisson count (Chi-square distribution), calculated in Excel 2010 using the function 'CHI2.INV' or in Excel 2016 using 'CHISQ.INV' on the responses in Hertz. The effect was considered significant when the total number of spikes during the optogenetic light emission was not within the 95% confidence interval of that for the control condition.

3 Results

3.1 Efficiency of the mouse lines

3.1.1 L6-Ntsr1 anatomy: where do they project and who is projecting to them

To understand the role of L6-Ntsr1 cells, it is important to position these cells in the whisker processing pathway by characterizing their inputs and outputs. Even if their projections are well characterized in the literature (Olsen et al., 2012, Bortone et al., 2014, Kim et al., 2014, Mease et al., 2014, Chevee et al., 2018), little is known about the cells that are responsible of their activation. The verification of L6-Ntsr1 projections allowed me to estimate which regions are modulated by these cells. Comparing the results with the current literature will grant me verifying their projections and checking the quality of my mouse line. Furthermore, investigating the cell identity and location of the Ntsr1-projecting cells allows me to estimate how these CT cells are activated in physiological conditions. L6-Ntsr1 input/output characterization will help in understanding the role of this cell population within the somatosensory processing pathway and be beneficial in interpreting the electrophysiology data following the photo-modulation of the Ntsr1 cells.

To characterize L6-Ntsr1 projections, I used the help of a retrograde tracer, the cholera toxin B. While injected in both POm and VPM thalamus (see materials and methods) in Ntsr1-tdTomato animals, the tracer is taken up by axon terminals in the area of injection and thus, by transport toward the cell body, label cells that project onto this area. Two small identical injections (200nL) were made: one in POm and one in VPM thalamus. The results suggest that 65% of this population of L6 cells project to the VPM and 18% project to the POm (Figure 2 A-D). It should be noted that these values apply for the injected target areas only (made small on purpose to avoid leaking), so the exact number of labelled cells is not relevant but rather the comparison between the two target areas. These somatosensory L6 CT neurons are thus mostly VPM projecting cells, in line with the current literature (Mease et al., 2014, Chevee et al., 2018). To label the cells projecting to L6-Ntsr1 cells, a modified floxed rabies virus that specifically labels cells presynaptic to the cre-cells, was used (see materials and methods and Figure 2E). Most of the neurons projecting to the L6 population are found in the barrel cortex, some are found in motor cortex, secondary somatosensory cortex, thalamus and striatum, and appear to label both excitatory and inhibitory cells in the BC. Finding sensory and motor function associated cells projecting to the L6-Ntsr1 cells lead me toward the hypothesis that both motor and sensory behavior can modulate the activity of these cells.

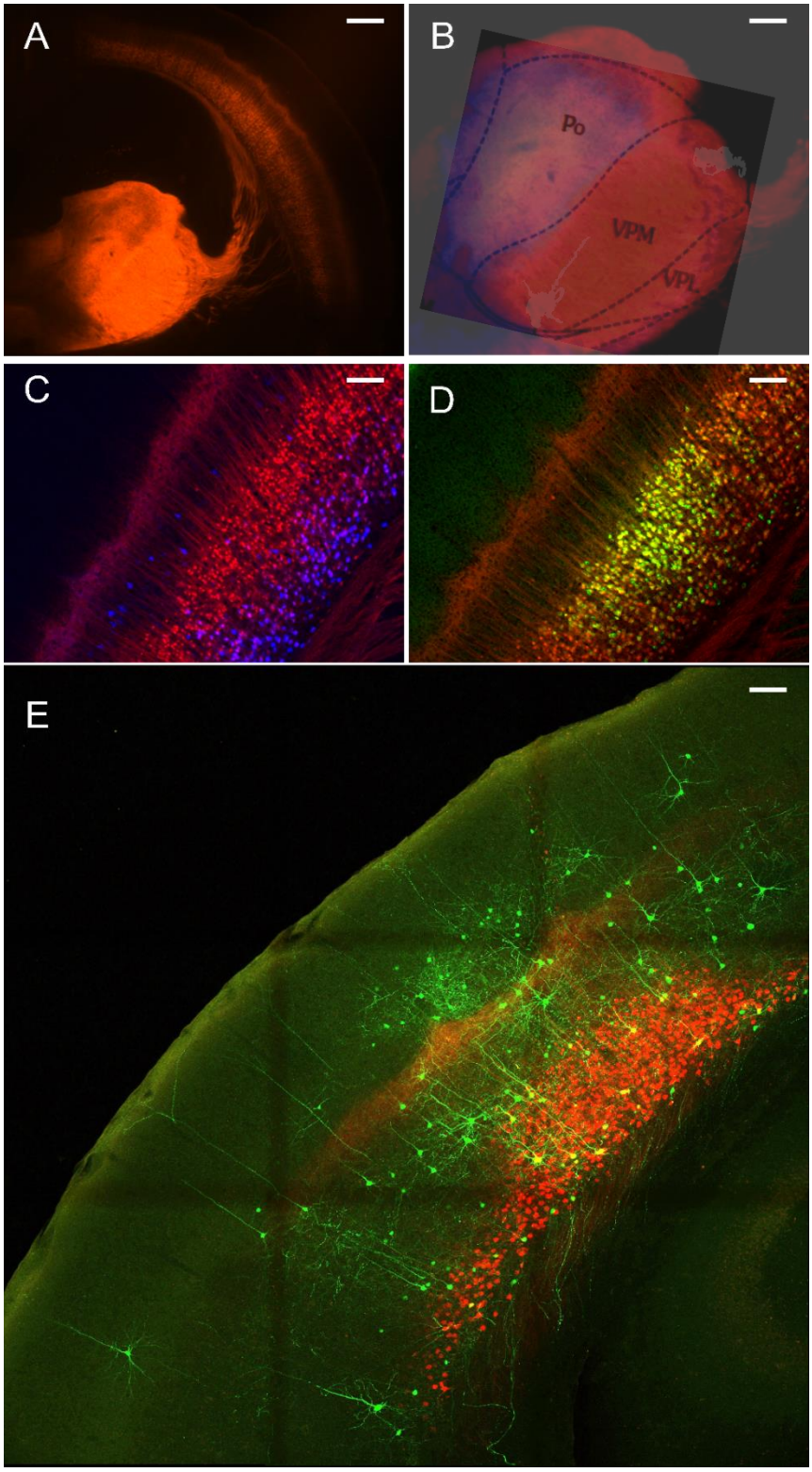

FIGURE 2: CHARACTERIZATION OF THE INPUT/OUTPUT PROPERTIES OF THE L6 NTSR1 POPULATION

A. L6-Ntsr1 neurons expressing tdTomato (in red) in the barrel cortex and thalamus in a Ntsr1-tdTomato animal. Obtained by crossing Ai14 and Ntsr1-cre animals (see material and methods).
B. Ntsr1 neurons appeared to project mainly to the VPM thalamus by looking at the axonal projections fluorescence (red). In blue, is the axonal projection of a known POm projecting mouse line: drd1a-tdTomato (see material and methods and (Hoerder-Suabedissen et al., 2018)).
C. Coronal brain slice showing Ntsr1 cells in red and POm projecting cells in blue due to injection of cholera toxin B in POm (see material and methods). 18% of Ntsr1 cells are purple (red + blue) so POm projecting.
D. Coronal brain slice showing Ntsr1 cells in red and VPM projecting cells in green due to injection of cholera toxin B in VPM (see material and methods). 65% of Ntsr1 cells are yellow (red + green) so VPM projecting.
E. Coronal brain slice showing Ntsr1 cells in red. Ntsr1 cells that incorporate both AAV of the first injection procedure and that were targeted by the RABΔV of the second injection step are yellow (see material and methods). Cells in green are the pre-synaptic to the yellow ones.

Scale bar: A = 450μm; B= 180 μm; C and D = 100 μm; E = 120 μm

3.1.2 Spiking activity in L6-Ntsr1 cells modulated by photostimulation

To examine the role of L6-Ntsr1 corticothalamic cells in somatosensory processing, I performed *in vivo* electrophysiology recordings in a transgenic mouse line (Ntsr1-cre) with genetically *cre*-labelled L6 cells (Gong et al., 2007, Olsen et al., 2012, Kim et al., 2014, Mease et al., 2014, Velez-Fort et al., 2014, Crandall et al., 2015, Denman and Contreras, 2015, Crandall et al., 2017, Guo et al., 2017). Virus mediated expression of channelrhodopsin-2 (ChR2-mCherry) or archaerhodopsin (ArchT-GFP) in the barrel cortex showed bright fluorescence from L6 somata and neuropil (Figure 3A-C). As has been previously shown in somatosensory cortex (Kim et al., 2014, Mease et al., 2014), neuronal somata expressing mCherry or GFP were restricted to L6 ensuring that optical stimulation of cortex specifically modulated the L6-Ntsr1 cell population. These cells make both cortico-cortical and cortico–thalamic projections (Figure 3A-C) predominately to ventroposteromedial thalamus (VPM) and to a lesser extent in the posterior medial nucleus (POm) and the thalamic reticular nucleus (nRT) (Lee et al., 2012, Mease et al., 2014, Chevee et al., 2018). To verify that single-unit spikes could be evoked by photo-activation, I made juxtacellular recordings from single ChR2-expressing L6 neurons (n = 14, Figure 3D) while applying blue light (470 nm) to the cortical surface via an optical fiber (400 µm in diameter); L6-Ntsr1 spike output scaled with the light intensity (Figure S1), and with the standard intensity used (2.6 mW) spiking increased from 0.07 ± 0.06 Hz to 35 ± 7 Hz. For the direction selectivity experiment, I used a really low light intensity (0.6mW), explanation on that in the corresponding result part, and spiking increased from 0.04 ± 0.01 Hz to 7.75 ± 6.6 Hz (n = 3). In L6-Ntsr1 neurons expressing ArchT (n = 2; Figure 3E), spiking was effectively blocked by photo-inactivation using yellow light at 2.4 mW (590 nm; 400 µm optical fiber diameter).

3.1.3 Spiking activity in GABAergic cells modulated by photostimulation

Evidence suggest that activation of L6-Ntsr1 CT cells in barrel cortex activates a sub-set of GABAergic interneurons (Olsen et al., 2012, Bortone et al., 2014, Kim et al., 2014, Guo et al., 2017). The effect on directional selectivity of recruiting a specific GABAergic microcircuit via L6-Ntsr1 CT activation, was compared with a general, unspecific activation of GABAergic interneurons. The Gad2-cre mouse line was used to target ChR2-expression to GABAergic interneurons, to thus achieve a non-specific activation of GABAergic interneurons. (Katzel et al., 2011, Taniguchi et al., 2011, Harris et al., 2014, Martinez et al., 2017). Virus mediated expression of ChR2-mCherry in the BC showed bright fluorescence from somata and neuropil

in all layers of BC (Figure 3F and Figure S9). To verify that single-unit spikes could be evoked by low intensity photo-activation, I made juxtacellular recordings from single ChR2-expressing GABAergic cell (Figure 3G) while applying blue light (470 nm; 0.6 mW) to the cortical surface via an optical fiber (400 µm in diameter). This activation lead to a decreased activity (chi-square test for a Poisson distribution; see material and methods) in most of the excitatory cells (16 of 29), an example shown in Figure 3H. Excitatory cells where photostimulation did not change spontaneous spiking (10 of 29) were also included in the analysis of directional selectivity, whereas the three cells, where there was in increased spiking, were excluded.

3.2 L6-Ntsr1 activation changes spontaneous activity in thalamus and cortex

We made juxtacellular recordings to characterize the effect of L6-Ntsr1 photo-activation on the spontaneous spiking rate of cortical excitatory cells and interneurons, as well as thalamic VPM cells (Figure 4). Averaged over all cells, in each respective layer, L6-Ntsr1 activation decreased spiking in L2/3 (n = 15), L5 (n = 42) and L6 non-Ntsr1 (n = 31), whereas on average spiking in L4 (n = 36) did not decrease significantly (Figure 4A). Analyzing the cells on a single cell basis it was, however, clear that the effect on spiking varied substantially (Figure 4 B-D) between cells, and therefore each cell was tested individually (chi-square test for a Poisson distribution; see materials and methods). The majority of the cells showed a significant change in spiking (Table 1, 64 of 96 cells; 28 cells excluded, see Methods), which in most cases was a decrease (86 %; 55 of 64 cells) in the spontaneous activity. An increase in spontaneous activity was found for some cells (14 %; 9 of 64 cells) in all layers, except L2/3 (Table 1). Furthermore, the decrease in spontaneous activity was dependent on light intensity (Figure S2). To compare the relative effect, of both the increase and decrease on spontaneous spiking, between layers the data was normalized and plotted as an Opto-Index "OI". An OI value of 0 indicates no effect, positive values an increase and negative values a decrease spiking. The cells showing a decreased activity (n = 55 cells) had an average Opto-Index of -0.67 ± 0.12; -0.63 ± 0.07; -0.59 ± 0.05 and -0.70 ± 0.08 for L2/3, L4, L5 and L6 non-Ntsr1 cells respectively, and with no significant difference between layers (one-way ANOVA; $p = 0.6608$; Figure 4E). The cells showing an increased activity had an average Opto-Index of 0.45 ± 0.10; 0.46 ± 0.08 and 0.75 for L4, L5 and L6, with no significant difference between layers (Mann-Whitney test between L4 and L5, $p > 0.9999$, L6 not included in the analysis since only one cell recorded in L6; data not shown).

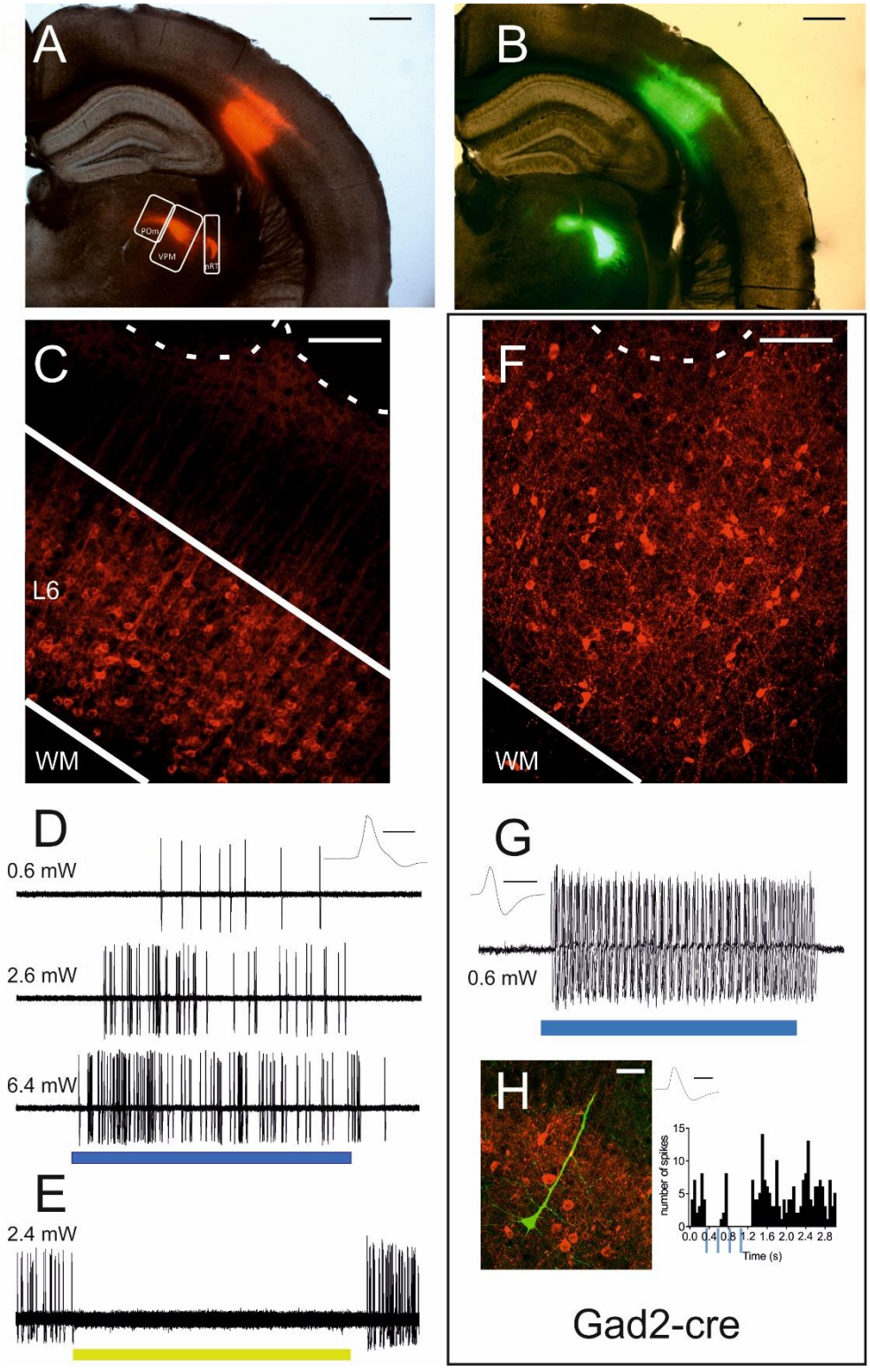

FIGURE 3: CRE-EXPRESSION OF NTSR1 AND GAD2 MOUSE LINES

A. L6-Ntsr1 neurons expressing ChR2-mCherry (in red) in the barrel cortex project mainly to the somatosensory thalamus and the reticular nucleus. The largest red area seen in somatosensory thalamus corresponds to the VPM part of sensory thalamus.
B. L6-Ntsr1 neurons expressing ArchT-GFP (in green) in the barrel cortex show the same projection pattern as that shown for ChR2-mCherry in panel A. With cortical and thalamic projections.
C. ChR2-mCherry expression in L6-Ntsr1 cells in the primary somatosensory barrel cortex. Fluorescent (in red) somata in L6 and dendritic tufts and/or terminals in L5. WM = white matter, L6 = Layer 6, the dotted lines represent the layer 4 barrels.
D. In vivo juxtacellular recording of a L6-Ntsr1 cell expressing channelrhodopsin that responds with spikes to the 470 nm light stimulation at varying intensities (blue bar is 50 ms). Recordings show the overlay of 5 sweeps for each light intensity.
E. In vivo juxtacellular recording of a L6-Ntsr1 cell expressing archaerhodopsin. Spiking was completely stopped in response to the 590 nm light stimulation (50ms; yellow bar) at 2.4 mW. Recording is the overlay of 50 sweeps.
F. GAD2-Interneurons expressing ChR2-mCherry (in red) in the barrel cortex. WM = white matter, the dotted line represents a layer 4 barrel.
G. In vivo juxtacellular recording of a L2/3 interneuron expressing channelrhodopsin that responds with spikes to the 470 nm light stimulation at 0.6 mW (blue bar is 80 ms). Recordings show the overlay of 5 sweeps.
H. Image of a pyramidal neuron (in green) associated with a PSTH showing it response to the 470nm light stimulation in a GAD2 animal expressing ChR2-mCherry in all layers (here 4 stimulations of 80ms at 4Hz). The cell was filled with biocytin after the in vivo recording using an electroporation method. Subsequently brain sections were labelled with Streptavidin Alexafluor 488 (in green), that binds to biocytin. PSTH shows the clear depression of the activity of the excitatory cell upon non-specific GABAergic activation.

Scale bar: A and B = 600 μm; C and F = 150 μm; H = 30 μm

Inset from D to H: Spike shape of the recorded neuron, scale bar = 1ms

Cells in which activation of L6-Ntsr1 cells decreased or had no effect on spiking had a control frequency over a relatively broad range (Figure S3; cells (n = 55) with a decrease: range 0.3-16.1 Hz; median 1.7 Hz; no effect (n = 32): range 0.1-10.7 Hz, median 0.8 Hz, whereas the cells (n = 9) that increased their firing, had a comparably much lower range of control activities: range 0.1 – 6.1 Hz; median 0.6 Hz; Kruskal-Wallis test, p = 0.0087).

Interestingly, following the photo-activation there was often an increased spiking occurring 200 – 500 ms after the offset of the light pulse. Averaged of the entire cell sample, 47% of the recorded cells showed this "rebound" response (58 of 124 cells; see Methods). The distribution per layer was: L2/3, 47% (7 of 15 cells); L4, 56% (20 of 36 cells); L5, 52% (22 of 42 cells); L6, 29% (9 of 31 cells). Furthermore, it appears that the strength of this rebound was depth dependent (Figure 4F). The Rebound-Index was the largest in L2/3 and decreased with depth (one-way ANOVA, p = 0.0174; post-test for linear trend p = 0.0046; L2/3: 0.88 ± 0.03; L4: 0.68 ± 0.04; L5: 0.62 ± 0.04; L6: 0.62 ± 0.09). To investigate if the rebound excitation was due to GABAergic interneurons, the effect of L6-Ntsr1 activation on interneurons was examined (Figure 4G-K). L2/3 interneurons displayed mostly no effect during L6-activation. 1 of 5 cells was inhibited by 93%. L4 interneurons displayed a mix of effects: 7 of 15 cells were inhibited on average by 78% (from 3.39 ± 1.87 Hz to 0.75 ± 0.48 Hz); no change in four cells, and four cells showed an increased spiking (from 0.85 ± 0.52 Hz to 3.24 ± 1.62 Hz). L5 interneurons displayed also a mixed effect: 5 of 11 cells inhibited on average by % (from 2.77 ± 0.79 Hz to 0.93 ± 0.56 Hz), in two cells no change, and four cells an increased spiking (from 0.13 ± 0.08 Hz to 1.48 ± 0.61 Hz). In contrast to the other layers, in L6 interneurons 3 of 6 cells showed a dramatic increase in their spiking with photostimulation (Figure 4I; 0.02 ± 0.02 Hz to 61.11 ± 13.3 Hz). The L6 interneurons responded to every light pulse with a relatively short and consistent response latency (14 ± 0.8 ms, 18 ± 0.5 ms, and 42 ± 0.7 ms after the onset of the light pulse; Figure S5). The four L4 cells and the four L5 cells that increased their spiking did not respond every time and when responding they had a longer onset latency of (L4: 278 ± 15 ms (12 % response probability), 158 ± 101 ms (12 %), 74 ± 4.8 ms (90 %) and 143 ± 96 ms (42%); L5: 114 ± 13 ms (24 %), 133 ± 87 ms (38 %), 155 ± 54 ms (70 %),186 ± 92 ms (10 %); Figure 4K). The strong, reliable and with short latency, activation of L6 interneurons suggests a direct activation of the interneurons via L6-Ntsr1 cells (the average latency to the first opto-induced spike was 8 ± 1 ms in L6-Ntsr1 cells (n = 14). Some interneurons were photo-activation decreased or had no effect of spiking also displayed the "rebound effect" (one example in Figure 4H), suggesting that they were also inhibited by infragranular interneurons. In summary,

the data indicate that the decrease in spontaneous activity recorded *in vivo* in excitatory neurons is due to the activation of infragranular GABAergic interneurons. This is consistent with data from somatosensory cortex recorded in the brain slice preparation (Kim et al., 2014) and *in vivo* in the visual cortex (Bortone et al., 2014).

The L6-Ntsr1 cells have both cortical and thalamic projections. In line with previous results (Mease et al., 2014), I found that photo-activation of L6-Ntsr1 cells can increase the spontaneous firing rate of VPM cells (Figure 4L; Control: 2.24 ± 0.49 Hz; L6-Ntsr1 activation: 5.28 ± 1.35 Hz; n = 11; p = 0.0088; paired t-test) with a peak at around 100 ms after the onset of the light pulse (Figure 4M). Interestingly, a rebound response occurs also in the VPM cells and with a shorter latency than in the cortical cells (Figure 4N). This indicates that the "rebound effect" in excitatory cells can be caused by both thalamic and cortical activity.

3.3 Limited Effect of L6-Ntsr1 Inactivation on Spontaneous Activity

Whereas the activation of L6-Ntsr1 cells on average decreased the spontaneous activity, their inactivation did not produce a clear opposite effect. In most of the cells (83 %, 82 of 99; 16 cells excluded, see Methods) there was no significant change in spontaneous spiking. In L4, the cells that did show a significant change (chi-square test for a Poisson distribution, see Methods), all decreased their activity (Table 2; Figure 5A). Averaged over all L4 cells, the L6-Ntsr1 inactivation decreased the resting activity (n = 28; control: 1.95 ± 0.67 Hz; L6-Ntsr1 inactivation: 1.44 ± 0.47 Hz; p = 0.0340; Wilcoxon test; Figure 5B). In L5/6, the cells that did show a significant change displayed a mix of effects (increase 7/12; decrease 5/12) but no significant change on average over the entire L5 and L6 non-Ntsr1 cells (Wilcoxon; L5: p = 0.8762; L6: p = 0.7960). Interestingly, in the L4 cells where L6-Ntsr1 inactivation decreased spontaneous activity, this decrease was, in contrast to the decrease induced by photo-activation, not followed by a rebound effect. This difference suggests that different underlying mechanisms are responsible for the decreased activity (Figure 5C).

Spontaneous spiking in GABAergic interneurons (3 cells in L2/3, 2 in L4, 5 in L5 and 7 in L6) was not significantly affected by photo-inactivation of L6-Ntsr1 cells (chi-square test for a Poisson distribution). In one L5 interneuron spiking decreased.

In VPM, (Figure 5D) spontaneous spiking was on average not affected (n = 16; control: 2.42 ± 0.48 Hz; L6-Ntsr1 inactivation: 2.19 ± 0.36 Hz; p = 0.2427, paired t-test). Notably, however, in 2 VPM cells, with a relatively high spontaneous activity, there was a significant decrease followed by a rebound effect (chi-square test for a Poisson distribution; cell 1: control, 2.9 Hz;

L6-Ntsr1 photo-inactivation, 1.8 Hz / cell 2: control, 8.1 Hz; L6-Ntsr1 photo-inactivation, 5.8 Hz; example in Figure 5E). If a proportion of VPM cells decrease there spiking with photo-inactivation (and none increase) this will contribute to the reduced activity seen in the cortical L4 cells (Figure 5B), which receives a strong VPM input. The much weaker effect on spontaneous activity when silencing the L6-Ntsr1 cells could be because the spontaneous activity in these cells is already relatively low (0.07 ± 0.06 Hz, n = 14; this average includes 10 cells that were confirmed to be L6-Ntsr1 cells with photo-activation, but where the spontaneous activity was zero in control; two cells (1 and 5.5 Hz spiking rate) were excluded since they were identified as outliers using the ROUT method (Motulsky and Brown, 2006) as implemented in GraphPad Prism (GraphPad Software, CA, USA).

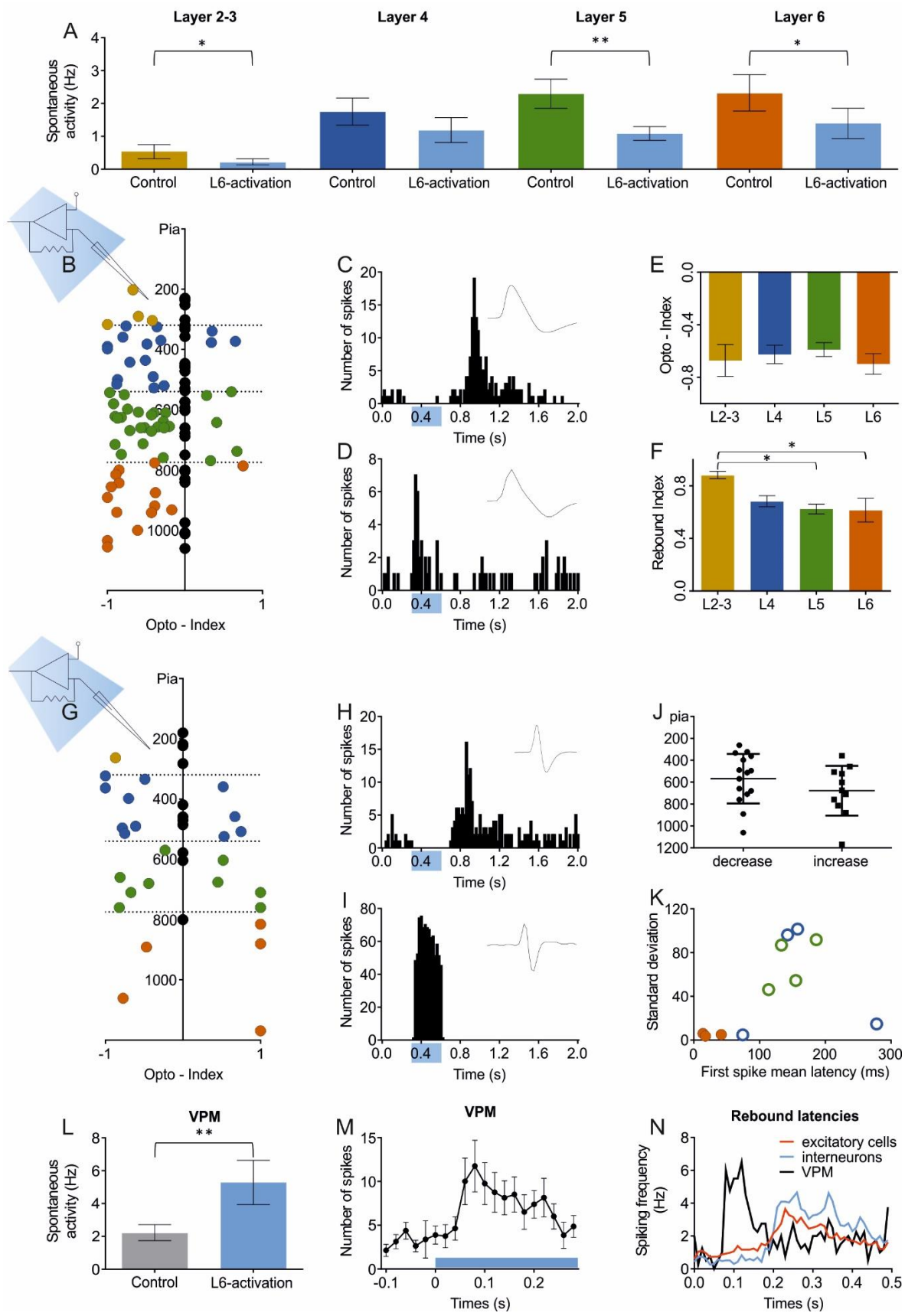

FIGURE 4: EFFECT OF L6-NTSR1 ACTIVATION ON SPONTANEOUS SPIKING

A. Effect of L6-Ntsr1 activation on the average spontaneous spiking rate in excitatory cells in the different cortical layers. The decrease was statistically significant in all layers expect layer 4 (L2/3: n=15, p = 0.0288; L4: n=36, p = 0.0811; L5: n=42, p = 0.0056; L6 non-Ntsr1: n=31, p = 0.0324. paired t-test) Data are represented as mean ± SEM (in all panels except J).
B. Although the effect on average was a decrease, it was clear that the effect of L6-Ntsr1 photo-activation varied substantially between cells. Therefore, cells were evaluated individually using a chi-square test and the effect was normalized and plotted as an "opto-index, OI" ((spiking in opto – spiking in ctrl) / (spiking in opto + spiking in ctrl)). Negative/positive OI means that spiking decreased/increased with light stimulation. Cells are classified by layer and the cells showing a significant change are shown in color. Black dots are cells with no significant effect and they are all placed at OI = zero. N = 96.
C. Example of a decrease in spontaneous spiking induced by L6-Ntsr1 photo-activation (L5 excitatory cell, depth: 655 μm). Note the rebound excitation at 1 s. Inset shows extracellularly recorded spike shape.
D. Example of an increase in spontaneous spiking induced by L6-Ntsr1 photo-activation (L5 excitatory cell, depth: 642 μm).
E. Average OI for the excitatory cells showing a significant decrease of their activity following the optogenetic light activation of L6-Ntsr1 cells. No significant difference between layers (one-way ANOVA, p = 0.6608).
F. Average "rebound index" ((1 – (spikes in ctrl/ spikes in opto)), the larger the value the stronger was the rebound) for excitatory cells showing a significant increase in spiking following the offset of the light pulse (one example of a rebound effect seen in panel C). The rebound showed a depth dependent effect being the strongest in L2/3 and weakest in L5 and L6 (One-way ANOVA; p = 0.0174).
G. Effect of the L6-Ntsr1 photo-activation on the spontaneous spiking in GABAergic interneurons. Effect quantified as an opto-index "OI" and plotted as described for the excitatory cells in panel B. Cells showing a significant change are shown in color. N = 37.
H. Example of the decreasing effect of L6 Ntsr1 photo-activation on an interneuron (L4 cell, depth: 323 μm).

I. Example of an increase in spontaneous spiking in an interneuron induced by L6-Ntsr1 photo-activation (L6 GABAergic interneurons, depth: 815 μm). Inset shows the extracellularly recorded spike shape typical of a GABAergic interneuron.

J. There was no depth dependent effect ($p = 0.2304$, unpaired t-test) of photo-activation with interneurons where L6-Ntsr1 photo-activation decreased spontaneous spiking (depth 568 ± 59 μm, n=15) and cells where the activity increased (678 ± 69 μm, n=11). Data presented as mean ± SD.

K. Plotted are all interneurons displaying a positive OI (meaning increased spiking with L6-activation). Same color code as G. Mean latency of the first spike (measured in 50 sweeps for each cell) emitted after the 470nm light onset plotted against the standard deviation. The L6-interneurons (orange filled circles) where activated on every stimulation (filled circle = responded to every light pulse), which was not the case for interneurons in other layers (median response probability (minimum one spike) = 31 %, range: 12-90 %). The three L6 interneurons thus appear to be directly activated by L6-Ntsr1 cells.

L. L6-Ntsr1 activation increased spontaneous spiking in VPM cells. (Control: 2.7 ± 0.6 Hz; L6-Ntsr1 activation: 7.1 ± 1.6 Hz; $p = 0.0085$; $n = 11$; paired t-test)

M. Recordings from 8 VPM cells with activity increasing with a 470 nm light pulse (blue bar = 300 ms). The increase activity peaks 100 ms after the onset of the blue light.

N. Difference in the latencies of the thalamic and cortical “rebound effect”. The thalamic one is triggered sooner in time than the cortical one. Time zero is at the offset of the light pulse.

Table 1, related to Figure 4. Effect of L6-Ntsr1 activation on spontaneous activity in excitatory cells

Total number of cells per layer		**Number of cells included**	**No significant change**	**Decreased spiking**		**Increased spiking**	
				% cells showing a decrease		% cells showing an increase	
				Control (Hz)	L6-Ntsr1 activation (Hz)	Control (Hz)	L6-Ntsr1 activation (Hz)
L2/3	15	8	50% (4)	50% (4)		zero	
				1.22 ± 0.74	0.42 ± 0.33		
L4	36	28	39% (11)	50% (14)		11% (3)	
				3.21 ± 0.82	1.25 ± 0.41	2.53 ± 1.80	5.71 ± 3.42
L5	42	36	22% (8)	64% (23)		14% (5)	
				3.21 ± 0.71	0.88 ± 0.21	0.57 ± 0.21	1.31 ± 0.35
L6	31	24	38% (9)	58% (14)		4% (1)	
				2.95 ± 0.88	0.71 ± 0.38	0.07	0.47
Total	124	96	32	55		9	

Data presented as mean ± SEM

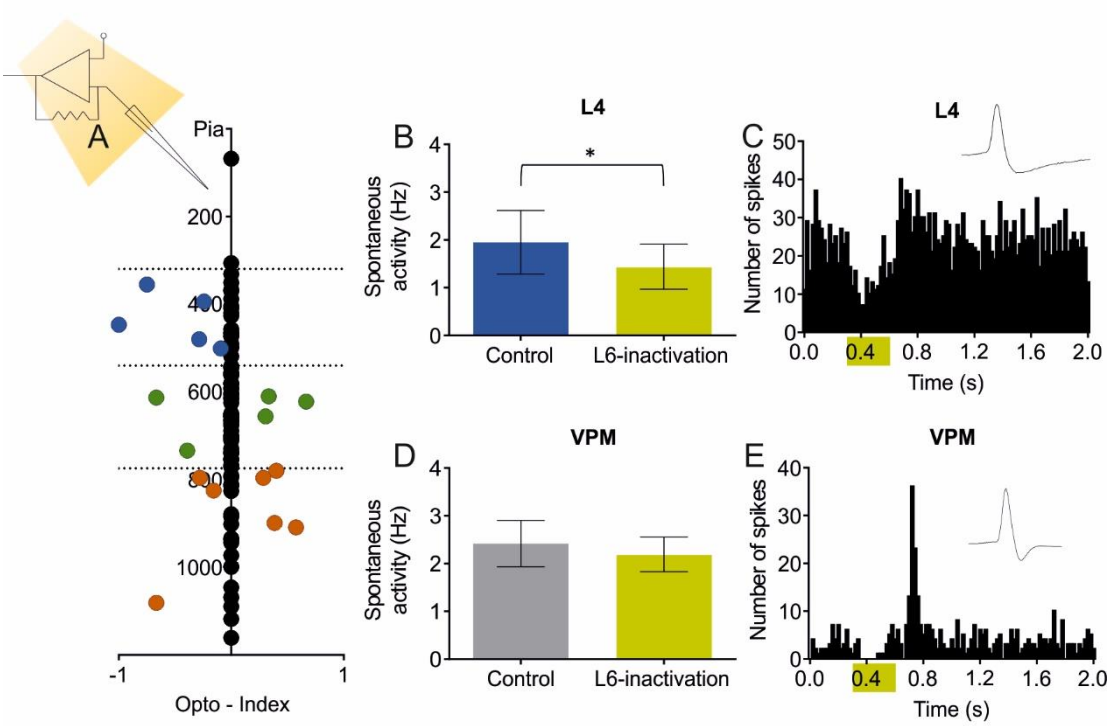

FIGURE 5: EFFECT OF L6-NTSR1 INACTIVATION ON SPONTANEOUS SPIKING

A. Effect of the L6-Ntsr1 inactivation on the resting activity of excitatory cells using the "optogenetic index, OI". Cells are classified by layer and the cells showing a significant change are shown in color (n = 99).

B. Photo-inactivation of L6- Ntsr1 cells decreased spontaneous spiking in L4 (n = 28; control: 1.95 ± 0.67; L6-Ntsr1 inactivated: 1.44 ± 0.47; p = 0.0340; Wilcoxon test). The average effect was not significant in the other layers (L2/3: n = 3; ctrl: 3.00 ± 2.42; L6-inact.: 2.47 ± 2.11; p = 0.2500); (L5: n = 52; ctrl: 2.49 ± 0.62; L6-inact.: 2.52 ± 0.63; p = 0.8762); (L6: n = 32; ctrl: 1.52 ± 0.32; L6-inact.: 1.56 ± 0.32; p = 0.7960). Data are represented as mean ± SEM

C. PSTH of a L4 excitatory cell showing a depressed activity with L6-Ntsr1 inactivation. Sum from 90 sweeps.

D. L6-Ntsr1 inactivation did not significantly modify the spontaneous spiking when averaging over the total VPM cell population (n = 16; control: 2.42 ± 0.48 Hz; L6-Ntsr1 inactivation: 2.19 ± 0.36 Hz; p = 0.2427, paired t-test). Data are represented as mean ± SEM

E. PSTH of a VPM cell where L6-Ntsr1 inactivation clearly decreased spontaneous activity and where this was followed by a rebound excitation ~100 ms after the offset of the light pulse.

Table 2, related to Figure 5. Effect of L6-Ntsr1 inactivation on spontaneous activity in excitatory cells

Total number of cells per layer		**Number of cells included**	**No significant change**	**% cells showing a decrease**		**% cells showing an increase**	
				Control freq. (Hz)	L6-Ntsr1 inhibition (Hz)		
L2/3	3	2	100% (2)	zero		zero	
L4	28	23	78% (18)	22% (5)		zero	
				6.28 ± 3.07	4.12 ± 2.30		
L5	52	48	90% (43)	4% (2)		6% (3)	
				0.70 ± 0.37	0.27 ± 0.20	1.09 ± 0.45	2.31 ± 0.66
L6	32	26	73% (19)	12% (3)		15% (4)	
				3.20 ± 2.03	2.16 ± 1.56	1.23 ± 0.58	2.90 ± 1.33
Total	115	99	82	10		7	

Data presented as mean ± SEM

3.4 L6-Ntsr1 activation alters whisker-evoked responses

Having established that photo-stimulation of L6-Ntsr1 cells changes cortical network excitability, I next investigated how this will influence whisker-evoked activity. Juxtacellular recordings were made from excitatory cells in layers 2 to 6 in barrel cortex while moving the principal whisker and photo-activating L6-Ntsr1 cells. The whisker-evoked response (spikes / 100 ms) was measured in 56 excitatory cells throughout all layers of barrel cortex (Table 3; no separation was made between cells where photo-activation increased, decreased or had no effect on spontaneous activity).

L6-Ntsr1 activation caused a significant reduction of the whisker-evoked response in all layers except L5. (Table 3; Figure 6A-B). The decrease in the average number of spikes per whisker-deflection, observed during L6-Ntsr1 activation, can be caused by a reduced response probability and/or a reduced number of whisker evoked spikes per successfully detected whisker deflection. To disentangle these different possibilities, I did complementary analyses. L6-Ntsr1 activation caused a reduced response probability in all layers except L5, contributing to the reduced whisker-evoked response (Figure 6C). Furthermore, it appears that activation of L6-Ntsr1 cells does not significantly change the number of spikes per successful response (defined as at least one spike in a 100 ms time window) for layers 2-5, but only in layer 6 (Figure 6D). In conclusion, the biggest reduction of the whisker-evoked response, caused by photo-activation of L6-Ntsr1 cells, was in layer 6 non-Ntsr1 cells. This is caused by a reduction of response probability and a reduced number of spikes per successful response.

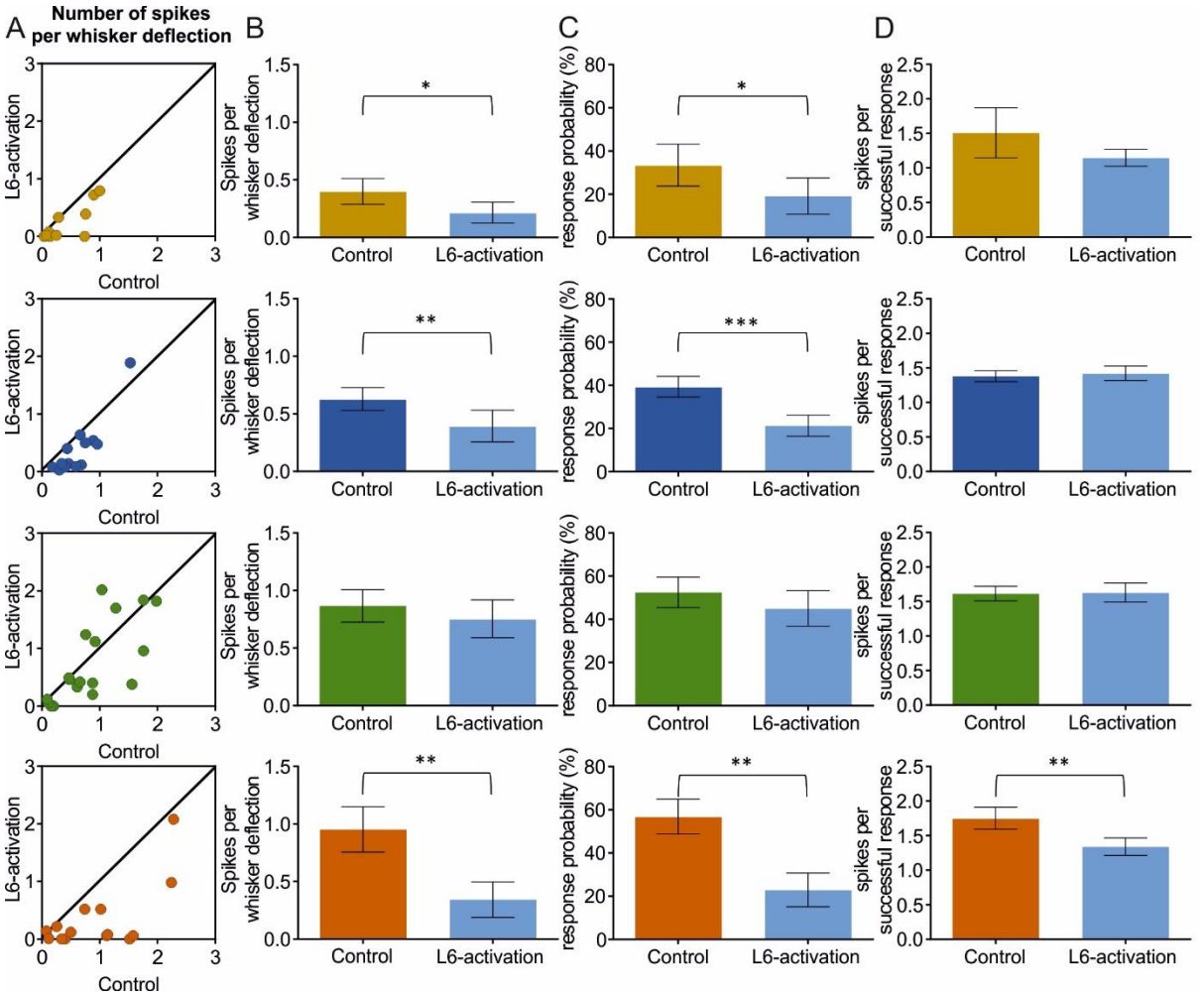

FIGURE 6: L6-NTSR1 ACTIVATION DECREASE EVOKED SPIKING

A. Scatter plot showing on the x-axis the average number of spikes elicited per whisker deflection (in a 100 ms time window) in control and on the y-axis with L6-Ntsr1 activation. The top panel is L2/3 (n = 11 cells) and the next panels in the vertical direction show, from top to bottom, L4 (n = 13), L5 (n = 18) and L6-non Ntsr1 (n = 14).

B. The same data as in panel A, but now shown as the averaged whisker-evoked response per layers for each condition. A significant decrease was found for all layers except L5. (L2/3: ctrl: 0.40 ± 0.11; L6-act.: 0.22 ± 0.09; p = 0.0181); (L4: ctrl: 0.63 ± 0.10; L6-act.: 0.39 ± 0.14; p = 0.0048); (L5: ctrl: 0.87 ± 0.14; L6-act.: 0.75 ± 0.16; p = 0.3435); (L6: ctrl: 0.95 ± 0.20; L6-act.: 0.34 ± 0.15; p = 0.0012). Data are represented as mean ± SEM in panels B-D.

C. The averaged response probability (whisker evoked responses with at least one spike) decreased in all layers. Data presented as: (n; RP in control; RP in L6-activation; p-value paired t-test); (L2/3: 11; 33 ± 10; 19 ± 8; 0.0161); (L4: 13; 39 ± 5; 21 ± 5; 0.0006); (L5: 18; 53 ± 7; 45 ± 8; 0.1663); (L6: 14; 57 ± 8; 23 ± 8; 0.0012).

D. The number of spikes per successful response (at least one spike in the 100 ms following the whisker deflection) averaged in each condition for all cells belonging to a specific layer (number of cells in this data lower due to RP = 0 for some opto condition. Significance is reach for L6 where a 24% decrease on the number of spikes per detected incoming information is triggered. Data presented as: (n; Number of spikes in control; Number of spikes in L6-activation; p); (L2/3: 8; 1.51 ± 0.36; 1.15 ± 0.12; 0.4036); (L4: 13; 1.38 ± 0.08; 1.42 ± 0.11; 0.6970); (L5: 16; 1.62 ± 0.11; 1.63 ± 0.14; 0.8933); (L6: 11; 1.75 ± 0.16; 1.34 ± 0.13; 0.0094).

Table 3, related to Figure 6. Effect of L6-Ntsr1 activation on cortical responses to whisker deflections recorded in excitatory cells

	Control Spikes per WD	L6-Ntsr1 activation Spikes per WD	Average decrease	Paired t-test, p-value
L2/3 (n=11)	0.40 ± 0.11	0.22 ± 0.09	45 %	0.0181
L4 (n=13)	0.63 ± 0.10	0.39 ± 0.14	38 %	0.0048
L5 (n=18)	0.87 ± 0.14	0.75 ± 0.16	-	0.3435
L6 (n=14)	0.95 ± 0.20	0.34 ± 0.15	64 %	0.0012

Data presented as mean ± SEM; WD = whisker deflection

3.5 L6 activation increases the evoked-to-spontaneous ratio in cortex

Photo-activation of L6-Ntsr1 cells decreased the whisker-evoked response and also spontaneous spiking. In cells where there was a decreased spontaneous spiking, the relative decrease of the spontaneous activity was larger than the decrease in the whisker-evoked activity (Figure 7A-C). A larger relative decrease in the spontaneous activity means that with L6 photo-activation the evoked-to-spontaneous ratio increased. The increased difference between evoked and spontaneous spiking can also be expressed by calculating the standard detection theory variable d-prime (Macmillan and Creelman, 2005). The spiking histogram used to calculate d-prime shows the increase sensitivity with L6-activation. A larger d-prime means a better detection of a true positive event (Figure 7B). Furthermore, it can be noticed that the spontaneous frequency distribution is sharper (SD is smaller) with L6-activation compared to control, thus allowing an easier detection of events outside the spontaneous spiking range.

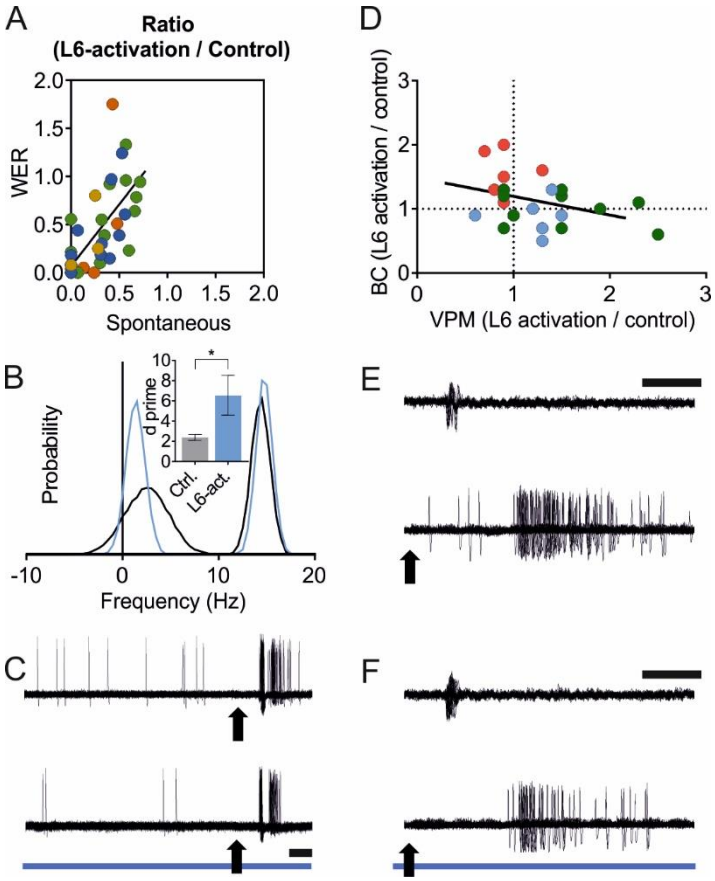

FIGURE 7: L6-NTSR1 ACTIVATION INCREASED EVOKED-TO-SPONTANEOUS RATIO

A. Scatter plot showing on the x-axis the relative change in spontaneous activity with L6-activation and on the y-axis, for the same respective cells, the relative change in the whisker-evoked response (WER). Only cells showing a significant decrease in their spontaneous spiking are plotted. Color coding same as in Figure 4. Linear regression analysis shows that the slope is significantly non-zero ($p < 0.0001$), with a slope = 1.2. A slope > 1 means that the evoked-response is less decreased then the spontaneous activity, leading to an increased evoked-to-spontaneous ratio with L6-activation.

B. A Gaussian spiking distribution generated based on mean and standard deviation from the respective spike counts of spontaneous spiking or whisker-evoked response in control or with L6-activation (n = 20 cells). *Inset*: The sensitivity index (d´), a measure of the separation of the signal and noise distributions, increased following L6-activation, implicating a better separation of true from false positive events (Bar graph: Control: 2.4 ± 0.3; L6-activation: 6.6 ± 2.0; $p = 0.0408$; paired t-test). Data are represented as mean ± SEM.

C. *Upper panel*: raw traces (50 sweeps overlaid). Arrow marks deflection of the principal whisker (every 3 seconds). *Lower panel*: L6-activation decreased both the spontaneous and the whisker-evoked response. But since the relative decrease of spontaneous spiking was larger the evoked-to-spontaneous ratio increased. Scale bar = 10 ms.

D. Simultaneous in vivo electrophysiology recording from a VPM cell and a L5 cell in a cortical barrel. Each cell pair (n = 13) was recorded with 1-3 different delays, varying between 100 (blue), 140 (red) or 320 ms (green), between onset of optogenetic stimulation and whisker stimulation. Both cells have the same principal whisker. The effect of L6-Ntsr1 activation on the WER in VPM is plotted on the y-axis and the corresponding effect of a simultaneous recorded L5 cell on the x-axis. No significant linear correlation between the relative change of the whisker-evoked response ($R^2 = 0.134$; $p = 0.0784$).

E. Example of a dual in vivo extracellular recording (aligned VPM barreloid neuron, and barrel cortex L5 excitatory neuron) in control condition. Arrow marks deflection of the principal whisker (every 3 seconds). *Upper panel*: Extracellular recorded spikes in a VPM neuron (50 aligned sweeps). *Lower panel*: Extracellular recorded spikes in a L5 excitatory neuron (50 aligned sweeps). Neurons were recorded simultaneously and the whisker-evoked response was recorded and plotted in D. Scale bar = 10 ms

F. Same dual recording as in E but with L6-activation (blue bar). Scale bar = 10 ms

3.6 L6 activity can modify cortical and thalamic activity independently

To investigate how the effect of L6-Ntsr1 activation on thalamic and cortical activity is related, dual aligned recordings were performed from aligned barreloid-barrel cells (corresponding to the same principal whisker). A tungsten electrode was used to obtain single-unit recordings in VPM and subsequently a glass pipette was used to search for a cortical L5 neuron in the aligned cortical barrel. I chose to record from layer 5 since it is an output layer and as such might better reflect the summed effect of L6-Ntsr1 cell activation in cortex. Furthermore, in layer 5, L6-Ntsr1 activation had the most diverse effect with both increased and decreased activity, and this in combination with using different latencies (100, 140 and 320 ms) between the optogenetic light onset and the whisker deflection, allowed that the cortical and thalamic responses could be studied over a broader range of activities. A possible correlation between the cortical and the thalamic response was quantified by comparing the relative change in the whisker-evoked response with L6-Ntsr1 photoactivation (Figure 7D-F). Each data point in figure 7D shows on the x-axis the relative change in the whisker-evoked activity measured in VPM with and without photoactivation (n = 13 for 24 data points). On the y-axis is plotted the simultaneously measured whisker-evoked response in a L5 cell (ratio between response with and without L6 photoactivation). The linear correlation between the relative change of the whisker-evoked response in cortex and thalamus did not quite reach statistical significance (Figure 7D; $R^2 = 0.134$; $p = 0.0784$). It can be concluded that the effect of L6-Ntsr1 activation on the cortical L5 output cannot strongly predict, at least not with a linear correlation, the effect of photo-activation on VPM spiking activity. A possible negative trend level correlation could be because in some cases L6-activation on the one hand depolarizes VPM neurons so that they increase their whisker-evoked response (x-axis), but then on the other hand decreases cortex activity (y-axis) via activation of GABAergic interneurons.

Sensory filtering in VPM thalamus is presumed to be dependent on the thalamic response mode, broadly characterized as “burst” vs. “tonic” (Mease et al., 2014, Mease et al., 2017). In the present study L6-Ntsr1 photo-activation increased spontaneous firing in VPM, an increase which provided an additive effect to the whisker-evoked responses in VPM (n = 13 single-unit recordings for 29 data points; more than one data point from some cells because data was acquired with different latencies between the optogenetic light onset and the whisker deflection onset; Interaction $p = 0.4722$; two-way ANOVA with repeated measures on both factors; data not shown). L6-Ntsr1 activation did not alter the response probability (control: 80.1 ± 2.7%; L6-activation: 80.5 ± 3.3%; $p = 0.9079$; paired t-test; data not shown), nor was there any change

in burstiness, quantified as percentage of successful response where at least one burst occurred (control: 26.1 ± 3.5%; L6-activation: 29.7 ± 4.1%; p = 0.0889; paired t-test; data not shown). That no change was seen in burstiness could imply that in these experiments the VPM cells were already quite depolarized, thus being in the "tonic" response mode (Mease et al., 2014, Urbain et al., 2015), where further L6 CT driven activation does not change burstiness.

3.7 Effect of L6-Ntsr1 inactivation on whisker responses in cortex and thalamus

Juxtacellular recordings were done in layers 4-6 and whisker-evoked responses were measured with and without L6-Ntsr1 inactivation. In all layers, there was no effect of photo-inhibition on the low-frequency (0.3 Hz) whisker-evoked response (no effect of total number of spikes, Figure 8A-B, Table 4), response probability (Figure 8C) and number of spikes per successful response.

The effect of L6-Ntsr1 photo-inhibition on whisker-evoked responses was also measured in VPM thalamus. Juxtacellular recordings were performed using a glass pipette to obtain single cell recordings in VPM. L6 inactivation did not affect the whisker-evoked response (n = 16 cells; control condition: 0.56 ± 0.18 spikes per whisker deflection (WD); L6-Ntsr1 inactivation: 0.60 ± 0.25 spikes per WD; p = 0.6413; paired t-test; data not shown), or the response probability (n = 16 cells; control condition: 28.6 ± 5.1 %; L6-Ntsr1 inactivation: 27.5 ± 6.4 %; p = 0.5885; paired t-test).

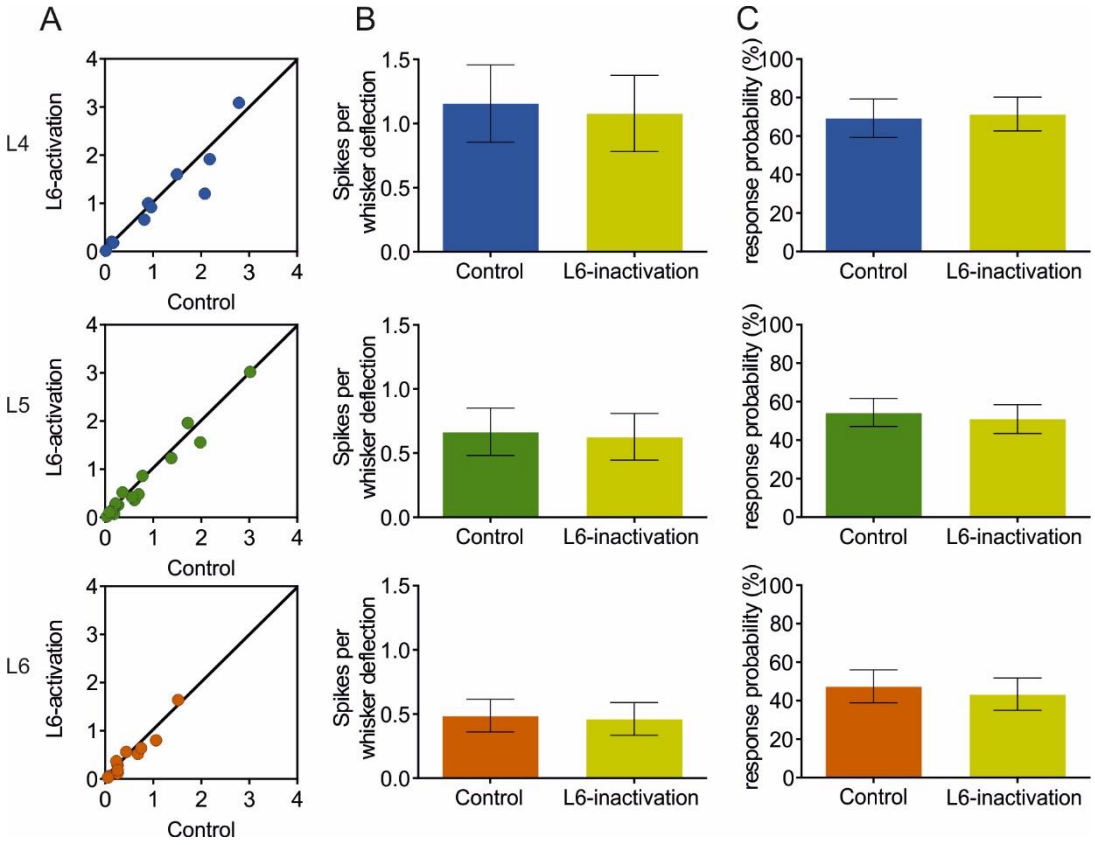

FIGURE 8: EFFECT OF L6-NTSR1 INACTIVATION ON EVOKED SPIKING

A. Scatter plot showing on the x-axis the average number of spikes elicited per whisker deflection (in a 100 ms time window) in control and on the y-axis with L6-Ntsr1 inactivation. The top panel is L4 (n = 10 cells) and the next panels in the vertical direction show, from top to bottom, L5 (n = 19) and L6-non Ntsr1 (n = 12).

B. The same data as in panel A, but now shown as the averaged whisker-evoked response per layer for each condition. No significant changes were found. (L4: ctrl: 1.16 ± 0.30; L6-inact.: 1.08 ± 0.30; p = 0.4666); (L5: ctrl: 0.67 ± 0.18; L6-inact.: 0.63 ± 0.18; p = 0.2708); (L6: ctrl: 0.49 ± 0.13; L6-inact.: 0.46 ± 0.13; p = 0.4889). Data are represented as mean ± SEM in panels B-C.

C. The averaged response probability (RP; whisker evoked responses with at least one spike) did not change in any of the layers. Data presented as: (n; RP in control; RP in L6-activation; p-value paired t-test); (L4: 10; 69 ± 10 %; 72 ± 9 %; p = 0.3403); (L5: 19; 54 ± 7 %; 51 ± 8 %; p = 0.1681); (L6: 12; 48 ± 9 %; 43 ± 8 %; p = 0.0838).

Table 4, related to Figure 8. Effect of L6-Ntsr1 inactivation on cortical responses to whisker deflections recorded in excitatory cells

	Control Spikes per WD	L6-Ntsr1 activation Spikes per WD	Average decrease	Paired t-test, p-value
L4 (n=10)	1.16 ± 0.30	1.08 ± 0.30	-	0.4666
L5 (n=19)	0.67 ± 0.18	0.63 ± 0.18	-	0.2708
L6 (n=12)	0.49 ± 0.13	0.46 ± 0.13	-	0.4889

Data presented as mean ± SEM; WD = whisker deflection

3.8 L6-Ntsr1 activation reduces sensory adaptation in cortex

It has been shown (Mease et al., 2014) that L6 stimulation reduces the adaptation of thalamic responses to repetitive whisker stimulation, thereby presumably allowing thalamic neurons to more reliably relay higher frequencies of sensory input. To study how L6 activation contributes to sensory adaptation in cortex, the whiskers were deflected with 8 Hz trains (Figure 9), similar to that done when examining thalamic responses (Mease et al., 2014). In control condition whisker-evoked responses (8 deflections at 8 Hz, every 3 seconds) decreased with successive whisker deflections (Figure 9A-D; Table 5). Adaptation was quantified comparing the whisker-evoked response (number of spikes without subtracting spontaneous activity) for the first compared to the last (8^{th}) stimulation. Activation of L6-Ntsr1 cells decreased the 1^{st} whisker deflection in all layers (control; L6 activation; two-way ANOVA repeated measures on both factors with Sidak's multiple comparisons test); L2/3: (0.40 ± 0.13 spikes/stim.; 0.20 ± 0.09 spikes/stim.; $p < 0.05$); L4: (1.42 ± 0.47; 0.50 ± 0.26; $p < 0.0001$); L5: (0.49 ± 0.12; 0.22 ± 0.06; $p < 0.0001$); L6: (0.76± 0.15; 0.30± 0.11; $p < 0.0001$). In contrast to control there was no adaptation of the whisker-evoked response when L6-Ntsr1 cells were activated, thus the response remained on average constant during the eight whisker deflections (Table 5). The lack of adaptation when L6-Ntsr1 cells were photo-activated was not caused by a decrease in L6-Ntsr1 spiking during the light pulse, because spiking in L6-Ntsr1 cells decreased rapidly after the first 100 ms preceding the whisker stimulation but then remained fairly constant during the whisker deflection protocol (Figure S4). Photo-inhibition of L6-Ntsr1 cells did not change sensory adaptation in cortex (Figure 9E-G; Table 6).

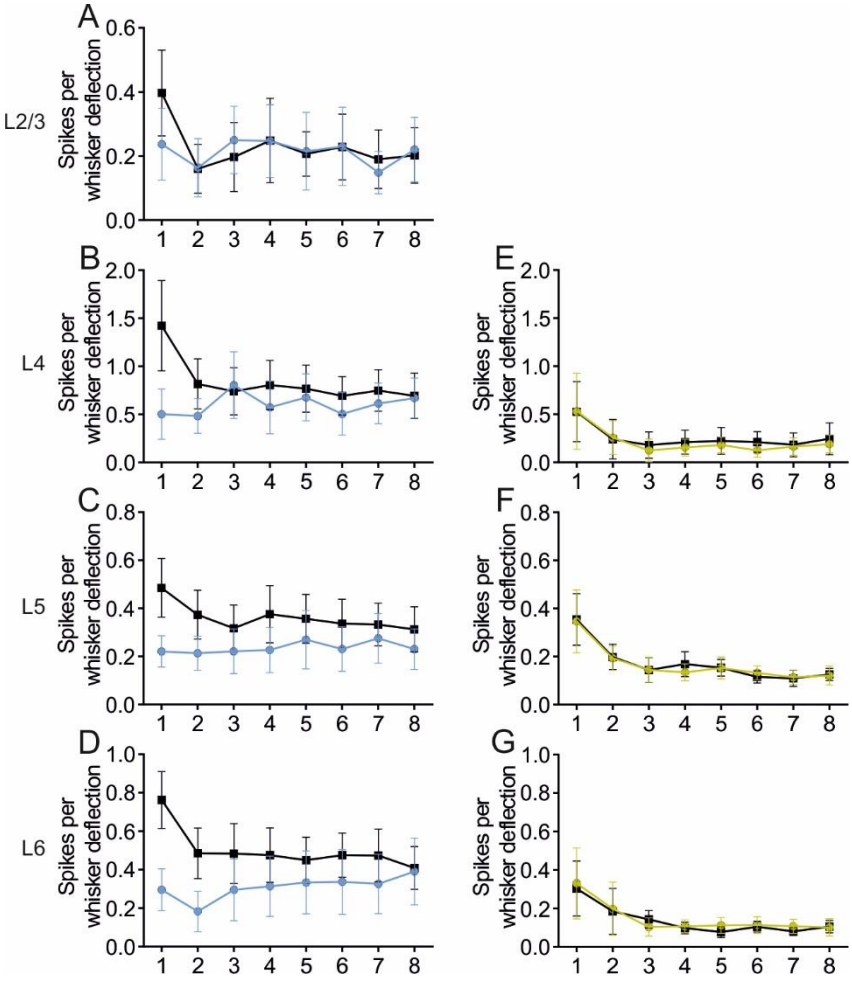

FIGURE 9: L6-NTSR1 REDUCED ADAPTATION

A. to D. Whisker stimulation at 8 Hz (8 deflections at 8 Hz). The first whisker deflection response is reduced with L6 activation condition, in line with low frequency data. The adaptation is seen in all layers in control, but is lost with L6-activation (blue line and symbols). Y-axis shows the average number of spikes evoked by each whisker deflection (L2/3: n = 6; L4: n = 9; L5: n = 16; L6 (non-Ntsr1): n = 13). In control the whisker evoked responses adapted in each layer (comparing 1st stim to average of stimulation 8), but not with L6-activation ("Opto"). (see Table 5 for numbers and statistics). Data are represented as mean ± SEM in all panels.

E. to G. L6-inactivation (yellow line and symbols) had no effect on adaptation to a train of 8 Hz whisker deflections. Plot showing the average number of spikes elicited per each whisker deflection in the 8Hz train in both conditions (control and L6 inactivation) for each layer (E: L4 (n = 3); F: L5 (n = 10); G: L6 (n = 6)). Numbers and statistics in Table 6.

Table 5, related to Figure 9. L6-Ntsr1 activation abolished adaptation to high frequency (8 Hz) whisker deflections

		1st stim	8th stim	Statistics
L2/3 (n=6)	Control	0.40 ± 0.13	0.20 ± 0.09	**
	Opto	0.24 ± 0.11	0.22 ± 0.10	ns
L4 (n=9)	Control	1.42 ± 0.47	0.69 ± 0.23	****
	Opto	0.50 ± 0.26	0.67 ± 0.21	ns
L5 (n=16)	Control	0.49 ± 0.12	0.31 ± 0.09	***
	Opto	0.22 ± 0.06	0.23 ± 0.08	ns
L6 (n=13)	Control	0.76 ± 0.15	0.41 ± 0.11	****
	Opto	0.30 ± 0.11	0.39 ± 0.17	ns

Average number of spikes per 100 ms following whisker deflection. Mean ± SEM
The first stimulation was reduced in all layers, comparing "control" with "opto" separately for each layer (L2/3, $p < 0.01$; L4, $p < 0.0001$; L5 $p < 0.001$, L6, $p < 0.0001$; repeated measures two-way ANOVA matching both factors with Sidak's multiple-comparisons test). In control the whisker evoked responses adapted in each layer (comparing 1st stim with stimulation 8), but not with L6-activation ("Opto") (repeated measures two-way ANOVA matching both factors with Dunnett's multiple comparisons test; *$p < 0.05$, **$p < 0.01$, ***$p < 0.001$, **** $p < 0.0001$.

Table 6, related to Figure 9. Effect of L6-Ntsr1 inactivation on cortical responses to high frequency (8 Hz) whisker deflection

		1st stim	8th stim	Statistics
L4 (n=3)	Control	0.53 ± 0.31	0.25 ± 0.17	**
	Opto	0.53 ± 0.40	0.19 ± 0.09	***
L5 (n=10)	Control	0.35 ± 0.11	0.13 ± 0.03	****
	Opto	0.35 ± 0.13	0.12 ± 0.04	****
L6 (n=6)	Control	0.30 ± 0.14	0.11 ± 0.03	****
	Opto	0.33 ± 0.18	0.10 ± 0.04	****

Average number of spikes per 100 ms following whisker deflection. Mean ± SEM

No significant effect on the first whisker stimulation comparing control and L6-activation ("opto"), and in both conditions the responses adapted (stim 8 smaller than 1st stim; One-way ANOVA with Dunnett post test; *$p < 0.05$, **$p < 0.01$, ***$p < 0.001$, **** $p < 0.0001$.)

3.9 L6-Ntsr1 and cortical direction selectivity

See (Figure 3F, Figure S9 and result part 3.1.2 & 3.1.3) for cortical expression of a double-floxed AAV expressing ChR2 in a Gad2-cre and Ntsr1-cre mouse line. Juxtacellular *in vivo* recordings were done from layer 4 and 5 excitatory cells in both Ntsr1-cre and Gad2-cre mice. Juxtacellular recordings of the VPM thalamus were made in Ntsr1-cre only. Around 30% of the cortical data in Ntsr1 animals have been recorded by Nadja Schwarz, a bachelor student of Ruhr-Universität Bochum.

Whisker-evoked spiking was measured in response to deflections of the whisker in 8 different directions (one full turn with 45 degree difference; establish by Simons, D.J. 1983). For each cell the direction that elicited the largest average number of spikes was called "principal direction" (PD; Figure 10). In a polar plot of the whisker-evoked responses, to different directions, both layer 4 and 5 excitatory cells (L4: n = 25 (13 cells from Ntsr1 animals and 12 cells from Gad2 animals); L5: n = 24 (12 cells from each mouse line)) show a typical "drop shape" (Figure 11A) indicative of orientation tuning (Kida et al., 2005, Wilent and Contreras, 2005a, Puccini et al., 2006, Bale and Petersen, 2009, Vilarchao et al., 2018). Calculating the directional selectivity individually for each L4 cell shows that on average the max response was 142% greater (range: 29 – 300%) to the preferred direction than to the response averaged over all directions. Furthermore the average OD response in L4 represent 38% of the average PD. Calculating the directional selectivity individually for each L5 cell shows that on average the max response was 112% greater (range: 29 – 430%) to the preferred direction than to the response averaged over all directions. Furthermore the average OD response in L5 represent 47% of the average PD. No specific direction appear to be the most responsive and the repartition of the PD appear to be well distributed (Figure S11). Figure 11B shows the normalized whisker-evoked responses, plotted against the distance (in degrees) from the Principal direction (PD). In fact, the response decrease with distance (in degrees) from the PD is slower in L5 than in L4. The greater direction selectivity index (see material and methods and (Wilent and Contreras, 2005a)) for L4 (DSI = 6.59) then L5 (DSI = 3.23) means that L4 is more directional selective than L5; this is in line with the fact that selectivity probably originates from the anatomically precise convergence of thalamic inputs (Wilent and Contreras, 2005b).

Furthermore, to emphasize the fact that excitatory cells in L4 are more orientation tuned than L5, I plotted the median first spikes latency (latency of first spike occurring minimally 5 ms

after the whisker deflection (WD) and maximally 100 ms after WD) of the principal direction against the median first spikes latency of all other directions (Figure 11C-D). It appeared that in L4 the median first spike latency for PD is shorter than the one for all other directions, which is not the case for L5. (Layer; n; latency of PD; latency of ALL except PD; Wilcoxon test p-value) (L4; n = 22; 16.92 ± 2.57 ms; 20.77 ± 3.39 ms; p = 0.0053) (L5; n = 23; 31.44 ± 4.34 ms; 30.78 ± 3.84 ms; p = 0.6010). Three cells in L4 and one in L5 were excluded since they were identified as outliers (latency of PD; latency of ALL except PD in L4: (cell1: 72.40 ms; 82.10 ms); (cell2: 49.40 ms; 19.01 ms); (cell3: 41.50 ms; 21.25 ms) and in L5: (cell1: 77.40 ms; 31.30 ms) using the ROUT method (Motulsky and Brown, 2006) as implemented in GraphPad Prism (GraphPad Software, CA, USA).

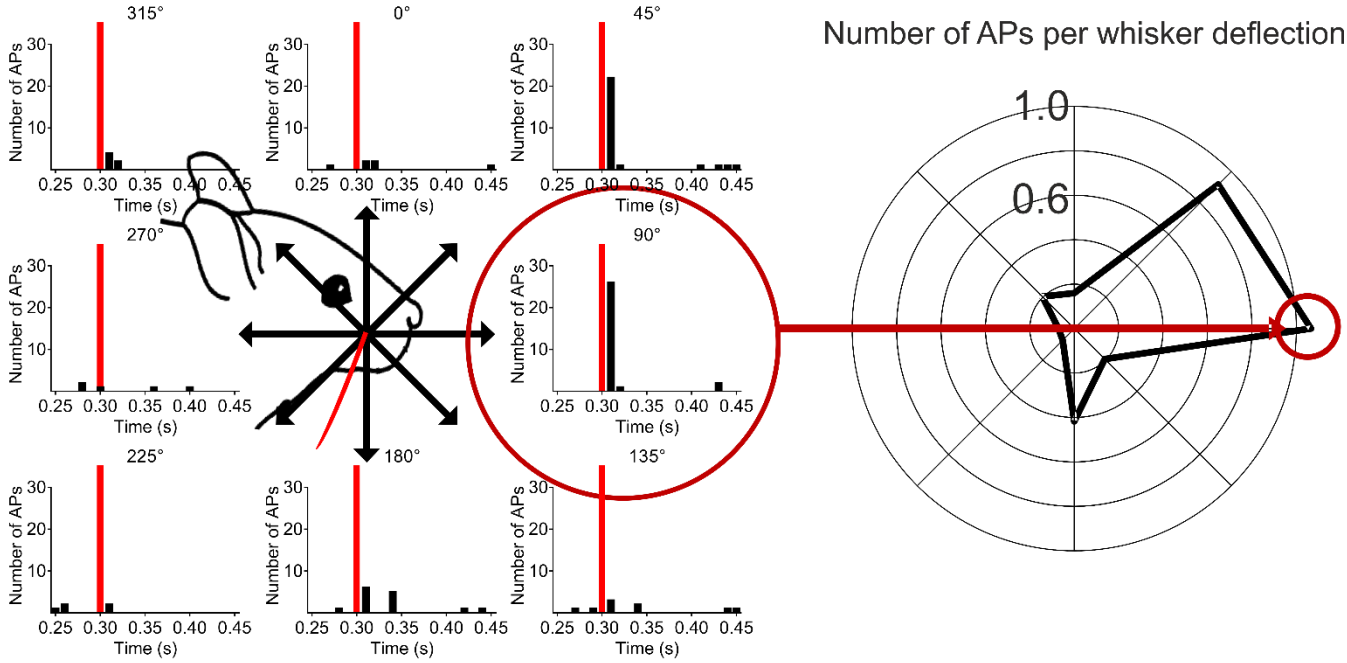

FIGURE 10: DIRECTION SELECTIVITY: EXPERIMENTAL PROTOCOL

Scheme of the experimental protocol. The whisker was deflected in 8 different directions separated by 45 degree. Here 25 whisker deflections per angle (so 5 turns), the whisker deflection time is marked as a vertical red bar at 0.3 seconds in the PSTH. The red circle shows the principal direction, meaning in which direction the recorded neuron answers the best in terms of spikes per WD in a 100ms time window. The right scheme display the number of spikes per WD for each angle in a 100ms time window.

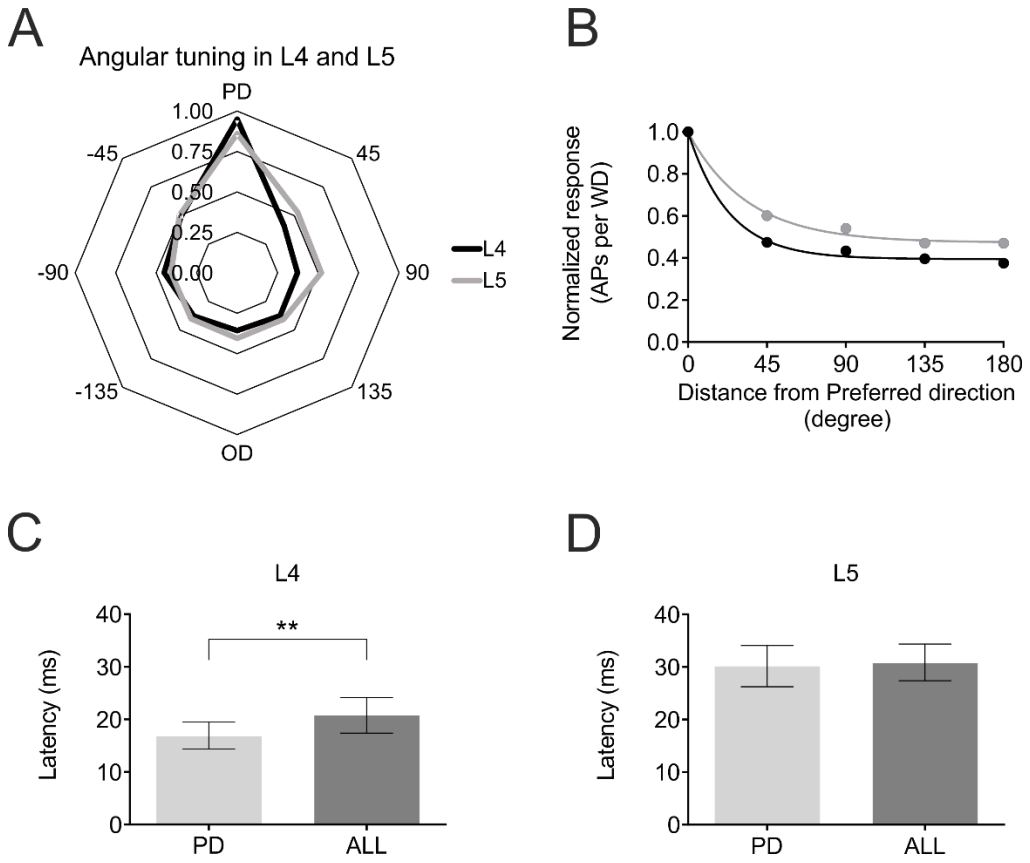

FIGURE 11: DIRECTION SELECTIVITY IS SHARPER IN LAYER 4

A. Averaged whisker-evoked response (number of spikes in 100 ms after whisker deflection) for each direction. PD = principal direction = direction in which individual cell triggered the most APs (see material and methods). It can be noticed that the L4 profile shape is looking like a drop and that the L5 profile is more roundish. For A to D: L4: n = 25; L5: n = 24.

B. Same data as in A. plotted as distance from PD. So 45 = average WER of +45 and -45. It can be noticed that L4 cells displayed a stronger decrease of the WER with distance to the PD since the direction selectivity index for L4 = 6.59 and L5 = 3.23.

C. Median of first spike latency for the principal direction (PD) and for the seven other directions (ALL) for 22 L4 excitatory cells in control condition in both mouse lines (Ntsr1 and Gad2). Data in ms, p-value of paired Wilcoxon test: ALL: 20.77 ± 3.39 ms; PD: 16.92 ± 2.57 ms; p = 0.0053.

D. Median of first spike latency for the principal direction (PD) and for the seven other directions (ALL) for 23 L5 excitatory cells in control condition in both mouse lines (Ntsr1 and Gad2). Data in ms, p-value of paired Wilcoxon test: ALL: 30.78 ± 3.84 ms; PD: 31.44 ± 4.34 ms; p = 0.6010.

3.10 L6-Ntsr1 activation abolished directional information in L4 and L5 excitatory cells.

Juxtacellular recordings were made from excitatory cells in layers 4 and 5 of barrel cortex while moving the principal whisker in eight different directions with or without photo-activating either L6-Ntsr1 cells conducting to the activation of infragranular FS-GABAergic interneurons either photo-activating non-specific GABAergic cells throughout the cortex (Gad2-cre mouse line; see Figure 3). The whisker-evoked response (spikes / 100 ms) was measured in 49 excitatory cells (Ntsr1: 13 L4 and 12 L5 cells; Gad2: 12 L4 and 12 L5 cells). Both L6-Ntsr1 and Gad2 photo-activation caused a significant reduction of the whisker-evoked responses. It can be noticed that for both mouse lines, photo-activation is causing a stronger decrease in L4 than in L5 for the same light intensity; in line with (Pauzin and Krieger, 2018) for the L6-activation condition data.

We used a low light intensity (0.6 mW), so that the whisker evoked response would only be slightly reduced. With a smaller reduction, plateau effects can be minimized. Spiking from recorded L6-Ntsr1 cells increased from 0.04 ± 0.01 Hz to 7.75 ± 6.6 Hz (n = 3). Based on my previous results (Pauzin and Krieger, 2018), this low level of L6 CT activation will reduce spontaneous spiking in excitatory cells by 30% (Figure S2).

To investigate the effect on directional selectivity when either driving a GABAergic circuit via L6-Ntsr1 activation or via direct activation of GABAergic cells (Gad2-cre mice), the optogenetic light activation was calibrated such that the effect on whisker-evoked response was similar between both conditions (Figure 12 A,B; L4: $p = 0.4552$, unpaired t-test; L5: $p = 0.6829$, unpaired t-test). This means that the average decreasing effect in all directions are similar between the two mouse lines, it does not mean that the distribution of the effect between directions is similar.

Interestingly, the effect of photo-activating different GABAergic circuits lead to different reduction strength of the evoked response depending on the directional preference of the excitatory cell. L6-Ntsr1 activation (leading to infragranular FS-interneurons activation) causes a loss of directional selectivity. The whisker-evoked response is decreased to achieve the same number of action potential per whisker deflection independently of the directional preference of the cells (repeated measures two-way ANOVA with Sidak's multiple-comparisons test shows no significant difference between the responses of each angle; Figure 12C). This effect leads to a normalization of the responses, abolishing directional preference in the L4 excitatory cells (Direction selectivity index (DSI) for control condition = 9.38 and for L6-act = 0; Figure

12D). A direction selectivity index equal to zero indicate that the data can be represented by a horizontal line in Figure 12 D and thus the cells display no direction preference.

For the non-specific GABAergic activation (Gad2 mice), the whisker-evoked response was decreased on the same way (in percentage) for all directions (interaction $p = 0.3046$; two-way ANOVA with repeated measures on both factors; Figure 12E). This homogeneous effect leads to a decreased but preserved direction selectivity the L4 excitatory cells (Direction selectivity index for control condition = 4.66 and for L6-act = 3.72; Figure 12F). Exactly the same conclusion for L5 excitatory cells (see statistics in Figure 12 G-J legend).

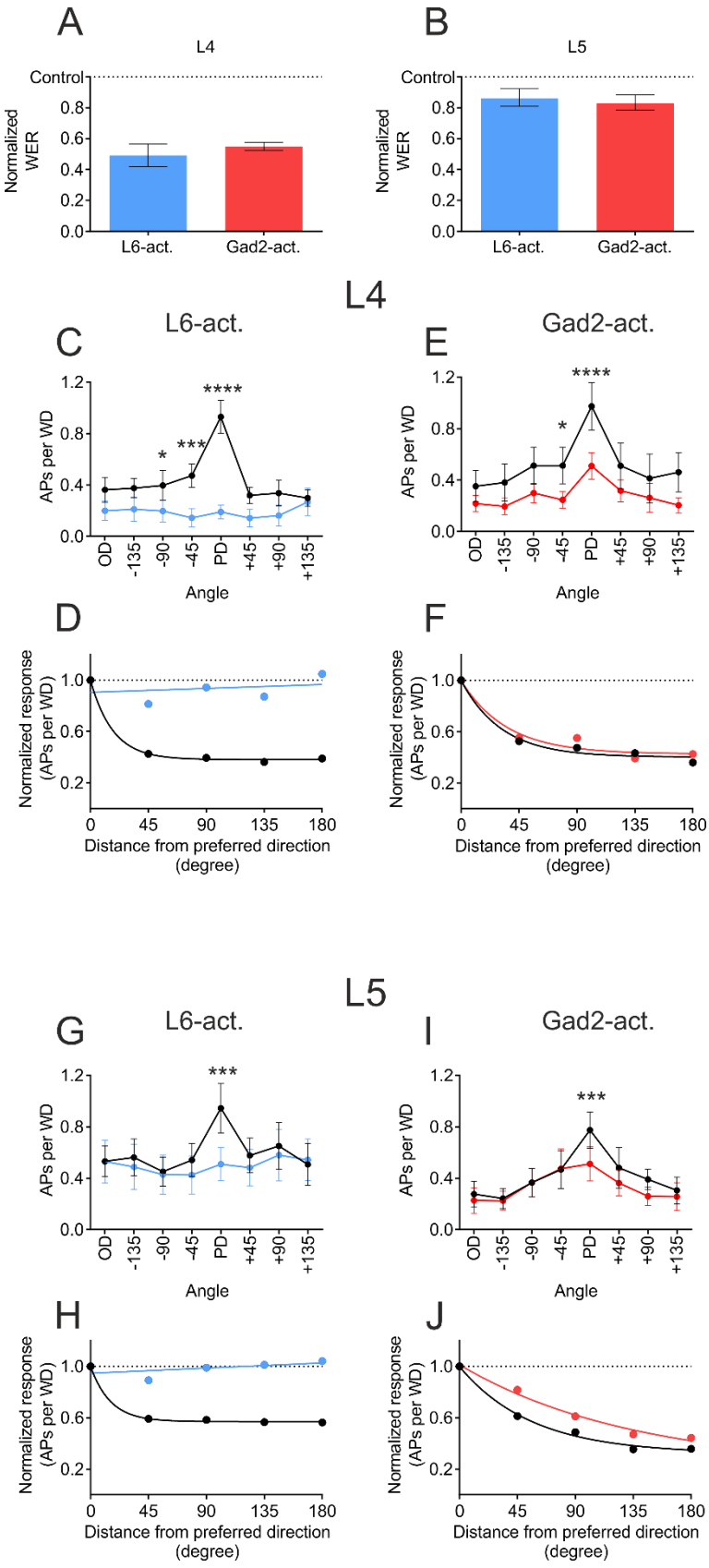

FIGURE 12: NTSR1-ACTIVATION ABOLISHED CORTICAL DIRECTION SELECTIVITY

A. and B. Normalized decrease of the WER with photo-activation for both mouse line (Ntsr1-cre and Gad2-cre). It can be noticed that we have decrease the WER with the same strength for both layers in both mouse line (layer, n, p-value of unpaired t-test: L4: n = 25; p = 0.4556; L5: n = 24; p = 0.6824). Used to prove that the differences find from C to J are not due to a difference in the strength of inhibition caused between the two photo-activation.

C. Averaged WER for layer 4 excitatory cells in Ntsr1 animals for each conditions and each directions. Multiple comparison with Two-way ANOVA show significant difference between control and Ntsr1-activation condition for PD (****), -45 (***) and -90 (*). As a reminder, keep in mind that I used a low light intensity in photo-activation condition in order to not shut completely down the sensory responses. It can be clearly seen that in Ntsr1 condition, the WER is independent of the whisker deflection direction. Interaction between the two conditions: $p < 0.0001$; two-way ANOVA with repeated measures on both factors

D. Normalized evolution of the whisker evoked response with distance (in degree) from the principal direction. Direction selectivity index (see material and methods) for control condition is 9.38 and for L6-activation condition = 0.

E. Averaged WER for layer 4 excitatory cells in Gad2 animals for each conditions and each directions. Multiple comparison with Two-way ANOVA show significant difference between control and Ntsr1-activation condition for PD (****) and -45 (*). Interaction between the two conditions: $p = 0.3046$; two-way ANOVA with repeated measures on both factors. Meaning that the two lines are parallel.

F. Normalized evolution of the whisker evoked response with distance (in degree) from the principal direction. Direction selectivity index (see material and methods) for control condition is 4.66 and for Gad-activation condition = 3.72.

G. Averaged WER for layer 5 excitatory cells in Ntsr1 animals for each conditions and each directions. Multiple comparison with Two-way ANOVA show significant difference between control and Ntsr1-activation condition for PD (***). It can be clearly seen that in Ntsr1 condition, the WER is independent of the whisker deflection direction. Interaction between the two conditions: $p = 0.0497$; two-way ANOVA with repeated measures on both factors

H. Normalized evolution of the whisker evoked response with distance (in degree) from the principal direction. Direction selectivity index (see material and methods) for control condition is 4.91 and for L6-activation = 0.

I. Averaged WER for layer 4 excitatory cells in Gad2 animals for each conditions and each directions. Multiple comparison with Two-way ANOVA show significant difference between control and Ntsr1-activation condition for PD (***). Interaction between the two conditions: $p = 0.0298$; two-way ANOVA with repeated measures on both factors.

J. Normalized evolution of the whisker evoked response with distance (in degree) from the principal direction. Direction selectivity index (see material and methods) for control condition is 3.31 and for Gad-activation condition = 1.04.

For all above: L4: Ntsr1: n = 13; Gad2: n = 12

L5: Ntsr1: n = 12; Gad2: n = 12

*$p < 0.05$, **$p < 0.01$, ***$p < 0.001$, **** $p < 0.0001$

3.11 Standardization of the responses in Ntsr1-photoactivation comes from a standardization of the detectability.

To investigate how Ntsr1-activation is able to abolish orientation tuning in L4 and L5 excitatory cells while Gad2-activation do not, I did complementary analysis on the characteristic of the responses. Indeed, burstiness (number of bursty events in 100 WD, n.s. so not shown), response probability (number of true event detected in 100 WD, Figure 13) and spikes per successful response (averaged number of emitted spike for each detected WD, n.s. so not shown). The largest difference in terms of average spikes triggered per whisker deflection is between the principal direction and its opposite direction; I decided to focus analysis on these two directions. In layer 4, in control condition, in both mouse line, detection of an incoming information is better if the whisker is deflected in the preferred direction of the cell than if it is deflected in the opposite direction (Figure 13A-B). This disparity in detection is decreased but conserved while a non-specific GABAergic activation is applied to barrel cortex (Figure 13B). This mean that the cell ability to detect an incoming information is still dependent on the orientation tuning of the input. (Response probability (RP) in control condition: PD: 64 ± 7.7 %; OD: 24 ± 6.4 %; Sidak´s multiple comparison: $p < 0.001$) (RP in Gad-activation condition: PD: 42 ± 6.6 %; OD: 20 ± 6.2 %; Sidak´s multiple comparison: $p < 0.05$). Conversely, the disparity in detection between PD and OD responses is abolished during Ntsr1-activation. This mean that the whisker-evoked response (average number of spikes per WD) and the detectability (number of true event detected (in %)) are not anymore influenced by the orientation tuning of the input. All responses become equal; it is a standardization of the responses (RP in control condition: PD: 55 ± 6.0 %; OD: 34 ± 6.9 %; Sidak´s multiple comparison: $p < 0.01$) (RP in Ntsr1-activation condition: PD: 25 ± 7.0 %; OD: 21 ± 7.7 %; Sidak´s multiple comparison: p = n.s.). The exact same conclusion is applied for the excitatory layer 5 cells (Figure 13C-D). (Gad mouse line: RP in control condition: PD: 49 ± 7.8 %; OD: 23 ± 7.2 %; Sidak´s multiple comparison: $p < 0.0001$) (RP in Gad-activation condition: PD: 39 ± 8.4 %; OD: 18 ± 8.2 %; Sidak´s multiple comparison: $p < 0.001$) (Ntsr1 mouse line: RP in control condition: PD: 52 ± 6.2 %; OD: 36 ± 6.5 %; Sidak´s multiple comparison: $p < 0.05$) (RP in Ntsr1-activation condition: PD: 37 ± 8.9 %; OD: 30 ± 8.6 %; Sidak´s multiple comparison: p = n.s.).

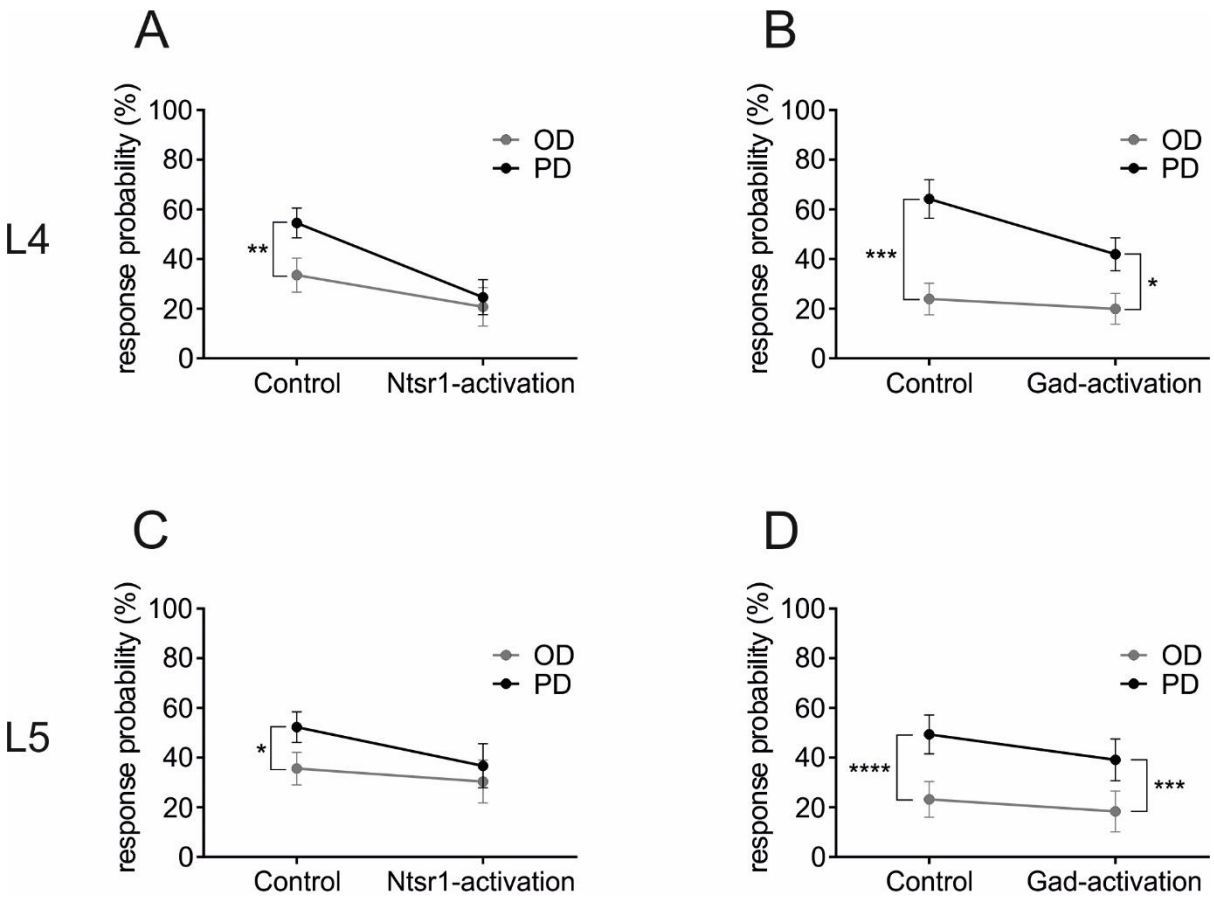

FIGURE 13: NTSR1-ACTIVATION STANDARDIZED DETECTABILITY OF INPUTS OF DIFFERENT DIRECTION

A. Response probability (see material and methods) in control and Ntsr1-activation conditions for the preferred (PD) and the opposite to preferred (OD) direction for n = 13 excitatory cells in layer 4. Repeated measure two-way ANOVA (Sidak´s multiple comparison test) found significance between PD and OD in control condition but this difference in detectability of the incoming information is lost with Ntsr1-activation.
B. Response probability in control and Gad-activation conditions for the preferred (PD) and the opposite to preferred (OD) direction for n = 12 excitatory cells in layer 4. Repeated measure two-way ANOVA (Sidak´s multiple comparison test) found significance between PD and OD in both conditions.
C. Response probability in control and Ntsr1-activation conditions for the preferred (PD) and the opposite to preferred (OD) direction for n = 12 excitatory cells in layer 5. Repeated measure two-way ANOVA (Sidak´s multiple comparison test) found significance between PD and OD in control condition but this difference in detectability of the incoming information is lost with Ntsr1-activation.
D. Response probability in control and Gad-activation conditions for the preferred (PD) and the opposite to preferred (OD) direction for n = 12 excitatory cells in layer 5. Repeated measure two-way ANOVA (Sidak´s multiple comparison test) found significance between PD and OD in both conditions.

Statistic can be found in result part 3.11

3.12 L6-Ntsr1 activation do not affect the grand average of the direction selectivity in VPM

Activation of L6-Ntsr1 CT cells changes whisker evoked activity not only in cortex but also in thalamus (Figure 7). To investigate if Ntsr1-activation abolished direction selectivity already in the thalamic VPM nucleus, in a new set of experiments the directional selectivity was determined for VPM cells with and without L6-Ntsr1 activation. The light intensity of the optogenetic LED, and the whisker deflection protocol was the same as for the cortical recordings. The whisker-evoked response (quantified as spikes / 50 ms) was measured in 8 VPM cells. The effect of L6-Ntsr1 photo-activation varied with an increased PD whisker-evoked response in some cells (n = 1), a decrease in others (n = 2), no significant change in (n = 5; calculated for the response in Hz with chi-square test for a Poisson distribution). Averaging over all eight cells, L6-activation did not change the PD response or the direction selectivity curve (interaction p = 0.9924; two-way ANOVA; Figure 14A).

The direction selectivity index is the same for both conditions because one curve fits for both data using the extra sum-of-squares F test (Keithley et al., 2009) as implemented in GraphPad Prism (GraphPad Software, CA, USA); p = 0.4924). Direction selectivity index for both condition = 3.08 (Figure 14B). Furthermore, the latency of the first spike seems to not be affected by the direction in which the principal whisker has been deflected (Figure 14C).

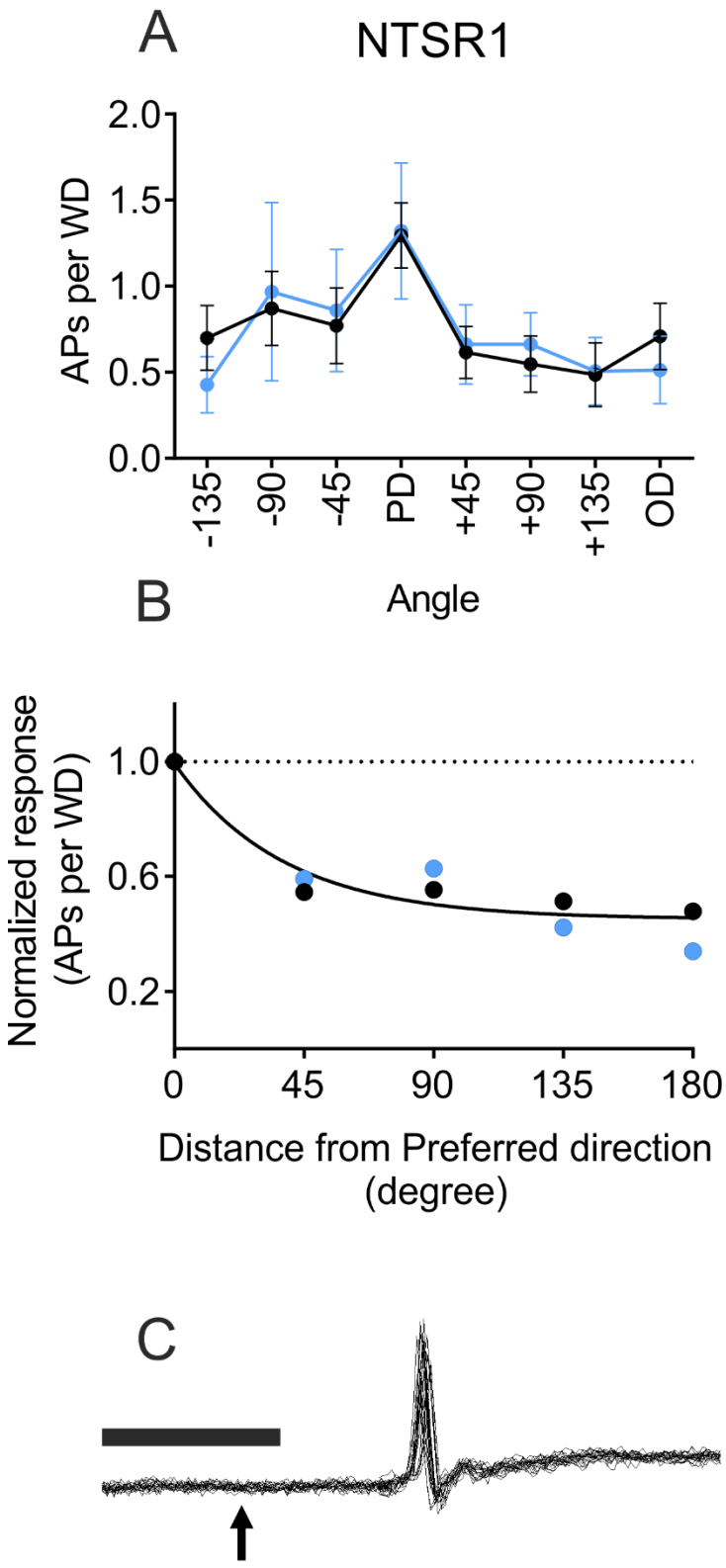

FIGURE 14: NTSR1-ACTIVATION DOES NOT AFFECT VPM DIRECTIONAL SELECTIVITY

A. Averaged WER for VPM cells in Ntsr1 animals for each conditions and each directions. Multiple comparison with Two-way ANOVA show no significant difference between control and Ntsr1-activation condition for all angles. Furthermore, there is no significant interaction between the two conditions, $p = 0.9924$. Here the balance of excitation/inhibition due to projection to nRT and VPM appear to be different than in Figure 4L, M and Figure 7.
B. Evolution of the WER with the distance from PD (in degree). WER of PD is normalized to 1. We can see that WER decreased similarly with distance from PD in both conditions. Direction selectivity index for both conditions = 3.08
C. Raw trace of a VPM recording. The arrow indicates the whisker deflection (5 times in four different directions so 20sweeps in total). It can be clearly seen that the latency of the first spike is not affected by the direction. Here response probability is 100%, so each whisker deflection in every direction produced a first spike of same latency.

Scale bar in C is 5ms.

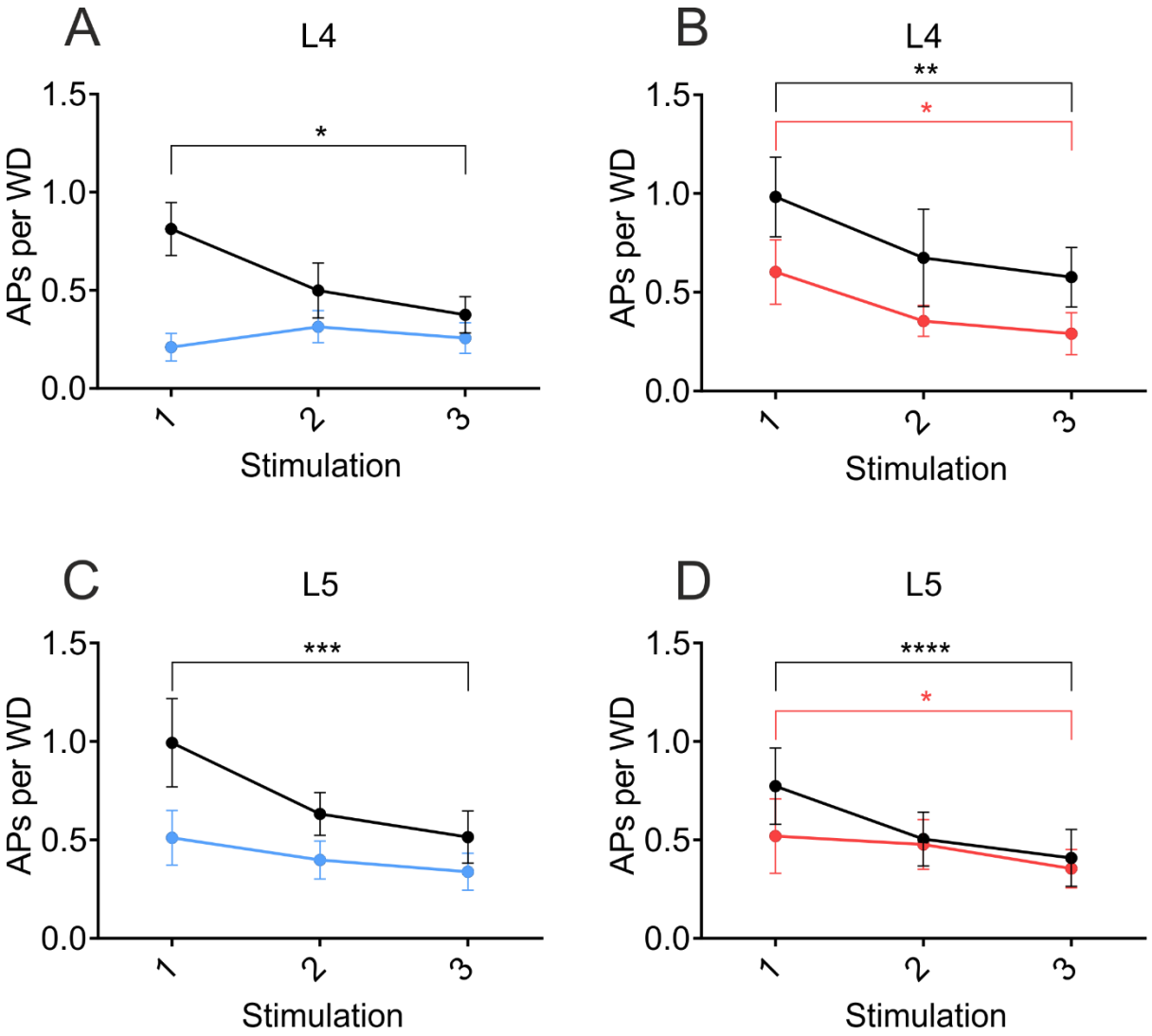

FIGURE 15: NTSR1-ACTIVATION ABOLISHED ADAPTATION WHILE AN UNSPECIFIC INCREASE OF INHIBITION DO NOT

Whisker stimulation at 4 Hz (4 deflections at 4 Hz) executed on the preferred direction of the cell. Only the three first stimulation are displayed. Y-axis shows the average number of spikes evoked by each whisker deflection.

A. (n = 10; (3 cells displaying facilitation were removed)). Two way ANOVA repeated measure with Sidak's multiple comparisons test showed adaptation in control (comparing 1st stim to stim 3): p = *; but not in L6 activation condition: p = ns.
B. (n = 11; (1 cell displaying facilitation was removed). Two way ANOVA repeated measure with Sidak's multiple comparisons test showed adaptation in control (comparing 1st stim to stim 3): p = **; and in Gad-activation condition: p = *.
C. (n = 10; (2 cells displaying facilitation were removed)). Two way ANOVA repeated measure with Sidak's multiple comparisons test showed adaptation in control (comparing 1st stim to stim 3): p = ***; but not in L6 activation condition: p = ns.
D. (n = 8; (4 cells displaying facilitation were removed)). Two way ANOVA repeated measure with Sidak's multiple comparisons test showed adaptation in control (comparing 1st stim to stim 3): p = ****; and in Gad-activation condition: p = *.

P-value: p > 0.05 = ns; p < 0.05 = *; p < 0.01 = **; p < 0.001 = ***; p < 0.0001 = ****

Data are represented as mean ± SEM in all panels.

3.13 Adaptation and directional selectivity

The contribution of L6 CT cells to sensory processing can vary depending on the sensory input characteristics (Temereanca and Simons, 2004, Li and Ebner, 2007, Mease et al., 2014, Crandall et al., 2015, Denman and Contreras, 2015, Guo et al., 2017, Pauzin and Krieger, 2018). An object detection task, for example, requires fewer touches, whereas a more complex task where object characteristics is analyzed would require more touches. To analyze how L6 CT modulates directional selectivity during, not only during a "detection" task mimicked with the low frequency stimulation reported above, the whiskers were stimulated with a train of 4 Hz whisker deflections, to mimic a more complex tactile processing task. Since my previous work (Pauzin and Krieger, 2018) claimed that the role of Ntsr1 cells appeared to be beneficial while the animal is whisking with high frequency, I decided to explore how adaptation evolved with following trains of whisker deflections with the activation of the two different GABAergic circuits.

In Figure 15, the averaged whisker-evoked responses for the three first stimulation of the 4Hz train of whisker deflections are plotted. I decided to not show the fourth one, since the rebound effect (see Figure 4) interfered with the calculation of the whisker-evoked response, increasing it abnormally. Furthermore, here are plotted only cells displaying adaptation in control, cells displaying facilitation in control were removed (a cell was considered as facilitatory if the response of the third stimulation of the train divided by the first one was superior at 1).

In L4 and L5, responses in control displayed adaptation, meaning that the cortical response to stimulation 1 is significantly stronger than the response to stimulation 3. This adaptation process is preserved in both layers with the unspecific GABAergic activation but is loss with the L6-activation. This phenomenon is an additional proof that the specific indirect activation of GABAergic interneurons by L6-Ntsr1 cells switches the cortex to an adapted mode. This switch is operated before the first input reaches cortex and additional whisker deflections failed to reduce the response even more.

4 Discussion

4.1 Summary

Activity in the somatosensory cortex and sub-cortical areas involved in tactile processing is dynamically regulated depending on behavioral context (Simons and Carvell, 1989, Nicolelis and Fanselow, 2002, Wilent and Contreras, 2005b, Fraser et al., 2006, Lee et al., 2008, Hirata et al., 2009, Musall et al., 2014, Whitmire et al., 2016). The cortical L6 cells could play an important role in this process because they can regulate both cortical and thalamic activity (Wörgötter et al., 2002, Thomson, 2010, Sherman, 2016).

In this thesis, I showed that activation of a genetically defined population of L6 corticothalamic cells decreases both cortical spontaneous spiking and whisker evoked responses, but the net effect is actually an increased evoked-to-spontaneous spiking ratio. Presumably leading to an improved tactile encoding depending on behavioral situation (Figure 16).

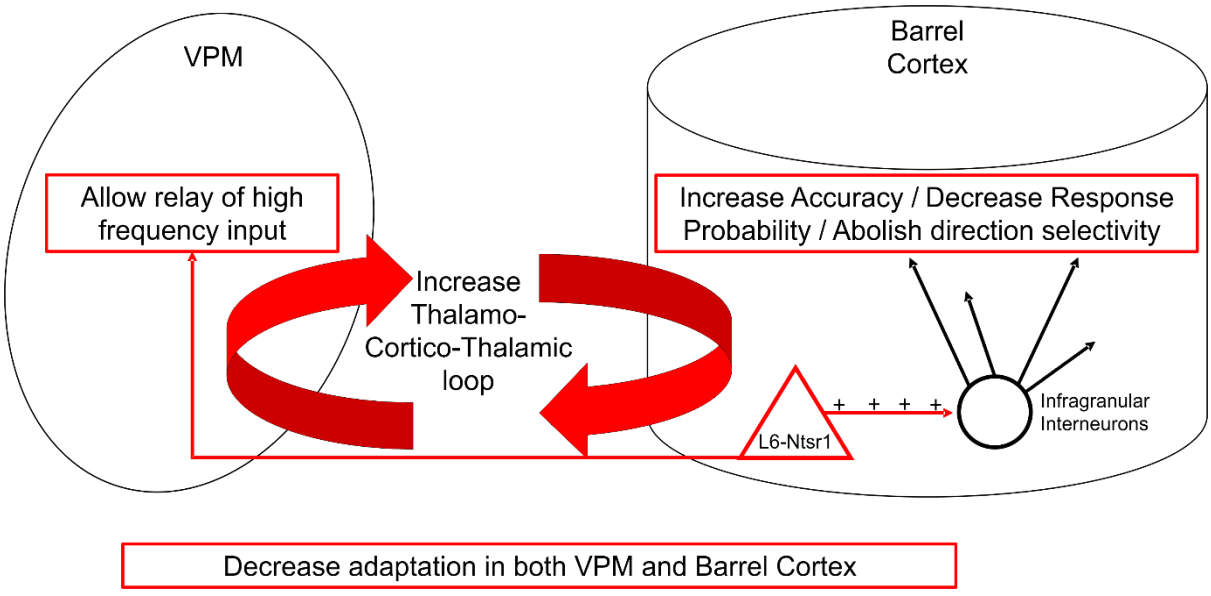

FIGURE 16: OVERVIEW

Furthermore, dual recordings from an aligned VPM barreloid and cortical barrel showed that the network effect of L6 activation is multi-faceted. For a given activation level of L6, the change in the VPM and the change in cortical L5 output activity are not strongly correlated. My interpretation of these data is that L6 activation can modulate the activity in the cortex and thalamus independently. In the present experimental paradigm, L6 activation appears to mostly excite the VPM, presumably because of the fast depression of the nRT mediated inhibition of the VPM (Mease et al., 2014, Crandall et al., 2015). The cortical effects of L6 activation are mediated mostly via infragranular GABAergic cells, putatively fast spiking GABAergic interneurons. This effect on low-frequency whisker deflections is combined with a reduced adaptation to repetitive whisker deflections in all layers of the barrel cortex, as well as in somatosensory thalamus (Mease et al., 2014). The reduced adaptation in VPM thalamus leads to an improved relay of high frequency input to cortex (Figure S8); cortex being simultaneously hyperpolarized by L6-activation. This thalamic and cortical switch of processing is presumably advantageous in a behavioral context (Musall et al., 2014, Ollerenshaw et al., 2014, Mohar et al., 2015), such as e.g., a discrimination task where the whisking frequency is high. L6 CT activation is thus switching the cortex to an adapted state via the specific activation of infragranular GABAergic interneurons. In this adapted state, cortical excitatory cells are answering to whisker deflection more accurately (less false positive), at the expense of response probability (less true positive) probably compensated by population coding and without directional feature (Figure 16). This adapted state does not appear to be reach with a similar strength of unspecific GABAergic activation.

4.2 Detailed discussion

In the present thesis, I investigated how one of the major cortical output, the L6 CT cells, directly impact cortical and thalamic function in the somatosensory processing. In this last part of the thesis, I will discuss about all results presented here to incorporate them with the most recent literature and explain why I suggest that these L6 CT cells are of great importance while the animal performs a discrimination task.

Layer 6 and recent literature

Each L4 barrel in the mouse appears as an ellipsoid shaped cell-dense ring that surrounds a less cell-dense hollow (Woolsey and Van der Loos, 1970, Welker and Woolsey, 1974). The claim that barrel cortex contains no cytoarchitecture outside of L4 is now obsolete (Feldmeyer et al., 2013). The recent identification of infrabarrels in L6 topographically aligned with L4 barrels (Crandall et al., 2017) are composed mostly of CT cells that span the full thickness of L6a. L6 occupies about one third of the cortical thickness. Deep in L6, close to the white matter, a light plexus of fibers divides L6, the upper part constituting L6a and the lower narrow stratum of cells constituting L6b (Zhang and Deschenes, 1997). L6 inhibitory interneurons appear not to respect infrabarrel boundaries.

L4 is the primary recipient layer of thalamic afferents in the lemniscal pathway, yet collaterals of these same axons also innervate L5 and L6 (Chmielowska et al., 1989, Diamond et al., 1992, Beierlein and Connors, 2002, Diamond et al., 2008, Cruikshank et al., 2010, Wimmer et al., 2010, Oberlaender et al., 2012, Constantinople and Bruno, 2013, Feldmeyer et al., 2013, Yang et al., 2014), suggesting a role for infragranular layers in early thalamocortical processing. Constantinople and Bruno, 2013 demonstrated that somatosensory responses in L5 and L6 of the rat barrel cortex might not require L4, implying that thalamus activates directly supra- and infra-granular layers in parallel. L6a receives direct excitatory input from VPM, with CC cells responding more strongly than CT cells (Crandall et al., 2017). Two additional pathways (paralemniscal and extralemniscal) also process information to thalamus and project to S1 (Killackey and Sherman, 2003). Unlike the lemniscal pathway, these pathways are thought to convey different information and project to septa in S1 (Pierret et al., 2000, Yu et al., 2006, Bokor et al., 2008, Furuta et al., 2009). Excitatory afferents from POm to L6a were even more selective to L6 CC than those from VPM (Zhang and Deschenes, 1997). L6 cells are therefore, in a unique position to integrate information from at least two parallel thalamocortical

pathways. It would be interesting to know whether the differences in CT and CC responses reflect properties of different afferent pathways, a convergence of inputs from within or across pathways, or synapse distributions along each neuron's somatodendritic axis; however, my approach cannot distinguish the relative contributions of these pathways to the responses of L6 CT cells. L6 CT fibers produce distinct synapses in VPM and POm nuclei. Upper L6 CT cells of barrel cortex leave a fiber collateral in the inhibitory part of the sensory thalamus, the nRT and also project mostly to VPM barreloid. In contrast, lower L6 CT cells innervate large sectors of POm and intralaminar thalamic nuclei (Deschenes et al., 1998, Hoerder-Suabedissen et al., 2018). This highlights a thalamo-infracorticothalamic loop, probably implicated in the refinement of sensory information in the thalamus and cortex, with nRT inputs modulating this loop.

To study how cortical activity can interact with these different sub-cortical pathways we used the GN220 Ntsr1-Cre mouse line where a sub-population of L6 CT cells are labelled (Olsen et al., 2012, Bortone et al., 2014, Kim et al., 2014, Mease et al., 2014, Crandall et al., 2015, Pauzin and Krieger, 2018). The organization of these cells is what constitutes the L6 infrabarrels describe in "Crandall et al., 2017". Optogenetic modulation of these L6 CT cells have been studied in cortex *in vitro* in the somatosensory system (Kim et al., 2014); *in vivo* in the visual (Olsen et al., 2012, Denman and Contreras, 2015) and auditory system (Guo et al., 2017), and in somatosensory thalamus (Mease et al., 2014). In all these sensory systems, the labelled cells are identified as glutamatergic pyramidal neurons. These previous studies of the L6 CT modulation of activity via optogenetic tools, do not create an entirely cohesive picture of their network functions. Furthermore, how somatosensory responses in cortex are affected by L6 activity has remained largely unexplored *in vivo* in the somatosensory barrel cortex. Furthermore, the fact that the role of L6 CT cells appear to have a diverse function in different sensory systems was the reason why we decided to focus mainly on the cortical role of L6 with regard to sensorimotor integration in the *in vivo* model of the mouse.

Effects of urethane anesthesia

In the experiments presented throughout this thesis, I used the urethane-anesthetized mouse to study the role of corticothalamic feedback in sensorimotor integration. Urethane is a widely used anesthetic for animal studies because of its minimal effects on cardiovascular, respiratory systems and maintenance of spinal reflexes (Maggi and Meli, 1986, Albrecht and Davidowa, 1989, Dringenberg and Vanderwolf, 1995).

While general anesthetics alter synaptic mechanisms (Nicoll et al., 1975, Franks and Lieb, 1994, Nishikawa and MacIver, 2000, Pittson et al., 2004); urethane was found to preserve synaptic signal transmission (Bindman et al., 1988, Sceniak and Maciver, 2006). So the thalamo-cortico-thalamic loop described in this thesis is not impaired in terms of synaptic transmission. The sensory response strength of cortical and thalamic cells systematically varies, however, with the depth of anesthesia (Armstrong-James and George, 1988, Armstrong-James and Callahan, 1991), thus the rate of respiration and the reflex status were monitored in all experiments in order to keep a stable and a similar depth of anesthesia between animals.

It was also shown that urethane non-selectively affected excitatory and inhibitory currents (Hara and Harris, 2002, Koblin, 2002), and since I showed here that L6 CT activation will increase inhibition, it is important that the anesthetic itself does not alter the excitation/inhibition balance.

Urethane has been reported to produce some depressive effects on neuronal excitability (Mercer et al., 1978, Scholfield, 1980, Dyer and Rigdon, 1987, Albrecht and Davidowa, 1989). In the result part of this thesis, I showed that optogenetic inactivation of L6-Ntsr1 cells had minor effects on somatosensory processing in both thalamus and cortex. Since the spontaneous firing rate of L6-Ntsr1 cells was rather low (on average 0.07 Hz, n=14 cells); the slight effect of their inactivation is not surprising. Studying the inactivation of L6 CT cells in awake animals could thus be more relevant.

The main role of the thalamus is to sift in relevant sensory inputs to the neocortex, this transfer of information is dependent on the behavioral state of the animal. PrV neurons are able to follow high-frequency sensory inputs during urethane anesthesia, whereas VPM neurons cannot (Ahissar et al., 2000). Similarly, the low-pass filtering of sensory inputs in the VPM during urethane anesthesia has been shown to be affected (Castro-Alamancos, 2002a) so that whisker stimulation above 2 Hz display a strong depression of the responses in time. Furthermore, the receptive field (number of whiskers evoking a response) of a VPM cells appear to be enlarged during urethane anesthesia (Simons and Carvell, 1989, Armstrong-James

and Callahan, 1991, Diamond et al., 1992, Minnery and Simons, 2003, Aguilar and Castro-Alamancos, 2005), due to feedback inhibition from the reticular nucleus (nRT) and the level of depolarization of VPM neurons themselves. These two factors have been shown to be instrumental in affecting the temporal response properties of VPM cells during activated states (Castro-Alamancos, 2002b, Minnery and Simons, 2003). L6 CT effects on somatosensory thalamus were concentrated to the VPM nucleus, where the transitions between firing modes are dynamic and extremely fast in the anesthetized thalamus, similar to that found in thalamus in awake animals (Guido et al., 1992, Bezdudnaya et al., 2006, Mease et al., 2014); thus, the principal actions of L6 on thalamic and cortical input/output properties, which are described here, likely also will apply in awake conditions, but in a more refined and spatio-temporally precise manner.

Cortical barrel neurons in rodents display single whisker receptive fields under deep barbiturate anesthesia but not during urethane anesthesia (Simons and Woolsey, 1979, Armstrong-James and Fox, 1987). In all experiments presented in this thesis, a hand-held probe was used to stimulate each individual whisker to search for the principal whisker (see material and methods). Since thalamic receptive field are enlarged with urethane anesthesia and cortical neurons displayed multi-whisker receptive field, the choice of the principal whisker has to be determined with certainty. If a clear choice could not be made, the recorded cell was discarded from the analysis.

The optogenetic modulation is always executed acutely in the same animal, leading to a brief neuronal modulation in time. Thus plasticity effects produced by complete and permanent changes in neuronal activity (e.g. using tetanus toxin) are not likely to contribute to the observed results. In summary: With each animal being its own control, the same depth of anesthesia, intact synaptic transmission and a normal excitation/inhibition balance, anesthesia is not expected to create the obtained results.

It is known that L6 cells can project to both VPM and POm (Zhang and Deschenes, 1997), and indeed the L6 Ntsr1 cells also project to POm (Mease et al., 2014, Pauzin and Krieger, 2018). In my thesis I have concentrated on the VPM projection. The paralemniscal pathway is unlikely to contribute strongly to sensory processing since a rapid GABAergic inhibition from zona incerta silences the POm nucleus in the anesthetized mouse (Trageser and Keller, 2004, Lavallee et al., 2005). I acknowledge that I am aware of the Ntsr1 cells projection to POm (Chevee et al., 2018), it would be interesting to investigate the effect of these L6 CT cells on the paralemniscal pathway. I would recommend to record the neuronal activity on awake animals.

L6-Ntsr1 affects spontaneous activity in cortex and thalamus

In this thesis, I showed that photoactivation of L6-Ntsr1 cells caused a general decrease in spontaneous spiking in cortex. Averaged over the entire recorded cortical cell sample (n = 124; Table 1) photo-activation lead to reduced spontaneous activity for around 57% of the excitatory cells and an increased spontaneous activity in only 9%. In L4 relatively few cells decreased spontaneous spiking, and in contrast to the other layers there was no cell where whisker-evoked response probability decreased to zero. This is presumably due to the fact the L4 receives a large part of the thalamic inputs, and since L6-Ntsr1 activation can also increase VPM activity (Figure 4L), this counterbalances the cortical inhibition.

Interestingly, following L6-Ntsr1 activation, around 50% of the cortical excitatory cells showed an increased spiking occurring 200 – 500 ms after the offset of the light pulse. Furthermore, some interneurons also displayed this "rebound effect" (Figure 4H), suggesting that they were also inhibited by infragranular interneurons.

The cause of the predominately reduced spontaneous activity is the activation of mostly infragranular GABAergic interneurons by L6-Ntsr1 cells (Figure 4I) that appear to inhibit excitatory cells in all layers. The activation of these interneurons occurred with a short and consistent latency, as expected of a direct activation by L6-Ntsr1 cells. Furthermore, the fast activation of these putative GABAergic cells (0.02 ± 0.02 Hz to 61.11 ± 13.3 Hz) triggering action potential with highly symmetrical shape with really short time from peak to trough (~ 0.3ms), is characteristic of fast spiking GABAergic interneurons (Petilla Interneuron Nomenclature et al., 2008, Cardin et al., 2009). The fact that L6-Ntsr1 cells can activate, fast-spiking GABAergic interneurons has been shown *in vivo* in visual cortex and in brain slices from somatosensory cortex (Bortone et al., 2014, Kim et al., 2014). L6-Ntsr1 cells can thus affect cortical excitability. Furthermore, it has been claimed that L6-Ntsr1 neurons directly excite neurons in L5a in both V1 and barrel cortex (Kim et al., 2014). I was not able to identify these projections in the experiments presented here. Despite the fact that I found L5 cells increasing their activity with light, I have no indication that it was due to a direct excitation from L6-Ntsr1 cells. Furthermore, excitatory cells increasing their activity with co-activation of L6-Ntsr1 cells were found in all layers of cortex except L2/3.

In line with previous results (Mease et al., 2014), we found that photo-activation of L6-Ntsr1 cells can increase the spontaneous firing rate of VPM cells (Figure 4L,M) with a peak at around 100 ms after the onset of the light pulse. Interestingly, a rebound response occurred also in the

VPM cells and with a shorter latency than in the cortical cells (Figure 4N). L6-Ntsr1 activation both excites VPM directly, and also indirectly – via nRT – inhibits VPM. If a population of VPM cells are inhibited by nRT the release of inhibition could cause a synchronized excitation in VPM causing the rebound excitation. The shorter latency in VPM also suggest that this rebound excitation contributes to the rebound excitation in cortex (Reinhold et al., 2015).

Changes in spontaneous spiking has also been seen in the visual (Olsen et al., 2012) and auditory (Guo et al., 2017) system, but in contrast to what was found in these two systems, photo-inactivation did not have a clear opposite effect to photo-activation in barrel cortex. This can, at least in part, be due to difference in the resting activity of the L6-Ntsr1 cells. L6 CT cells are often reported to have low spontaneous rates and weak sensory responses *in vivo* (Swadlow, 1989, Oberlaender et al., 2012). L6 CT in the mouse are less intrinsically excitable than L6 CC cells due to their higher spike threshold and rheobase (Kumar and Ohana, 2008). Photo-inactivation efficiently shuts down L6-Ntsr1 spiking (Figure 3E), but, presumably due to the relatively low spontaneous activity in the L6-Ntsr1 cells (0.07 ± 0.06 Hz, $n = 14$ including 10 cells where spontaneous spiking was zero), there was not a strong effect on spontaneous spiking activity in cortical L2-6 excitatory cells (no change in 83 % of 99 recorded cells). Spontaneous activity was reduced in only a few L4 cells. L4 being the main thalamo-cortical input layer, the decreased activity, seen in few VPM cells with photo-inactivation (Figure 5E) could lead to the decreased spontaneous activity in L4. Notably, in the around 22 % of the cells where spontaneous spiking actually decreased, no rebound spiking was recorded after the offset of the photo-inactivation. When cells were inactivated by photo-activation of L6-Ntsr1 cells, there was often a rebound excitation presumably due to synchronized activity following the release from inhibition. The lack of a rebound suggests that L6-inactivation decreases spontaneous spiking through a different mechanism, presumably a decrease in direct excitation from VPM thalamus. It would be interesting to investigate the mechanisms underlying a decrease in thalamocortical transmission. Is it a direct decrease of excitation from L6 to VPM thalamus or an indirect decrease via activation of nRT?

Bortone et al., (2014) claimed that L6-Ntsr1 cells in primary visual cortex provide excitation via their cortical projections to most excitatory and inhibitory neurons across all cortical layers. However, due to their particularly strong excitation of fast spiking inhibitory cells, the resulting disynaptic or multisynaptic inhibition overpowers the modest direct excitation mediated by L6 CTs (Bortone et al., 2014). This direct excitation provided by L6-Ntsr1 cells was not identifiable for the majority of cells in my dataset. Paired whole-cell patch-clamp recordings

would be the appropriate technic for further investigation of the intracortical connectivity. Anyway, my data would be consistent with the report that L6 CT cells preferentially innervate cortical inhibitory neurons and that connections between excitatory L6 CT and excitatory L6 CC neurons are relatively sparse and not reciprocal, (Beierlein and Connors, 2002, Mercer et al., 2005, West et al., 2006, Lefort et al., 2009). Identifying molecular markers that would selectively label the L6 fast spiking interneurons activated by L6-Ntsr1 cells will be of great help for future anatomical and functional studies.

The amount of effect exerted by L6-Ntsr1 in S1 and VPM thalamus may have a spatial profile (in the context of somatotopic organization within the lemniscal pathway), reflecting the ratio of direct excitation and di- or multi- synaptic inhibition received by each neuron (Murphy and Sillito, 1987, Bortone et al., 2014). Meaning that the L6 CT activation of a specific cortical column has probably different effects on its own cortical column than on the neighboring ones (not investigated in this thesis). In my experiment paradigm, ChR injection infected around 6 cortical column per animal, so the synchronous photoactivation of the L6 CT of six barrel column was studied rather than an undoubtedly more fine regulation in behaving animals. Furthermore, because of the multisynaptic nature of inhibition, the onset of L6 CT activity may transiently excite the target neurons before the onset of inhibition. By contrast, the net effect of activating L6 CT neurons in the primary auditory cortex is excitatory in all layers (Guo et al., 2017). This sign reversal does not reflect the absence of disynaptic inhibition evoked by L6 CT neurons, because the strong activation of FS interneurons during light stimulation has also been observed in this study. Apparently, in A1, the combined effect of feedforward excitatory inputs from the L6 CTs and disynaptic inhibition from FS interneurons tips toward net excitation across the column. These differences may reflect important differences in the set point of local inhibitory networks between brain areas, as has also been suggested from the opposite effects of locomotion on sensory-evoked responses in A1 and V1 for example (Niell and Stryker, 2010, Fu et al., 2014, Schneider et al., 2014, Zhou et al., 2014, McGinley et al., 2015, Guo et al., 2017).

Whisker-evoked responses in cortex

Concept of detection vs discrimination

The effect of photo-activation on sensory processing was tested with two tactile input frequencies, mimicking different behavioral contexts (Moore, 2004, Ollerenshaw et al., 2014). The low frequency (0.3 Hz) whisker deflections are mimicking a detectability task, where only the object position matters. The uncovering of this object is the important feature while the nature of this object (size, shape, texture, etc.…) can hardly be solved without multiple successive touches. The high frequency (8 Hz) whisker deflections in the anesthetized animal mimics, on the other hand, a discriminability task.

With active exploration of the environment, the somatosensory system is placed into a so called "adapted state", reducing the magnitude of the cortical response, but improving the ability of the system to discern some of the finer features of sensory stimuli (Fanselow and Nicolelis, 1999, Kohn and Whitsel, 2002, Moore, 2004, Maravall et al., 2007). Indeed, detectability of sensory inputs can be sacrificed in favor of improved discriminability and the process of adaptation may regulate this trade-off (Moore et al., 1999, Sherman, 2001, Moore, 2004). Adaptation lead to an overall decrease in time of the responses in regard to persistent stimulation. (Ahissar et al., 2000, Fairhall et al., 2001, Chung et al., 2002, Higley and Contreras, 2006, Maravall et al., 2007, Khatri et al., 2009, Ollerenshaw et al., 2014).

Choosing the two different protocols of whisker deflections is thus important for mimicking two different behavioral situations. In the low frequency paradigm, inputs are arriving when the pathway is in the non-adapted state meaning that the cortical response was recorded in absence of any prior deflection of the vibrissae (Ollerenshaw et al., 2014). In this state, whisker inputs are more likely to generate a large cortical response with the recruitment of a large number of cortical neurons. The functional role of the large unadapted responses that occur at low frequencies during quiescent states has been proposed to serve as a mechanism of heightened sensitivity for detecting stimuli, alerting an "inattentive animal" to the presence of an unexpected stimulus (Fanselow and Nicolelis, 1999, Moore et al., 1999, Sherman, 2001, Chung et al., 2002, Khatri et al., 2009, Diamond and Arabzadeh, 2013, Ollerenshaw et al., 2014). Indeed, detectability (how good inputs can be detected) is significantly improved in the absence of whisking (Ollerenshaw et al., 2012), potentially part of an active strategy by the animal to facilitate information flow in this very specific context.

In the high frequency paradigm, the adaptation caused by passively moving the whisker multiple time (like in my experimental paradigm) is leading to a similar cortical state as when

the animal is freely whisking, thus switching the system from a state in which it is more sensitive, to one in which it is more selective to sensory inputs (Moore et al., 1999, Castro-Alamancos, 2004, Moore, 2004, Leiser and Moxon, 2007, Poulet et al., 2012, Ollerenshaw et al., 2014). Even in humans, sensory adaptation can lead to improved discriminability of tactile stimuli (Vierck and Jones, 1970, Goble and Hollins, 1993, Tannan et al., 2006). Interestingly, in the barrel cortex of rodents, receptive fields of cortical neurons are restrained during adapted states as compared to non-adapted states, posited as a potential mechanism for enhanced spatial acuity (Vierck and Jones, 1970, Simons and Carvell, 1989, Lee and Whitsel, 1992, Sheth et al., 1998, Moore et al., 1999, Castro-Alamancos and Oldford, 2002, Tommerdahl et al., 2002, Wörgötter et al., 2002, Simons et al., 2005). Sensory adaptation caused by repetitive sensory stimulation has been proposed as a way to focus sensory representations in neocortex (Sheth et al., 1998, Moore et al., 1999, Kohn and Whitsel, 2002). Changes in the thalamocortical path may also play a role in this process (Castro-Alamancos and Oldford, 2002). How adaptation may modulate the relationship between object contact detection versus discrimination of object surfaces is unknown. Across sensory modalities and across features within a sensory modality, the adaptive changes could act to improve the ability of the system to discriminate between stimuli, consistent with the theoretical notion that adaptation acts to enhance information transmission in sensory pathways (Moore et al., 1999, Moore, 2004, Ollerenshaw et al., 2014). Increasing or decreasing the degree of sensory adaptation shifts the system from transmitting information about one aspect of the environment to another, potentially a hallmark of sensory processing in the natural sensory world (Lesica and Stanley, 2004).

Detection mimicking task

By deflecting the principal whisker once every three seconds, I found that L6-Ntsr1 cells decreased the whisker evoked response in all layer except in L5. Decreasing spontaneous more strongly, L6 activation is actually leading to an increased sensory responsiveness by increasing the evoked-to-spontaneous spiking ratio. The reduced activity is mediated via L6 CT activation of infragranular inhibitory interneurons, putatively fast spiking interneurons. With the implicit assumption that ongoing spontaneous activity represents the “noisy” background against which a tactile stimulation can be detected, an increased evoked-to-spontaneous ratio would mean improved detection accuracy (accuracy = true positive / all positive). A decreased response probability in combination with an increased evoked-to-spontaneous ratio reduces the false positives (low alpha level), at the expense of power (reduced response probability). In other

words, the appearance of a spike in a cortical cell during the L6-Ntsr1 activation condition increases the probability that this spike is coding for tactile information. In essence we get "un neurone vérité" – a truthful neuron. This response gain modulation via regulation of inhibition is a fundamental cortical operation, crucially involved in sensory representation and sensorimotor integration (Garabedian et al., 2003, Moore, 2004). It may underlie the effects of attention on cortical responses to tactile stimuli. VPM inputs to the cortex can directly activate L6 (Constantinople and Bruno, 2013) thus tactile activity itself is directly influencing the L6-mediated gating.

The reduction of the whisker-evoked response in a layer specific manner, was mostly due to a decrease in the response probability (Figure 6C). Furthermore, L6 displayed the strongest reduction of sensory responses, this was due to a loss of detectability plus a reduction in the number of spikes triggered per successful detected input (Figure 6D). Burstiness of the response as well as average latency of the sensory responses were not affected (data not shown). The fine balance of excitatory and inhibitory cortical networks is essential for gating incoming TC input (Higley and Contreras, 2006, Sun et al., 2006, Miceli et al., 2017), it is thus surprising that L4 excitatory cells latency was not affected in L6 CT activation condition.

The L6 photo-activation started 100 ms before the whisker deflection to achieve a "steady-state" condition, meaning that the L6-Ntsr1 spiking stays at a constant rate (Figure S4), where both cortex and thalamus has been affected by the optogenetic modulation before that the input reached it. From experiments were the onset time was varied (Figure S6) it is, however, clear that activation of L6-Ntsr1 cells can induce its effect even when activated simultaneously with the whisker deflection. This shows that L6 activity can regulate the whisker evoked response over a large temporal range, and with a fast onset. The L6 modulation is thus rapid enough to be able to modulate whisker evoked activity on a cycle-by-cycle basis.

The effect on the whisker-evoked response was the most heterogeneous in L5 excitatory cells (Figure 6A) – both increase and decrease - likely due to L6 projections directly to L5a (Kim et al., 2014) thus, on the one hand, exciting them via this direct connection, and on the other hand decreasing activity via di/poly-synaptic inhibition. Notice here that the recorded cells in L5 were not divided into L5a and L5b; considered nowadays as two genuine layers (Schubert et al., 2006). It would be interesting to know more precisely how L6 CT modulate these two layer 5. My data cannot distinguish L5a and L5b well enough to investigate this further.

To analyses to what extent the L6 induced effect on thalamus predicts what the net effect on cortical output will be, dual recordings were made from the VPM thalamus and the cortical

output layer 5 (Figure 7). No clear (linear) correlation was found between the VPM activity and L5 output (Figure 7D). The fine tuning of the relative changes in VPM and cortical activity appears to be regulated by the L6 firing frequency (Crandall et al., 2015) and it remains to be investigated in which behavioral situations L6 activity would influence thalamic and cortical activity to different degrees. The p-value of the linear correlation was close to reach significance ($p = 0.0784$), indicating a negative correlation between the thalamic and cortical effects. It could be interpreted as: the stronger the L6 CT activation, the stronger the thalamic activity is increased due to direct excitation and rapid nRT depression. On the other hand, the stronger the L6 CT activation, the stronger the cortical activity is decreased via projections onto GABAergic cells.

Keeping in mind that L6 CT cells are weakly answering to sensory inputs (Velez-Fort et al., 2014, Crandall et al., 2017), it is perhaps not surprising that L6-Ntsr1 inactivation did not have a clear opposite effect to photo-activation. In L4 spontaneous activity decreased in a few cells (5 of 23 cells; Table 2 and Figure 5). Averaging over the whole L4 cell sample there was, however, no significant effect on the whisker-evoked response (Figure 8). Response probability (Figure 8C) was not affected by L6-Ntsr1 inactivation in neither thalamic nor excitatory cortical cells.

Guo et al., (2017) proposed that L6 CT cells could reset the phase of low-frequency rhythms and thus dynamically regulate the importance of the input. Indeed, stimuli that arrive at expected times are more rapidly and accurately processed than stimuli that occur at unexpected times (Jones et al., 2002, Wright and Fitzgerald, 2004, Nobre et al., 2007, Jaramillo and Zador, 2011, Buran et al., 2014). A time-dependent modulation of neural and perceptual salience may arise from fluctuations in the underlying low-frequency cortical electric field not only because perceptual salience is modulated by oscillation phase, but because phase itself can be actively controlled through attention and expectation (Luo and Poeppel, 2007, Schroeder and Lakatos, 2009). Here I propose, in line with Guo et al., (2017), that L6 CT neurons may be able to resolve the competing demands of detection and discrimination by coordinating their spiking at appropriate moments during the analysis of a sensory scene, probably by a communication between the motor system and the somatosensory system. The anatomical study (Figure 2) is thus reinforcing this idea since the cells responsible of L6 CT activation (pre-synaptic cells) are not exclusively found in BC, but also in motor cortex. If the animal changes its whisking behavior to solve a task, motor cortex modulation of L6 activity in the barrel cortex at the

appropriate time would optimize thalamic and cortical processing toward the resolution of the special demands of the present task (Zhang and Deschenes, 1998, Lee et al., 2008).

Discrimination mimicking task

The understanding of the physiology underlying perception must be based on knowledge of the properties of the neural circuits involved in the brain's sensory systems. As a part of the somatosensory system, the whisker system is critical to many species (mouse, rat, hamster, gerbil, chinchilla, porcupine, etc, (Fox, 2008)) for the ability to obtain information about the surrounding world. Thus, it is a logical inference that the whisking frequency itself is an essential element of barrel cortex information processing. Mice whisk in the frequency range of 5-20 Hz during exploration. Suppression of spontaneous activity after initial whisker movement last around 130 ms. Recovery from this suppression coincide with subsequent excitation by a second deflection at around 8 Hz (Garabedian et al., 2003). At low frequencies, inhibition does not suppress the "noisy" spikes that occur between longer inter-stimulus intervals (>130 ms). At higher frequencies (>10 Hz), interactions between the slow inhibition and thalamocortical depression effectively diminish the response and undermine the consistency of a greater number of spikes from cycle to cycle. These band-pass characteristics of S1 neurons overlap closely with the reported range of whisking sampling frequencies of the vibrissae, suggesting that whisking frequencies reflect the optimal range for sensory information processing in the vibrissa to cortex pathway (Garabedian et al., 2003). Sampling tactile information at 8 Hz could mediate a compromise between having an ample number of spikes per stimulus and collecting information at an optimal rate (Garabedian et al., 2003).
Furthermore, it is known that L6 depolarization controls not only the firing mode but also the adaptation in the VPM (whiskers deflected at 8 Hz in this study) (Mease et al., 2014). To reproduce this scheme (Figure S8), I stimulated the principal whisker repetitively at 8 Hz, a frequency known to evoke adaptation (Ahissar et al., 2000, Castro-Alamancos, 2002a, Mease et al., 2014).

A key function of L6 corticothalamic cells appears to be that they can regulate sensory adaptation in both cortex and thalamus (Maravall et al., 2007). With my results, I would claim that the subpopulation of L6 CT cells targeted in the Ntsr1-cre mouse line is regulating adaptation in both cortex and thalamus simultaneously. I haven't observed a cortical effect without a thalamic one and vice-versa; L6 CT activation switches both areas synchronously. Keep in mind that L6 CT activation can regulate thalamus and cortex independently (when one

goes up the other goes down). The investigation of other population of CT cells that could modulate the activity of thalamus only would be of great interest for future studies.

At the most general level, theoretical considerations suggest that adaptation may be an efficient coding mechanism that maximizes available channel capacity, in the sense that the nervous system normalizes (e.g., reduce) the magnitude of the response to a stimulus as a function of stimulus strength (e.g., increase in stimulus frequency) (Whitmire and Stanley, 2016, Whitmire et al., 2016). These views only indirectly address the following intuitive problem related to touch: given that the magnitude of a single-neuron's response provides a major source of information about the stimulus (e.g. stimulus location or stimulus intensity), adaptation increases the ambiguity of the response, limiting the information conveyed about the most recent stimulus. Therefore, it has been suggested that there is a trade-off between tracking the dynamics of sensory input and optimal coding of current context (Fairhall et al., 2001, Panzeri and Diamond, 2010, Liu et al., 2017, Pitas et al., 2017). L6-Ntsr1 activation decreases adaptation to high frequency (8 Hz) whisker deflections in thalamus (Figure S8 and (Mease et al., 2014)) and abolish it completely in cortex (Figure 9). L6-Ntsr1 activation appear to switch cortex to an adapted mode. In agreement with earlier studies (Simons, 1978, Ahissar and Zacksenhouse, 2001, Castro-Alamancos and Oldford, 2002, Chung et al., 2002, Garabedian et al., 2003), I found that almost all responses of individual neurons adapted to repetitive stimulation and this adaptation was more robust with increasing frequency (unpublished data). The magnitude of adaptation within the VPM is significantly smaller than that observed in the cortex (Diamond et al., 1992, Hartings and Simons, 1998, Sosnik et al., 2001, Chung et al., 2002). Data from whole cell recordings in barrel cortex have demonstrated that repetitive vibrissa stimulation depressed EPSPs evoked at the thalamocortical synapse and that depression at this synapse can account for the consistently observed cortical adaptation in spiking activity (Chung et al., 2002).

My prediction is that stronger L6-Ntsr1 activity – switching cortex to an adapted mode – would be beneficial when the frequency of tactile input is high, such as during texture or vibration discrimination. The higher the input frequency/stimulation strength the more difficult it is for an individual cell to follow each input. During L6-Ntsr1 activation condition, spontaneous activity is considerably reduced, so the probability that a triggered spike is coding for tactile information (and not spontaneous) is increased. This phenomenon is caused by an increased cortical GABAergic activity, in particular the infragranular FS GABAergic cells activated by L6-Ntsr1 cells. This increased inhibition also decreased the cells probability to respond to

inputs; a decreased response probability doesn't mean that the cell never fires with increasing frequency only less frequent, and this decrease in a single cells response probability is compensated by population coding (Abbott and Dayan, 1999, Farkhooi et al., 2013, Liu et al., 2017). Neurons share the work in order to process the signal with higher accuracy (less spontaneous spike) and each input of the high frequency train can be followed by population coding.

Once more, not surprisingly, L6-Ntsr1 inactivation did not display an opposite effect to photo-activation. L6 CT inactivation had no significant effect on the responses of persistent whisker deflections (Figures 9E-G).

Corticothalamic loops

Corticothalamic loops have been hypothesized to help increase the sensitivity of thalamic and cortical responses during brief thalamic bursting modes but not to play this role during tonic thalamic firing (Nicolelis and Fanselow, 2002). This result being in line with a previous study (Mease et al., 2014) who proved that L6 CT activation can switch VPM cell firing mode from burst to tonic.

Urethane anesthesia shift thalamic firing toward burstiness (Steriade et al., 1993, Huh and Cho, 2013). The fact that any change in burstiness was found with L6-activation could imply that, in my experiments, the VPM cells were already quite depolarized, thus being in the tonic response mode (Mease et al., 2014, Urbain et al., 2015), where further L6 CT-driven activation does not change burstiness. In this thesis, thalamic responses displaying bursts where representing 26% of the responses and L6 CT photoactivation did not modify these firing properties. The presented thalamic depolarization could be due to ascending neuromodulatory input and/or descending excitatory input from the cortex, both of which are known to cause thalamocortical cells to change from bursting to tonic mode (Castro-Alamancos, 2002a). Furthermore, low dose of urethane anesthesia (1.5 mg / kg of animal) is often reported as a light anesthesia state (Armstrong-James and Callahan, 1991, Bartho et al., 2007, Fox, 2008) and this could be a reason for the non-pronounce shift to burstiness of the thalamic cells in this set of experiment.

High frequency whisker deflections would sends an ascending excitatory volley to the VPM thalamus (via the trigeminothalamic pathways). The signals are then detected by VPM neurons and transmitted to the S1 cortex, in part as bursts. The following combination of L6 CT activation and the excitatory signal from the periphery also activates the reticular formation of brainstem, which sends cholinergic input to the thalamus. This cholinergic input depolarizes

VPM neurons but inhibits nRT cells, leading to an overall reduction in GABAergic inhibition of VPM (Destexhe et al., 1998, Destexhe, 2000) and the L6 CT activation would decreases the amplitude of the IT-mediated calcium spiking (Mease et al., 2014). The combination of these events (VPM depolarization, reduction in RT-mediated inhibition and reduction of IT-mediated calcium spiking) would allow VPM neurons to remain sufficiently depolarized and hence switch from a bursting to a tonic mode of firing. By remaining in tonic mode, VPM neurons would be able to respond more rapidly and accurately to the multi-whisker stimuli that would likely be experienced as the whiskers move over objects and surfaces during the whisking behavior.

Whisking frequency map in barrel cortex

It has been shown that in the somatotopic frequency map in the somatosensory cortex the part of barrel field, corresponding to the rostral part of the whisker's pad, is more sensitive to the higher frequency while the caudal part more sensitive to the low frequency (Andermann et al., 2004). Furthermore, it has been reported that sensory transduction and neural processing of whisker frequency information parallels the transduction and neural representation of the auditory stimuli in the auditory cortex (Sadovsky and MacLean, 2013, Tsytsarev et al., 2016). However, in contrast to the auditory system, in the whisker system the neurons most sensitive to the particular frequency are not organized into a morphological pool, therefore the frequency-selective functional map can't be observed in the neocortex. Whisker stimuli with different frequencies led to different activation patterns in the barrel field. In the set of experiments presented here, the injection of different opsins was made to target the C2 barrel (see material and methods). So it would mean that the recorded neurons presented here have a slight shift in processing low frequency inputs. It would be interesting to study the impact of L6 CT activation in a more rostral cortical column.

Direction selectivity

At all levels of the sensory processing pathway, single neurons can be found that are tuned to certain features of the sensory input. In the visual system, neurons in mouse primary visual cortex are tuned to different orientations (Hubel and Wiesel, 1962, Niell and Stryker, 2008, Olsen et al., 2012). Response selectivity is organized by the input organization in different subregions of cortex (Schummers et al., 2002, Monier et al., 2003). In primary auditory cortex, excitation and inhibition are seemingly balanced,tuning is largely a product of the tuning of the total synaptic input (Wehr and Zador, 2003).

In the somatosensory system neurons in the trigeminal nucleus, thalamus and cortex of the rodent whisker system are sensitive to the direction of whisker deflection (Simons and Carvell, 1989, Lichtenstein et al., 1990, Minnery and Simons, 2003). The selectivity of the primary afferents is due to the restricted distributions of receptors around the follicle (Zucker and Welker, 1969, Lichtenstein et al., 1990, Shoykhet et al., 2000). The afferents impose their selectivity on the neurons of the PrV, which in turn project to neurons in the VPM thalamus, where a map of direction preference emerges along the length of the barreloids. VPM cells with similar direction selectivity are clustered within barreloids (Temereanca and Simons, 2003, Timofeeva et al., 2003). In the thalamic input layers of barrel cortex, selectivity probably originates from the anatomically precise convergence of tuned thalamic inputs (Wilent and Contreras, 2005b). In L4, there are "minicolumns" in which convergent thalamic inputs share a similar direction preference (Mountcastle, 1957, Hubel and Wiesel, 1974, Hubel and Wiesel, 1977, Favorov and Whitsel, 1988a, Favorov and Whitsel, 1988b, McCasland and Woolsey, 1988, Favorov and Diamond, 1990, Tommerdahl et al., 1993, Kohn et al., 1997, Bruno et al., 2003, Krieger et al., 2007). Direction selectivity may be sharpened by increased inhibition, which modulates the membrane potential (Bruno and Simons, 2002, Wilent and Contreras, 2004, Wilent and Contreras, 2005b). Inhibition sharpens selectivity by limiting the ability of weaker inputs to evoke an action potential (Miller et al., 2001, Pouille and Scanziani, 2001, Monier et al., 2003, Wehr and Zador, 2003, Douglas and Martin, 2004). Spike threshold increases as the direction of deflection diverges from the principal direction (Hodgkin and Huxley, 1952, Noble and Stein, 1966, Traub and Miles, 1991, Fleidervish et al., 1996, Martina and Jonas, 1997). The main thalamic input layer, L4 is also displaying shorter latency of the first spike following a whisker deflection if it was moved in the preferred direction of the recorded cells (Wilent and Contreras, 2004, Wilent and Contreras, 2005b, Wilent and Contreras, 2005a).

In visual system, Olsen et al., 2012 investigated the effect of L6-Ntsr1 photoactivation on orientation tuning in cortex. Remarkably, photo-stimulation of L6 reduced visually evoked responses by a similar fraction irrespective of presented orientation. Photo-stimulation of L6 did not affect preferred orientation, tuning width, or the orientation selectivity index of cortical neurons throughout layers 2/3, 4 and 5 (Olsen et al., 2012). But visual orientation grating and tactile direction selectivity are two different phenomenon, and the genetically defined population L6 CT-Ntsr1 appear to show different effect depending on the sensory system. L6-Ntsr1 cells have both cortical and thalamic projections and I investigated their role in

modulating directional selectivity in VPM thalamus and in barrel cortex. In S1, recordings of single excitatory cells were recorded in both the main input layer, L4 and the main output layer, L5 to have an overview of how the cortical input/output feature selectivity is affected by L6-Ntsr1 activation.

Whiskers were deflected in eight different directions (Figure 10) in three different conditions. The first one, control condition, without any optogenetic modulation. Secondly, with co-photoactivation of L6-Ntsr1, leading to an increased cortical inhibition via infragranular FS interneurons (Pauzin and Krieger, 2018). Lastly, with co-photoactivation of unspecific GABAergic interneurons, leading also to a hyperpolarized cortex (Katzel et al., 2011, Taniguchi et al., 2011, Harris et al., 2014, Martinez et al., 2017) via photoactivation of Gad2 positive cells.. The idea behind the third condition, is to compare the specific cortical inhibition imposed by the L6 CT cells via infragranular GABAergic interneurons with a global hyperpolarization of the neocortex via unspecific GABAergic cells. In this set of experiments, I used a low light intensity in all photo-activation conditions in order to just slightly decrease cortical somatosensory responses.

Effect of different GABAergic circuits on the direction selectivity

In cortex

During a detection mimicking task (whisker deflection at low frequency, in the present experiments every 5 seconds), where the position of an object is the main cue to solve the task, the cells directional selectivity is useful to localize an object. As has been previously shown, I found that excitatory cells in both L4 and L5 displayed direction selectivity (Figure 11 A, B). It appears that L4 is more selective than L5 while comparing the direction selectivity index (DSI); probably due to the fact that L4 is the main recipient of tuned input from VPM thalamus (Wilent and Contreras, 2005b). Furthermore, the median latency of the first spike emitted is shorter in L4 for the preferred direction compared to the others. This known characteristic of cortical cells (Wilent and Contreras, 2005a, Puccini et al., 2006) was not found in my data for L5; suggesting again a sharper tuning of whisker direction in L4 excitatory cells (Figure 11 C, D).

The activation of two different GABAergic populations decreases whisker–evoked responses of these excitatory cells. I could by modulating the light intensity, achieve the same reduction of the average whisker-evoked response (averaged over all directions) in both mouse lines (Gad2 and Ntsr1;) and thus allowing the comparison of the effect of two different GABAergic

circuits on direction selectivity. It can be noticed that three excitatory cells displayed increased activity with co-activation of GABAergic cells in the in Gad2 mouse. The increased activity presumably due to disinhibition.

The first intriguing phenomenon, is the fact that for both mouse lines, photo-activation lead to a stronger reduction of the whisker-evoked responses in L4 compared to L5. In (Pauzin and Krieger, 2018), we showed that Ntsr1-activation on average decreased WER in all layers of barrel cortex except in L5. In Figure 12 G, the effectiveness of the L5 response reduction is dependent on the direction of the whisker deflection; being significant only for the principal direction. This phenomenon could contribute to the non-significant decrease seen in L5 with L6-activation (Pauzin and Krieger, 2018).

The fact that the unspecific GABAergic increase of activity (using Gad2) decreased the whisker evoked responses of L4 excitatory cells more powerfully than for L5 excitatory cells, push me toward the hypothesis that cortical inhibition is more efficient to reduce the cortical input than the cortical output (Figure 12 A and B).

The unspecific GABAergic activation (Channelrhodopsin activation in Gad2-cre mouse line) reduced the whisker-evoked response of all directions with the same strength (in %). Direction selectivity is thus reduced, but conserved (Figure 12 F, J). In contrast, L6-Ntsr1 activation, leading to the specific activation of infragranular GABAergic interneurons (putatively fast spiking), reduced the whisker-evoked response with different strength resulting in an equal response on average for all directions (Figure 12 D, H). This normalization of the responses leads to a loss of the direction selectivity, which thus was not the case for the unspecific GABAergic photoactivation condition (Figure 13).

My explanation for the difference between the two mouse lines is based on the fact that different populations of interneurons were recruited with the optogenetic light stimulation. Indeed, different interneuron population display different strength of direction tuning. In rat barrel cortex for example, L2/3 chandelier cells have broad sensitivity to the direction of the whisker deflection while L1 deep-projecting GABAergic neurons are well tuned (Zhu et al., 2004, Zhu and Zhu, 2004). In the mouse barrel cortex, somatostatin neurons are inhibited during whisker deflections via VIP interneurons while fast spiking and parvalbumin interneurons are activated (Gentet, 2012, Gentet et al., 2012).

In my experimental paradigm, the Gad2 activation lead to an activation of a proportional amount of interneurons displaying or not displaying direction selectivity, responding or not

responding to the whisker deflection and thus the responses of excitatory cells are reduced but keep the same characteristics in average. We are basically increasing the "natural" inhibition. On the other hand, Ntsr1-activation leads to an increase activity of a specific population of fast spiking interneurons, so we are deranging the "natural" inhibition toward a specific inhibition. Indeed, even if CT neurons are known to display direction preferences ((Li and Ebner, 2007, Kwegyir-Afful and Simons, 2009); not investigated in this thesis) it appear that the GABAergic interneurons activated by Ntsr1 are not displaying direction selectivity characteristic (Figure S10; results have to be taken with precaution since only one of these cells have been recorded). So, photo-activation is deregulating the direction selectivity toward an abolishment of it by levelling the responses. Furthermore, these interneurons are displaying a clear facilitation with train of whisker deflections (Figure S10) directing me to claim that Ntsr1 cells are useful while the frequency of inputs is high. To strengthen this idea, (Pauzin and Krieger, 2018) have claimed that L6 modulation is rapid enough to be able to modulate whisker evoked activity on a cycle-by-cycle basis. (Figure S6).

In thalamus

Sensory thalamus serves to gate information flow, switching between dynamics that would facilitate detection of transient inputs at the level of cortex and those that would enable transmission of details of the input required for discrimination (Sherman, 2001, Mease et al., 2014). Direction selectivity displayed by cortical neurons depending on the direction of the whisker deflection is abolished (at least for L4 and L5) with L6-Ntsr1 activation, while it is preserved for VPM sensory cells. This is another example of how L6-Ntsr1 cells can control the thalamic and cortical activity independently. A 2007 study conducted by Li and Ebner showed that electrical stimulation of L6 in the rat somatosensory cortex sharpens the directional selectivity curves of VPM neurons that are tuned to the same direction as the stimulation site in the cortex and rotates the directional preference of VPM neurons initially tuned to a different direction toward the direction that cortical neurons prefer. In my experimental paradigm, the optogenetic activation of L6 CTs is broad and synchronous leading to an increase spiking of cells displaying undoubtedly different direction preferences.

Computational neuroscience methods have been successfully applied for modelling the frequency and directional selectivity in the whisker system by tuning the synaptic amplitude and latency (Puccini et al., 2006). It was shown that directional selectivity is modulated by the frequency of an ongoing stimulus. Directional selectivity is based on the synaptic tuning which is sensitive to the stimulus temporal structure. Directional selectivity may be prominent in

behavior, primarily in the discrimination of the object location, but more likely to be negligible in other behavioral acts such as texture discrimination, which is based on the frequency selectivity. In fact, during a discriminability mimicking task, the object has already been detected and position in space and need to be characterized.

Effect of different GABAergic circuits during a discrimination mimicking task

In Figure 9 of this thesis, I showed that L6 CT activation switches barrel cortex to an adapted state where sensory responses given at 8Hz do not adapt anymore. In this new set of experiment, I deflected the principal whisker at four times at 4Hz and compared the L6 CT activation effect on adaptation against an unspecific increase of inhibition (using Gad2-cre mouse line). I used a 4 Hz stimulation instead of the previous 8 Hz stimulation for two reasons: first to check if the abolishment of adaptation is seen with different input frequencies with co-activation of L6 CT. Secondly, because with lower frequency, the number of action potentials per whisker deflection is increased and by that I augment the power of my analysis (especially that adaptation has to be scrutinized after a reduction of the whisker-evoked responses via GABAergic activation; Figure 15).

Only the three first whisker deflection responses are analyzed due to the L6 CT data. Indeed, the rebound effect seen in Figure 4 appear to be triggered earlier in time with a low light intensity (used in these experiments). I interpret this shorter latency due to the fact that with stronger light intensity, the effect produced (here increase inhibition) lasts longer after the light offset (can be seen in Figure 3D), the release of inhibition with a stronger light intensity appear thus after a longer time than with a low light intensity.

In both L4 and L5, the unspecific GABAergic activation decreases each response of the train but preserve the adaptation. Contrariwise, L6 CT brings all responses to a similar strength, abolishing adaptation, the cortex seems to be already in an adapted state from the first whisker deflection (Figure 15).

It has to be noticed that in order to see a nice adaptation process in control condition and in both layers, I decided to plot the preferred direction. In this direction, the decrease of the WER in L6 CT activation condition is stronger than the decrease caused by Gad2-activation. The different effect concerning adaptation could only come from a difference in the strength of inhibition.

Photo-activation (low light intensity) in both mouse line failed to reduce the response of any whisker deflection of the train in OD direction. Meaning that a response should be strong enough to be affected by these two GABAergic circuits.

How Ntsr1 cells are physiologically activated?

Sensory perception is in general terms thought to rely on three basic pathways of information transfer. In the case of tactile perception in the whisker system, sensory information is transmitted from the whisker pad in a bottom up fashion via thalamus to cortex where it is transmitted via horizontal connections to other cortical areas, and then top-down connections control the earlier processing stages. Intriguingly, the L6 CT cells can regulate both cortical and thalamic excitability. Activation of L6 can switch thalamic cells from burst to tonic response mode to facilitate transmission of high frequency inputs. The question is then: in which behavioral situations are L6 cells modulating activity in cortex and thalamus? A switch to "tonic" response mode where presumably more complex object features can be more faithfully relayed, can be driven either by corticothalamic input (Sherman and Guillery, 1996, Mease et al., 2014) or an increase in the ongoing bottom-up sensory adaptation (Whitmire and Stanley, 2016, Whitmire et al., 2016). Another scenario is that cross-modal activation, presumably relayed via higher-order thalamic nuclei (Rouiller and Welker, 2000), can cause activation of L6. And finally L6 cells could be driven by motor cortex (Zhang and Deschenes, 1998, Lee et al., 2008) during active sensing. If the animal changes to active exploration of an object, which necessitates to discriminate, e.g., different textures, motor cortex input to L6 in somatosensory barrel cortex would make sense in order to optimize thalamic activity via a cortical feedback mechanism. Thus presumably it is a combination of changes in the sensory input and a change in active whisking, and thus increased motor cortex activity, that optimize L6 activity depending on the behavioral task.

Popular science explanation

Imaging sitting on your bed at night with the lights on. Suddenly, blackout! So you decide to leave your room. You are “blinded”, you get up from your bed and you walk slowly in the direction of the door doing high amplitude movements with your arms until you touch the door. After the first touch, your motor strategy will unconsciously change to low frequency movements of your arms to palp the door and find the handle. This switch in motor output, and the probable increase of attention, helps the somatosensory system to identify the fine details of that door, until the handle is found. In this example, you unconscientiously switched feature detection to feature discrimination. To only detect the door, the low frequency with large amplitude movements of your arms appear to be the best strategy; after the localization of the door, a switch in the motor output to high frequency and low amplitude movement is executed to identify the handle.

Open questions

For future experiments, since I hypothesized that L6-Ntsr1 cells are especially useful during high frequency input processing, it is necessary to study L6-Ntsr1 modulation in different behavioral contexts, for example, a head-restricted discriminability task such as pole localization, texture discrimination, frequency discrimination, etc (Helmchen et al., 2018).

Since L6-Ntsr1 activation appear to switch neocortex to an adapted state, where the directional stimulus detection is reduced, I wonder if it is the same for other characteristics of the response like velocity, amplitude, principal whisker versus surrounding whisker deflection responses. The investigation of different cortical responses features with L6-Ntsr1 activation would refine the precise role of these CT cells.

Furthermore, all electrophysiology data presented here are recorded from the anesthetized mouse model. It would be of great importance to study Ntsr1 modulation in the awake model. Especially for the inhibition of L6-Ntsr1 cells since only slight effects have been found here in somatosensory system while awake recordings in other sensory systems showed a reversed effect of Ntsr1 inactivation compared to its activation (Olsen et al., 2012, Guo et al., 2017). Furthermore, POm recordings were not included in this thesis. Recordings of somatosensory POm in awake animal would help in understanding L6-Ntsr1 feedback in its entirety. In addition, since L6-Ntsr1 cells leave a fiber collateral in the nRT, it would be of great importance to dissect how cortex can modulate the inhibition of somatosensory thalamic nuclei via the reticular nucleus.

(Chevee et al., 2018) showed that the L6-Ntsr1 population is composed of at least two sub-populations. One with corticothalamic cells projecting only to the VPM part of sensory thalamus and another one composed of cells projecting to both VPM and POm sensory thalamus. Injection of a floxed retrograde Channelrhodopsin virus in POm would make possible the specific activation of Ntsr1 CT cells projecting to both POm and VPM. This modulation of a more specific L6 CT population would undoubtedly refine and improve our knowledge concerning corticothalamic feedback in tactile processing.

Conclusions

A genetically defined population of L6 corticothalamic cells regulates both cortical and thalamic activity simultaneously. Activation of these L6 corticothalamic cells decreases both cortical spontaneous spiking and whisker evoked responses, but the net effect is actually an increased evoked-to-spontaneous spiking ratio. L6 corticothalamic activation switches cortex to an adapted mode where persistent inputs responses do not adapt anymore; they are already "adapted". Cortical excitatory cells are answering to whisker deflection more accurately (less false positive), at the expense of response probability (less true positive) and without directional feature. This adapted state does not appear to be reach with an unspecific increase of inhibition of similar strength.

Our prediction is, therefore, that stronger L6 corticothalamic activity, leading to a cortical switch toward an adapted state, would be beneficial when the frequency of tactile input is high, such as during texture or vibration discrimination. The higher the input frequency, the more difficult it is for an individual cell to follow each input. Thus, spontaneous activity, representing the background noise is tremendously decrease, this is leading to the fact that the low occurrence of a spike has great probability to be coding for an input. This hyperpolarization effect, removing almost entirely the background noise is influencing the responsiveness of the neocortex to incoming information. Indeed, response probability is decreased for each individual cell. So an individual neuron spikes only when it has to process an input but many input will be undetected. In essence we get "un neurone vérité" – a truthful neuron. Less true positive is compensated by population coding. Neurons share the work to process the signal with higher accuracy.

5 References

ABBOTT, L. F. & DAYAN, P. 1999. The effect of correlated variability on the accuracy of a population code. *Neural Comput,* 11**,** 91-101.

ADINEH, V. R., LIU, B., RAJAN, R., YAN, W. & FU, J. 2015. Multidimensional characterisation of biomechanical structures by combining Atomic Force Microscopy and Focused Ion Beam: A study of the rat whisker. *Acta Biomater,* 21**,** 132-41.

AGUILAR, J. R. & CASTRO-ALAMANCOS, M. A. 2005. Spatiotemporal gating of sensory inputs in thalamus during quiescent and activated states. *J Neurosci,* 25**,** 10990-1002.

AHISSAR, E., SOSNIK, R. & HAIDARLIU, S. 2000. Transformation from temporal to rate coding in a somatosensory thalamocortical pathway. *Nature,* 406**,** 302-6.

AHISSAR, E. & ARIELI, A. 2001. Figuring space by time. *Neuron,* 32**,** 185-201.

AHISSAR, E. & ZACKSENHOUSE, M. 2001. Temporal and spatial coding in the rat vibrissal system. *Prog Brain Res,* 130**,** 75-87.

AHISSAR, E., GOLOMB, D., HAIDARLIU, S., SOSNIK, R. & YU, C. 2008. Latency coding in POm: importance of parametric regimes. *J Neurophysiol,* 100**,** 1152-4; author reply 1155-7.

AHMED, B., ANDERSON, J. C., DOUGLAS, R. J., MARTIN, K. A. & NELSON, J. C. 1994. Polyneuronal innervation of spiny stellate neurons in cat visual cortex. *J Comp Neurol,* 341**,** 39-49.

ALBRECHT, D. & DAVIDOWA, H. 1989. Action of urethane on dorsal lateral geniculate neurons. *Brain Res Bull,* 22**,** 923-7.

ALITTO, H. J. & USREY, W. M. 2003. Corticothalamic feedback and sensory processing. *Curr Opin Neurobiol,* 13**,** 440-5.

ANDERMANN, M. L., RITT, J., NEIMARK, M. A. & MOORE, C. I. 2004. Neural correlates of vibrissa resonance; band-pass and somatotopic representation of high-frequency stimuli. *Neuron,* 42**,** 451-63.

ANDERSON, J. C., DOUGLAS, R. J., MARTIN, K. A. & NELSON, J. C. 1994. Map of the synapses formed with the dendrites of spiny stellate neurons of cat visual cortex. *J Comp Neurol,* 341**,** 25-38.

ANDOLINA, I. M., JONES, H. E., WANG, W. & SILLITO, A. M. 2007. Corticothalamic feedback enhances stimulus response precision in the visual system. *Proc Natl Acad Sci U S A,* 104**,** 1685-90.

ARABZADEH, E., ZORZIN, E. & DIAMOND, M. E. 2005. Neuronal encoding of texture in the whisker sensory pathway. *PLoS Biol,* 3**,** e17.

ARMSTRONG-JAMES, M. & FOX, K. 1987. Spatiotemporal convergence and divergence in the rat S1 "barrel" cortex. *J Comp Neurol,* 263**,** 265-81.

ARMSTRONG-JAMES, M. & GEORGE, M. J. 1988. Influence of anesthesia on spontaneous activity and receptive field size of single units in rat Sm1 neocortex. *Exp Neurol,* 99**,** 369-87.

ARMSTRONG-JAMES, M. & CALLAHAN, C. A. 1991. Thalamo-cortical processing of vibrissal information in the rat. II. spatiotemporal convergence in the thalamic ventroposterior medial nucleus (VPm) and its relevance to generation of receptive fields of S1 cortical "barrel" neurones. *J Comp Neurol,* 303**,** 211-24.

ASHER, R. 1960. Clinical sense. The use of the five senses. *Br Med J,* 1**,** 985-93.

BALE, M. R. & PETERSEN, R. S. 2009. Transformation in the neural code for whisker deflection direction along the lemniscal pathway. *J Neurophysiol,* 102**,** 2771-80.

BARTHO, P., SLEZIA, A., VARGA, V., BOKOR, H., PINAULT, D., BUZSAKI, G. & ACSADY, L. 2007. Cortical control of zona incerta. *J Neurosci,* 27**,** 1670-81.

BEIERLEIN, M. & CONNORS, B. W. 2002. Short-term dynamics of thalamocortical and intracortical synapses onto layer 6 neurons in neocortex. *J Neurophysiol,* 88**,** 1924-32.

BEZDUDNAYA, T., CANO, M., BERESHPOLOVA, Y., STOELZEL, C. R., ALONSO, J. M. & SWADLOW, H. A. 2006. Thalamic burst mode and inattention in the awake LGNd. *Neuron,* 49**,** 421-32.

BINDMAN, L. J., MEYER, T. & PRINCE, C. A. 1988. Comparison of the electrical properties of neocortical neurones in slices in vitro and in the anaesthetized rat. *Exp Brain Res,* 69**,** 489-96.

BINZEGGER, T., DOUGLAS, R. J. & MARTIN, K. A. 2004. A quantitative map of the circuit of cat primary visual cortex. *J Neurosci,* 24**,** 8441-53.

BINZEGGER, T., DOUGLAS, R. J. & MARTIN, K. A. 2007. Stereotypical bouton clustering of individual neurons in cat primary visual cortex. *J Neurosci,* 27**,** 12242-54.

BISHOP, G. H. 1959. The relation between nerve fiber size and sensory modality: phylogenetic implications of the afferent innervation of cortex. *J Nerv Ment Dis,* 128**,** 89-114.

BOKOR, H., ACSADY, L. & DESCHENES, M. 2008. Vibrissal responses of thalamic cells that project to the septal columns of the barrel cortex and to the second somatosensory area. *J Neurosci,* 28**,** 5169-77.

BORTONE, D. S., OLSEN, S. R. & SCANZIANI, M. 2014. Translaminar inhibitory cells recruited by layer 6 corticothalamic neurons suppress visual cortex. *Neuron,* 82**,** 474-85.

BOSMAN, L. W., HOUWELING, A. R., OWENS, C. B., TANKE, N., SHEVCHOUK, O. T., RAHMATI, N., TEUNISSEN, W. H., JU, C., GONG, W., KOEKKOEK, S. K. & DE ZEEUW, C. I. 2011. Anatomical pathways involved in generating and sensing rhythmic whisker movements. *Front Integr Neurosci,* 5**,** 53.

BOURASSA, J. & DESCHENES, M. 1995. Corticothalamic projections from the primary visual cortex in rats: a single fiber study using biocytin as an anterograde tracer. *Neuroscience,* 66**,** 253-63.

BOURASSA, J., PINAULT, D. & DESCHENES, M. 1995. Corticothalamic projections from the cortical barrel field to the somatosensory thalamus in rats: a single-fibre study using biocytin as an anterograde tracer. *Eur J Neurosci,* 7**,** 19-30.

BRECHT, M. & SAKMANN, B. 2002. Whisker maps of neuronal subclasses of the rat ventral posterior medial thalamus, identified by whole-cell voltage recording and morphological reconstruction. *J Physiol,* 538**,** 495-515.

BRECHT, M., ROTH, A. & SAKMANN, B. 2003. Dynamic receptive fields of reconstructed pyramidal cells in layers 3 and 2 of rat somatosensory barrel cortex. *J Physiol,* 553**,** 243-65.

BRIGGS, F. & USREY, W. M. 2008. Emerging views of corticothalamic function. *Curr Opin Neurobiol,* 18**,** 403-7.

BRIGGS, F. 2010. Organizing principles of cortical layer 6. *Front Neural Circuits,* 4**,** 3.

BRIGGS, F., KILEY, C. W., CALLAWAY, E. M. & USREY, W. M. 2016. Morphological Substrates for Parallel Streams of Corticogeniculate Feedback Originating in Both V1 and V2 of the Macaque Monkey. *Neuron,* 90**,** 388-99.

BRUNO, R. M. & SIMONS, D. J. 2002. Feedforward mechanisms of excitatory and inhibitory cortical receptive fields. *J Neurosci,* 22**,** 10966-75.

BRUNO, R. M., KHATRI, V., LAND, P. W. & SIMONS, D. J. 2003. Thalamocortical angular tuning domains within individual barrels of rat somatosensory cortex. *J Neurosci,* 23**,** 9565-74.

BURAN, B. N., VON TRAPP, G. & SANES, D. H. 2014. Behaviorally gated reduction of spontaneous discharge can improve detection thresholds in auditory cortex. *J Neurosci,* 34**,** 4076-81.

CALLAWAY, E. M. 1998. Local circuits in primary visual cortex of the macaque monkey. *Annu Rev Neurosci,* 21**,** 47-74.

CARDIN, J. A., CARLEN, M., MELETIS, K., KNOBLICH, U., ZHANG, F., DEISSEROTH, K., TSAI, L. H. & MOORE, C. I. 2009. Driving fast-spiking cells induces gamma rhythm and controls sensory responses. *Nature,* 459**,** 663-7.

CASAGRANDE, V. A. 1994. A third parallel visual pathway to primate area V1. *Trends Neurosci,* 17**,** 305-10.

CASANOVA, M. F. 2005. *Neocortical modularity and the cell minicolumn,* Hauppauge, N.Y., Nova Biomedical Books.

CASTEJON, C., BARROS-ZULAICA, N. & NUNEZ, A. 2016. Control of Somatosensory Cortical Processing by Thalamic Posterior Medial Nucleus: A New Role of Thalamus in Cortical Function. *PLoS One,* 11**,** e0148169.

CASTRO-ALAMANCOS, M. A. 2002a. Properties of primary sensory (lemniscal) synapses in the ventrobasal thalamus and the relay of high-frequency sensory inputs. *J Neurophysiol,* 87**,** 946-53.

CASTRO-ALAMANCOS, M. A. 2002b. Different temporal processing of sensory inputs in the rat thalamus during quiescent and information processing states in vivo. *J Physiol,* 539**,** 567-78.

CASTRO-ALAMANCOS, M. A. & OLDFORD, E. 2002. Cortical sensory suppression during arousal is due to the activity-dependent depression of thalamocortical synapses. *J Physiol,* 541**,** 319-31.

CASTRO-ALAMANCOS, M. A. 2004. Absence of rapid sensory adaptation in neocortex during information processing states. *Neuron,* 41**,** 455-64.

CHAKRABARTI, S. & ALLOWAY, K. D. 2006. Differential origin of projections from SI barrel cortex to the whisker representations in SII and MI. *J Comp Neurol,* 498**,** 624-36.

CHEN, C. C., ABRAMS, S., PINHAS, A. & BRUMBERG, J. C. 2009. Morphological heterogeneity of layer VI neurons in mouse barrel cortex. *J Comp Neurol,* 512**,** 726-46.

CHEVEE, M., ROBERTSON, J. J., CANNON, G. H., BROWN, S. P. & GOFF, L. A. 2018. Variation in Activity State, Axonal Projection, and Position Define the Transcriptional Identity of Individual Neocortical Projection Neurons. *Cell Rep,* 22**,** 441-455.

CHMIELOWSKA, J., CARVELL, G. E. & SIMONS, D. J. 1989. Spatial organization of thalamocortical and corticothalamic projection systems in the rat SmI barrel cortex. *J Comp Neurol,* 285**,** 325-38.

CHUNG, S., LI, X. & NELSON, S. B. 2002. Short-term depression at thalamocortical synapses contributes to rapid adaptation of cortical sensory responses in vivo. *Neuron,* 34**,** 437-46.

CONSTANTINOPLE, C. M. & BRUNO, R. M. 2013. Deep cortical layers are activated directly by thalamus. *Science,* 340**,** 1591-4.

COX, C. L., HUGUENARD, J. R. & PRINCE, D. A. 1997. Nucleus reticularis neurons mediate diverse inhibitory effects in thalamus. *Proc Natl Acad Sci U S A,* 94**,** 8854-9.

CRANDALL, S. R., CRUIKSHANK, S. J. & CONNORS, B. W. 2015. A corticothalamic switch: controlling the thalamus with dynamic synapses. *Neuron,* 86**,** 768-82.

CRANDALL, S. R., PATRICK, S. L., CRUIKSHANK, S. J. & CONNORS, B. W. 2017. Infrabarrels Are Layer 6 Circuit Modules in the Barrel Cortex that Link Long-Range Inputs and Outputs. *Cell Rep,* 21**,** 3065-3078.

CRUIKSHANK, S. J., URABE, H., NURMIKKO, A. V. & CONNORS, B. W. 2010. Pathway-specific feedforward circuits between thalamus and neocortex revealed by selective optical stimulation of axons. *Neuron,* 65**,** 230-45.

CUDEIRO, J. & SILLITO, A. M. 2006. Looking back: corticothalamic feedback and early visual processing. *Trends Neurosci,* 29**,** 298-306.

DANTZKER, J. L. & CALLAWAY, E. M. 2000. Laminar sources of synaptic input to cortical inhibitory interneurons and pyramidal neurons. *Nat Neurosci,* 3**,** 701-7.

DE KOCK, C. P., BRUNO, R. M., SPORS, H. & SAKMANN, B. 2007. Layer- and cell-type-specific suprathreshold stimulus representation in rat primary somatosensory cortex. *J Physiol,* 581**,** 139-54.

DENMAN, D. J. & CONTRERAS, D. 2015. Complex Effects on In Vivo Visual Responses by Specific Projections from Mouse Cortical Layer 6 to Dorsal Lateral Geniculate Nucleus. *J Neurosci,* 35**,** 9265-80.

DESCHENES, M., VEINANTE, P. & ZHANG, Z. W. 1998. The organization of corticothalamic projections: reciprocity versus parity. *Brain Res Brain Res Rev,* 28**,** 286-308.

DESTEXHE, A., CONTRERAS, D. & STERIADE, M. 1998. Mechanisms underlying the synchronizing action of corticothalamic feedback through inhibition of thalamic relay cells. *J Neurophysiol,* 79**,** 999-1016.

DESTEXHE, A. 2000. Modelling corticothalamic feedback and the gating of the thalamus by the cerebral cortex. *J Physiol Paris,* 94**,** 391-410.

DIAMOND, M. E., ARMSTRONG-JAMES, M. & EBNER, F. F. 1992. Somatic sensory responses in the rostral sector of the posterior group (POm) and in the ventral posterior medial nucleus (VPM) of the rat thalamus. *J Comp Neurol,* 318**,** 462-76.

DIAMOND, M. E. 2000. Neurobiology. Parallel sensing. *Nature,* 406**,** 245, 247.

DIAMOND, M. E., VON HEIMENDAHL, M., KNUTSEN, P. M., KLEINFELD, D. & AHISSAR, E. 2008. 'Where' and 'what' in the whisker sensorimotor system. *Nat Rev Neurosci,* 9**,** 601-12.

DIAMOND, M. E. & ARABZADEH, E. 2013. Whisker sensory system - from receptor to decision. *Prog Neurobiol,* 103**,** 28-40.

DOUGLAS, R. J. & MARTIN, K. A. 2004. Neuronal circuits of the neocortex. *Annu Rev Neurosci,* 27**,** 419-51.

DRINGENBERG, H. C. & VANDERWOLF, C. H. 1995. Some general anesthetics reduce serotonergic neocortical activation and enhance the action of serotonergic antagonists. *Brain Res Bull,* 36**,** 285-92.

DYER, R. S. & RIGDON, G. C. 1987. Urethane affects the rat visual system at subanesthetic doses. *Physiol Behav,* 41**,** 327-30.

EBARA, S., KUMAMOTO, K., MATSUURA, T., MAZURKIEWICZ, J. E. & RICE, F. L. 2002. Similarities and differences in the innervation of mystacial vibrissal follicle-sinus complexes in the rat and cat: a confocal microscopic study. *J Comp Neurol,* 449**,** 103-19.

ESCOBAR, M. I., PIMIENTA, H., CAVINESS, V. S., JR., JACOBSON, M., CRANDALL, J. E. & KOSIK, K. S. 1986. Architecture of apical dendrites in the murine neocortex: dual apical dendritic systems. *Neuroscience,* 17**,** 975-89.

FAIRHALL, A. L., LEWEN, G. D., BIALEK, W. & DE RUYTER VAN STEVENINCK, R. R. 2001. Efficiency and ambiguity in an adaptive neural code. *Nature,* 412**,** 787-92.

FANSELOW, E. E. & NICOLELIS, M. A. 1999. Behavioral modulation of tactile responses in the rat somatosensory system. *J Neurosci,* 19**,** 7603-16.

FANSELOW, E. E., SAMESHIMA, K., BACCALA, L. A. & NICOLELIS, M. A. 2001. Thalamic bursting in rats during different awake behavioral states. *Proc Natl Acad Sci U S A,* 98**,** 15330-5.

FARKHOOI, F., FROESE, A., MULLER, E., MENZEL, R. & NAWROT, M. P. 2013. Cellular adaptation facilitates sparse and reliable coding in sensory pathways. *PLoS Comput Biol,* 9**,** e1003251.

FAVOROV, O. & WHITSEL, B. L. 1988a. Spatial organization of the peripheral input to area 1 cell columns. II. The forelimb representation achieved by a mosaic of segregates. *Brain Res,* 472**,** 43-56.

FAVOROV, O. & WHITSEL, B. L. 1988b. Spatial organization of the peripheral input to area 1 cell columns. I. The detection of 'segregates'. *Brain Res,* 472**,** 25-42.

FAVOROV, O. V. & DIAMOND, M. E. 1990. Demonstration of discrete place-defined columns--segregates--in the cat SI. *J Comp Neurol,* 298**,** 97-112.

FELDMEYER, D. 2012. Excitatory neuronal connectivity in the barrel cortex. *Front Neuroanat,* 6**,** 24.

FELDMEYER, D., BRECHT, M., HELMCHEN, F., PETERSEN, C. C., POULET, J. F., STAIGER, J. F., LUHMANN, H. J. & SCHWARZ, C. 2013. Barrel cortex function. *Prog Neurobiol,* 103**,** 3-27.

FELDMEYER, D., QI, G., EMMENEGGER, V. & STAIGER, J. F. 2018. Inhibitory interneurons and their circuit motifs in the many layers of the barrel cortex. *Neuroscience,* 368**,** 132-151.

FLEIDERVISH, I. A., FRIEDMAN, A. & GUTNICK, M. J. 1996. Slow inactivation of Na+ current and slow cumulative spike adaptation in mouse and guinea-pig neocortical neurones in slices. *J Physiol,* 493 (Pt 1)**,** 83-97.

FLEISCHHAUER, K., PETSCHE, H. & WITTKOWSKI, W. 1972. Vertical bundles of dendrites in the neocortex. *Z Anat Entwicklungsgesch,* 136**,** 213-23.

FOX, K., WRIGHT, N., WALLACE, H. & GLAZEWSKI, S. 2003. The origin of cortical surround receptive fields studied in the barrel cortex. *J Neurosci,* 23**,** 8380-91.

FOX, K. 2008. *Barrel cortex,* Cambridge ; New York, Cambridge University Press.

FRANKS, N. P. & LIEB, W. R. 1994. Molecular and cellular mechanisms of general anaesthesia. *Nature,* 367**,** 607-14.

FRASER, G., HARTINGS, J. A. & SIMONS, D. J. 2006. Adaptation of trigeminal ganglion cells to periodic whisker deflections. *Somatosens Mot Res,* 23**,** 111-8.

FRIEDBERG, M. H., LEE, S. M. & EBNER, F. F. 1999. Modulation of receptive field properties of thalamic somatosensory neurons by the depth of anesthesia. *J Neurophysiol,* 81**,** 2243-52.

FU, Y., TUCCIARONE, J. M., ESPINOSA, J. S., SHENG, N., DARCY, D. P., NICOLL, R. A., HUANG, Z. J. & STRYKER, M. P. 2014. A cortical circuit for gain control by behavioral state. *Cell,* 156**,** 1139-1152.

FUNDIN, B. T., BERGMAN, E. & ULFHAKE, B. 1997a. Alterations in mystacial pad innervation in the aged rat. *Exp Brain Res,* 117**,** 324-40.

FUNDIN, B. T., PFALLER, K. & RICE, F. L. 1997b. Different distributions of the sensory and autonomic innervation among the microvasculature of the rat mystacial pad. *J Comp Neurol,* 389**,** 545-68.

FUNDIN, B. T., SILOS-SANTIAGO, I., ERNFORS, P., FAGAN, A. M., ALDSKOGIUS, H., DECHIARA, T. M., PHILLIPS, H. S., BARBACID, M., YANCOPOULOS, G. D. & RICE, F. L. 1997c. Differential dependency of cutaneous mechanoreceptors on neurotrophins, trk receptors, and P75 LNGFR. *Dev Biol,* 190**,** 94-116.

FURUTA, T., KANEKO, T. & DESCHENES, M. 2009. Septal neurons in barrel cortex derive their receptive field input from the lemniscal pathway. *J Neurosci,* 29**,** 4089-95.

GARABEDIAN, C. E., JONES, S. R., MERZENICH, M. M., DALE, A. & MOORE, C. I. 2003. Band-pass response properties of rat SI neurons. *J Neurophysiol,* 90**,** 1379-91.

GENTET, L. J. 2012. Functional diversity of supragranular GABAergic neurons in the barrel cortex. *Front Neural Circuits,* 6**,** 52.

GENTET, L. J., KREMER, Y., TANIGUCHI, H., HUANG, Z. J., STAIGER, J. F. & PETERSEN, C. C. 2012. Unique functional properties of somatostatin-expressing GABAergic neurons in mouse barrel cortex. *Nat Neurosci,* 15**,** 607-12.

GOBLE, A. K. & HOLLINS, M. 1993. Vibrotactile adaptation enhances amplitude discrimination. *J Acoust Soc Am,* 93**,** 418-24.

GOLOMB, D., AHISSAR, E. & KLEINFELD, D. 2006. Coding of stimulus frequency by latency in thalamic networks through the interplay of GABAB-mediated feedback and stimulus shape. *J Neurophysiol,* 95**,** 1735-50.

GOLSHANI, P., LIU, X. B. & JONES, E. G. 2001. Differences in quantal amplitude reflect GluR4- subunit number at corticothalamic synapses on two populations of thalamic neurons. *Proc Natl Acad Sci U S A,* 98**,** 4172-7.

GONG, S., DOUGHTY, M., HARBAUGH, C. R., CUMMINS, A., HATTEN, M. E., HEINTZ, N. & GERFEN, C. R. 2007. Targeting Cre recombinase to specific neuron populations with bacterial artificial chromosome constructs. *J Neurosci,* 27**,** 9817-23.

GROH, A., MEYER, H. S., SCHMIDT, E. F., HEINTZ, N., SAKMANN, B. & KRIEGER, P. 2010. Cell-type specific properties of pyramidal neurons in neocortex underlying a layout that is modifiable depending on the cortical area. *Cereb Cortex,* 20**,** 826-36.

GROH, A. & KRIEGER, P. 2013. Structure-function analysis of genetically defined neuronal populations. *Cold Spring Harb Protoc,* 2013**,** 961-9.

GROH, A., BOKOR, H., MEASE, R. A., PLATTNER, V. M., HANGYA, B., STROH, A., DESCHENES, M. & ACSADY, L. 2014. Convergence of cortical and sensory driver inputs on single thalamocortical cells. *Cereb Cortex,* 24**,** 3167-79.

GUIDO, W., LU, S. M. & SHERMAN, S. M. 1992. Relative contributions of burst and tonic responses to the receptive field properties of lateral geniculate neurons in the cat. *J Neurophysiol,* 68**,** 2199-211.

GUIDO, W. & WEYAND, T. 1995. Burst responses in thalamic relay cells of the awake behaving cat. *J Neurophysiol,* 74**,** 1782-6.

GUILLERY, R. W. & SHERMAN, S. M. 2002. Thalamic relay functions and their role in corticocortical communication: generalizations from the visual system. *Neuron,* 33**,** 163-75.

GUO, W., CLAUSE, A. R., BARTH-MARON, A. & POLLEY, D. B. 2017. A Corticothalamic Circuit for Dynamic Switching between Feature Detection and Discrimination. *Neuron,* 95**,** 180-194 e5.

HAGIHARA, K. M. & OHKI, K. 2013. Long-term down-regulation of GABA decreases orientation selectivity without affecting direction selectivity in mouse primary visual cortex. *Front Neural Circuits,* 7**,** 28.

HALASSA, M. M., SIEGLE, J. H., RITT, J. T., TING, J. T., FENG, G. & MOORE, C. I. 2011. Selective optical drive of thalamic reticular nucleus generates thalamic bursts and cortical spindles. *Nat Neurosci,* 14**,** 1118-20.

HARA, K. & HARRIS, R. A. 2002. The anesthetic mechanism of urethane: the effects on neurotransmitter-gated ion channels. *Anesth Analg,* 94**,** 313-8, table of contents.

HARRIS, J. A., HIROKAWA, K. E., SORENSEN, S. A., GU, H., MILLS, M., NG, L. L., BOHN, P., MORTRUD, M., OUELLETTE, B., KIDNEY, J., SMITH, K. A., DANG, C., SUNKIN, S., BERNARD, A., OH, S. W., MADISEN, L. & ZENG, H. 2014. Anatomical characterization of Cre driver mice for neural circuit mapping and manipulation. *Front Neural Circuits,* 8**,** 76.

HARRIS, K. D. & MRSIC-FLOGEL, T. D. 2013. Cortical connectivity and sensory coding. *Nature,* 503**,** 51-8.

HARTINGS, J. A. & SIMONS, D. J. 1998. Thalamic relay of afferent responses to 1- to 12-Hz whisker stimulation in the rat. *J Neurophysiol,* 80**,** 1016-9.

HARTMANN, M. J., JOHNSON, N. J., TOWAL, R. B. & ASSAD, C. 2003. Mechanical characteristics of rat vibrissae: resonant frequencies and damping in isolated whiskers and in the awake behaving animal. *J Neurosci,* 23**,** 6510-9.

HE, J. & HU, B. 2002. Differential distribution of burst and single-spike responses in auditory thalamus. *J Neurophysiol,* 88**,** 2152-6.

HELMCHEN, F., GILAD, A. & CHEN, J. L. 2018. Neocortical dynamics during whisker-based sensory discrimination in head-restrained mice. *Neuroscience,* 368**,** 57-69.

HIGLEY, M. J. & CONTRERAS, D. 2003. Nonlinear integration of sensory responses in the rat barrel cortex: an intracellular study in vivo. *J Neurosci,* 23**,** 10190-200.

HIGLEY, M. J. & CONTRERAS, D. 2006. Balanced excitation and inhibition determine spike timing during frequency adaptation. *J Neurosci,* 26**,** 448-57.

HILL, D. N., CURTIS, J. C., MOORE, J. D. & KLEINFELD, D. 2011. Primary motor cortex reports efferent control of vibrissa motion on multiple timescales. *Neuron,* 72**,** 344-56.

HIRATA, A., AGUILAR, J. & CASTRO-ALAMANCOS, M. A. 2009. Influence of subcortical inhibition on barrel cortex receptive fields. *J Neurophysiol,* 102**,** 437-50.

HODGKIN, A. L. & HUXLEY, A. F. 1952. A quantitative description of membrane current and its application to conduction and excitation in nerve. *J Physiol,* 117**,** 500-44.

HOERDER-SUABEDISSEN, A., HAYASHI, S., UPTON, L., NOLAN, Z., CASAS-TORREMOCHA, D., GRANT, E., VISWANATHAN, S., KANOLD, P. O., CLASCA, F., KIM, Y. & MOLNAR, Z. 2018. Subset of Cortical Layer 6b Neurons Selectively Innervates Higher Order Thalamic Nuclei in Mice. *Cereb Cortex,* 28**,** 1882-1897.

HOOGLAND, P. V., WOUTERLOOD, F. G., WELKER, E. & VAN DER LOOS, H. 1991. Ultrastructure of giant and small thalamic terminals of cortical origin: a study of the projections from the barrel cortex in mice using Phaseolus vulgaris leuco-agglutinin (PHA-L). *Exp Brain Res,* 87**,** 159-72.

HUBEL, D. H. & WIESEL, T. N. 1962. Receptive fields, binocular interaction and functional architecture in the cat's visual cortex. *J Physiol,* 160**,** 106-54.

HUBEL, D. H. & WIESEL, T. N. 1974. Sequence regularity and geometry of orientation columns in the monkey striate cortex. *J Comp Neurol,* 158**,** 267-93.

HUBEL, D. H. & WIESEL, T. N. 1977. Ferrier lecture. Functional architecture of macaque monkey visual cortex. *Proc R Soc Lond B Biol Sci,* 198**,** 1-59.

HUH, Y. & CHO, J. 2013. Urethane anesthesia depresses activities of thalamocortical neurons and alters its response to nociception in terms of dual firing modes. *Front Behav Neurosci,* 7**,** 141.

JACQUIN, M. F., RENEHAN, W. E., KLEIN, B. G., MOONEY, R. D. & RHOADES, R. W. 1986. Functional consequences of neonatal infraorbital nerve section in rat trigeminal ganglion. *J Neurosci,* 6**,** 3706-20.

JADHAV, S. P. & FELDMAN, D. E. 2010. Texture coding in the whisker system. *Curr Opin Neurobiol,* 20**,** 313-8.

JARAMILLO, S. & ZADOR, A. M. 2011. The auditory cortex mediates the perceptual effects of acoustic temporal expectation. *Nat Neurosci,* 14**,** 246-51.

JONES, E. G. 2003. Chemically defined parallel pathways in the monkey auditory system. *Ann N Y Acad Sci,* 999**,** 218-33.

JONES, E. G. 2007. *The thalamus,* Cambridge ; New York, Cambridge University Press.

JONES, L. M., DEPIREUX, D. A., SIMONS, D. J. & KELLER, A. 2004a. Robust temporal coding in the trigeminal system. *Science,* 304**,** 1986-9.

JONES, L. M., LEE, S., TRAGESER, J. C., SIMONS, D. J. & KELLER, A. 2004b. Precise temporal responses in whisker trigeminal neurons. *J Neurophysiol,* 92**,** 665-8.

JONES, M. R., MOYNIHAN, H., MACKENZIE, N. & PUENTE, J. 2002. Temporal aspects of stimulus-driven attending in dynamic arrays. *Psychol Sci,* 13**,** 313-9.

JUCZEWSKI, K., VON RICHTHOFEN, H., BAGNI, C., CELIKEL, T., FISONE, G. & KRIEGER, P. 2016. Somatosensory map expansion and altered processing of tactile inputs in a mouse model of fragile X syndrome. *Neurobiol Dis,* 96**,** 201-215.

KANOLD, P. O. & LUHMANN, H. J. 2010. The subplate and early cortical circuits. *Annu Rev Neurosci,* 33**,** 23-48.

KATZ, L. C. 1987. Local circuitry of identified projection neurons in cat visual cortex brain slices. *J Neurosci,* 7**,** 1223-49.

KATZEL, D., ZEMELMAN, B. V., BUETFERING, C., WOLFEL, M. & MIESENBOCK, G. 2011. The columnar and laminar organization of inhibitory connections to neocortical excitatory cells. *Nat Neurosci,* 14**,** 100-7.

KEITHLEY, R. B., HEIEN, M. L. & WIGHTMAN, R. M. 2009. Multivariate concentration determination using principal component regression with residual analysis. *Trends Analyt Chem,* 28**,** 1127-1136.

KHATRI, V., BRUNO, R. M. & SIMONS, D. J. 2009. Stimulus-specific and stimulus-nonspecific firing synchrony and its modulation by sensory adaptation in the whisker-to-barrel pathway. *J Neurophysiol,* 101**,** 2328-38.

KIDA, H., SHIMEGI, S. & SATO, H. 2005. Similarity of direction tuning among responses to stimulation of different whiskers in neurons of rat barrel cortex. *J Neurophysiol,* 94**,** 2004-18.

KILLACKEY, H. P. & SHERMAN, S. M. 2003. Corticothalamic projections from the rat primary somatosensory cortex. *J Neurosci,* 23**,** 7381-4.

KIM, J., MATNEY, C. J., BLANKENSHIP, A., HESTRIN, S. & BROWN, S. P. 2014. Layer 6 corticothalamic neurons activate a cortical output layer, layer 5a. *J Neurosci,* 34**,** 9656-64.

KIM, U. & EBNER, F. F. 1999. Barrels and septa: separate circuits in rat barrels field cortex. *J Comp Neurol,* 408**,** 489-505.

KLEINFELD, D., AHISSAR, E. & DIAMOND, M. E. 2006. Active sensation: insights from the rodent vibrissa sensorimotor system. *Curr Opin Neurobiol,* 16**,** 435-44.

KLEINFELD, D. & DESCHENES, M. 2011. Neuronal basis for object location in the vibrissa scanning sensorimotor system. *Neuron,* 72**,** 455-68.

KOBLIN, D. D. 2002. Urethane: help or hindrance? *Anesth Analg,* 94**,** 241-2.

KOHN, A., PINHEIRO, A., TOMMERDAHL, M. A. & WHITSEL, B. L. 1997. Optical imaging in vitro provides evidence for the minicolumnar nature of cortical response. *Neuroreport,* 8**,** 3513-8.

KOHN, A. & WHITSEL, B. L. 2002. Sensory cortical dynamics. *Behav Brain Res,* 135**,** 119-26.

KREILE, A. K., BONHOEFFER, T. & HUBENER, M. 2011. Altered visual experience induces instructive changes of orientation preference in mouse visual cortex. *J Neurosci,* 31**,** 13911-20.

KRIEGER, P., KUNER, T. & SAKMANN, B. 2007. Synaptic connections between layer 5B pyramidal neurons in mouse somatosensory cortex are independent of apical dendrite bundling. *J Neurosci,* 27**,** 11473-82.

KRIEGER, P. & GROH, A. 2015. *Sensorimotor integration in the whisker system,* New York, Springer.

KUMAR, P. & OHANA, O. 2008. Inter- and intralaminar subcircuits of excitatory and inhibitory neurons in layer 6a of the rat barrel cortex. *J Neurophysiol,* 100**,** 1909-22.

KWEGYIR-AFFUL, E. E. & SIMONS, D. J. 2009. Subthreshold receptive field properties distinguish different classes of corticothalamic neurons in the somatosensory system. *J Neurosci,* 29**,** 964-72.

LAKATOS, P., KARMOS, G., MEHTA, A. D., ULBERT, I. & SCHROEDER, C. E. 2008. Entrainment of neuronal oscillations as a mechanism of attentional selection. *Science,* 320**,** 110-3.

LAM, Y. W. & SHERMAN, S. M. 2010. Functional organization of the somatosensory cortical layer 6 feedback to the thalamus. *Cereb Cortex,* 20**,** 13-24.

LAND, P. W., BUFFER, S. A., JR. & YASKOSKY, J. D. 1995. Barreloids in adult rat thalamus: three-dimensional architecture and relationship to somatosensory cortical barrels. *J Comp Neurol,* 355**,** 573-88.

LANDISMAN, C. E. & CONNORS, B. W. 2007. VPM and PoM nuclei of the rat somatosensory thalamus: intrinsic neuronal properties and corticothalamic feedback. *Cereb Cortex,* 17**,** 2853-65.

LAVALLEE, P., URBAIN, N., DUFRESNE, C., BOKOR, H., ACSADY, L. & DESCHENES, M. 2005. Feedforward inhibitory control of sensory information in higher-order thalamic nuclei. *J Neurosci,* 25**,** 7489-98.

LEE, C. C., LAM, Y. W. & SHERMAN, S. M. 2012. Intracortical convergence of layer 6 neurons. *Neuroreport,* 23**,** 736-40.

LEE, C. J. & WHITSEL, B. L. 1992. Mechanisms Underlying Somatosensory Cortical Dynamics .1. Invivo Studies. *Cerebral Cortex,* 2**,** 81-106.

LEE, K. J. & WOOLSEY, T. A. 1975. A proportional relationship between peripheral innervation density and cortical neuron number in the somatosensory system of the mouse. *Brain Res,* 99**,** 349-53.

LEE, S., CARVELL, G. E. & SIMONS, D. J. 2008. Motor modulation of afferent somatosensory circuits. *Nat Neurosci,* 11**,** 1430-8.

LEE, S. H. & SIMONS, D. J. 2004. Angular tuning and velocity sensitivity in different neuron classes within layer 4 of rat barrel cortex. *J Neurophysiol,* 91**,** 223-9.

LEFORT, S., TOMM, C., FLOYD SARRIA, J. C. & PETERSEN, C. C. 2009. The excitatory neuronal network of the C2 barrel column in mouse primary somatosensory cortex. *Neuron,* 61**,** 301-16.

LEISER, S. C. & MOXON, K. A. 2007. Responses of trigeminal ganglion neurons during natural whisking behaviors in the awake rat. *Neuron,* 53**,** 117-33.

LESICA, N. A. & STANLEY, G. B. 2004. Encoding of natural scene movies by tonic and burst spikes in the lateral geniculate nucleus. *J Neurosci,* 24**,** 10731-40.

LEV, D. L. & WHITE, E. L. 1997. Organization of pyramidal cell apical dendrites and composition of dendritic clusters in the mouse: emphasis on primary motor cortex. *Eur J Neurosci,* 9**,** 280-90.

LI, L. & EBNER, F. F. 2007. Cortical modulation of spatial and angular tuning maps in the rat thalamus. *J Neurosci,* 27**,** 167-79.

LI, Y. T., MA, W. P., LI, L. Y., IBRAHIM, L. A., WANG, S. Z. & TAO, H. W. 2012. Broadening of inhibitory tuning underlies contrast-dependent sharpening of orientation selectivity in mouse visual cortex. *J Neurosci,* 32**,** 16466-77.

LICHTENSTEIN, S. H., CARVELL, G. E. & SIMONS, D. J. 1990. Responses of rat trigeminal ganglion neurons to movements of vibrissae in different directions. *Somatosens Mot Res,* 7**,** 47-65.

LIU, C., FOFFANI, G., SCAGLIONE, A., AGUILAR, J. & MOXON, K. A. 2017. Adaptation of Thalamic Neurons Provides Information about the Spatiotemporal Context of Stimulus History. *J Neurosci,* 37**,** 10012-10021.

LLANO, D. A. & SHERMAN, S. M. 2008. Evidence for nonreciprocal organization of the mouse auditory thalamocortical-corticothalamic projection systems. *J Comp Neurol,* 507**,** 1209-27.

LLINAS, R. & JAHNSEN, H. 1982. Electrophysiology of mammalian thalamic neurones in vitro. *Nature,* 297**,** 406-8.

LORENTE DE NÓ, R. 1938. Analysis of the activity of the chains of internuncial neurons. *J. Neurophysiol.,* 1**,** 207-244.

LUBKE, J. & FELDMEYER, D. 2007. Excitatory signal flow and connectivity in a cortical column: focus on barrel cortex. *Brain Struct Funct,* 212**,** 3-17.

LUO, H. & POEPPEL, D. 2007. Phase patterns of neuronal responses reliably discriminate speech in human auditory cortex. *Neuron,* 54**,** 1001-10.

MACMILLAN, N. A. & CREELMAN, C. D. 2005. *Detection theory: A user's guide, 2nd ed,* Mahwah, NJ, US, Lawrence Erlbaum Associates Publishers.

MAGGI, C. A. & MELI, A. 1986. Suitability of urethane anesthesia for physiopharmacological investigations in various systems. Part 1: General considerations. *Experientia,* 42**,** 109-14.

MARAVALL, M., PETERSEN, R. S., FAIRHALL, A. L., ARABZADEH, E. & DIAMOND, M. E. 2007. Shifts in coding properties and maintenance of information transmission during adaptation in barrel cortex. *PLoS Biol,* 5**,** e19.

MARTINA, M. & JONAS, P. 1997. Functional differences in Na+ channel gating between fast-spiking interneurones and principal neurones of rat hippocampus. *J Physiol,* 505 (Pt 3)**,** 593-603.

MARTINEZ, J. J., RAHSEPAR, B. & WHITE, J. A. 2017. Anatomical and Electrophysiological Clustering of Superficial Medial Entorhinal Cortex Interneurons. *eNeuro,* 4.

MASRI, R., BEZDUDNAYA, T., TRAGESER, J. C. & KELLER, A. 2008. Encoding of stimulus frequency and sensor motion in the posterior medial thalamic nucleus. *J Neurophysiol,* 100**,** 681-9.

MCCASLAND, J. S. & WOOLSEY, T. A. 1988. High-resolution 2-deoxyglucose mapping of functional cortical columns in mouse barrel cortex. *J Comp Neurol,* 278**,** 555-69.

MCCORMICK, D. A. & VON KROSIGK, M. 1992. Corticothalamic activation modulates thalamic firing through glutamate "metabotropic" receptors. *Proc Natl Acad Sci U S A,* 89**,** 2774-8.

MCGINLEY, M. J., DAVID, S. V. & MCCORMICK, D. A. 2015. Cortical Membrane Potential Signature of Optimal States for Sensory Signal Detection. *Neuron,* 87**,** 179-92.

MCGUIRE, B. A., HORNUNG, J. P., GILBERT, C. D. & WIESEL, T. N. 1984. Patterns of synaptic input to layer 4 of cat striate cortex. *J Neurosci,* 4**,** 3021-33.

MEASE, R. A., KRIEGER, P. & GROH, A. 2014. Cortical control of adaptation and sensory relay mode in the thalamus. *Proc Natl Acad Sci U S A,* 111**,** 6798-803.

MEASE, R. A., SUMSER, A., SAKMANN, B. & GROH, A. 2016a. Cortical Dependence of Whisker Responses in Posterior Medial Thalamus In Vivo. *Cereb Cortex,* 26**,** 3534-43.

MEASE, R. A., SUMSER, A., SAKMANN, B. & GROH, A. 2016b. Corticothalamic Spike Transfer via the L5B-POm Pathway in vivo. *Cereb Cortex,* 26**,** 3461-75.

MEASE, R. A., KUNER, T., FAIRHALL, A. L. & GROH, A. 2017. Multiplexed Spike Coding and Adaptation in the Thalamus. *Cell Rep,* 19**,** 1130-1140.

MERCER, A., WEST, D. C., MORRIS, O. T., KIRCHHECKER, S., KERKHOFF, J. E. & THOMSON, A. M. 2005. Excitatory connections made by presynaptic cortico-cortical pyramidal cells in layer 6 of the neocortex. *Cereb Cortex,* 15**,** 1485-96.

MERCER, L. F., JR., REMLEY, N. R. & GILMAN, D. P. 1978. Effects of urethane on hippocampal unit activity in the rat. *Brain Res Bull,* 3**,** 567-70.

MEYER, H. S., WIMMER, V. C., HEMBERGER, M., BRUNO, R. M., DE KOCK, C. P., FRICK, A., SAKMANN, B. & HELMSTAEDTER, M. 2010. Cell type-specific thalamic innervation in a column of rat vibrissal cortex. *Cereb Cortex,* 20**,** 2287-303.

MICELI, S., NADIF KASRI, N., JOOSTEN, J., HUANG, C., KEPSER, L., PROVILLE, R., SELTEN, M. M., VAN EIJS, F., AZARFAR, A., HOMBERG, J. R., CELIKEL, T. & SCHUBERT, D. 2017. Reduced Inhibition within Layer IV of Sert Knockout Rat Barrel Cortex is Associated with Faster Sensory Integration. *Cereb Cortex,* 27**,** 933-949.

MILLER, K. D., PINTO, D. J. & SIMONS, D. J. 2001. Processing in layer 4 of the neocortical circuit: new insights from visual and somatosensory cortex. *Curr Opin Neurobiol,* 11**,** 488-97.

MINNERY, B. S., BRUNO, R. M. & SIMONS, D. J. 2003. Response transformation and receptive-field synthesis in the lemniscal trigeminothalamic circuit. *J Neurophysiol,* 90**,** 1556-70.

MINNERY, B. S. & SIMONS, D. J. 2003. Response properties of whisker-associated trigeminothalamic neurons in rat nucleus principalis. *J Neurophysiol,* 89**,** 40-56.

MOHAR, B., GANMOR, E. & LAMPL, I. 2015. Faithful Representation of Tactile Intensity under Different Contexts Emerges from the Distinct Adaptive Properties of the First Somatosensory Relay Stations. *J Neurosci,* 35**,** 6997-7002.

MONIER, C., CHAVANE, F., BAUDOT, P., GRAHAM, L. J. & FREGNAC, Y. 2003. Orientation and direction selectivity of synaptic inputs in visual cortical neurons: a diversity of combinations produces spike tuning. *Neuron,* 37**,** 663-80.

MOORE, C. I. & NELSON, S. B. 1998. Spatio-temporal subthreshold receptive fields in the vibrissa representation of rat primary somatosensory cortex. *J Neurophysiol,* 80**,** 2882-92.

MOORE, C. I., NELSON, S. B. & SUR, M. 1999. Dynamics of neuronal processing in rat somatosensory cortex. *Trends Neurosci,* 22**,** 513-20.

MOORE, C. I. 2004. Frequency-dependent processing in the vibrissa sensory system. *J Neurophysiol,* 91**,** 2390-9.

MOORE, J. D., MERCER LINDSAY, N., DESCHENES, M. & KLEINFELD, D. 2015. Vibrissa Self-Motion and Touch Are Reliably Encoded along the Same Somatosensory Pathway from Brainstem through Thalamus. *PLoS Biol,* 13**,** e1002253.

MOTULSKY, H. J. & BROWN, R. E. 2006. Detecting outliers when fitting data with nonlinear regression - a new method based on robust nonlinear regression and the false discovery rate. *BMC Bioinformatics,* 7**,** 123.

MOUNTCASTLE, V. B. 1957. Modality and topographic properties of single neurons of cat's somatic sensory cortex. *J Neurophysiol,* 20**,** 408-34.

MOUNTCASTLE, V. B. 1997. The columnar organization of the neocortex. *Brain,* 120 (Pt 4)**,** 701-22.

MOUNTCASTLE, V. B. 2003. Introduction. Computation in cortical columns. *Cereb Cortex,* 13**,** 2-4.

MURPHY, P. C. & SILLITO, A. M. 1987. Corticofugal feedback influences the generation of length tuning in the visual pathway. *Nature,* 329**,** 727-9.

MUSALL, S., VON DER BEHRENS, W., MAYRHOFER, J. M., WEBER, B., HELMCHEN, F. & HAISS, F. 2014. Tactile frequency discrimination is enhanced by circumventing neocortical adaptation. *Nat Neurosci,* 17**,** 1567-73.

NEIMARK, M. A., ANDERMANN, M. L., HOPFIELD, J. J. & MOORE, C. I. 2003. Vibrissa resonance as a transduction mechanism for tactile encoding. *J Neurosci,* 23**,** 6499-509.

NICOLELIS, M. A. & FANSELOW, E. E. 2002. Thalamocortical [correction of Thalamcortical] optimization of tactile processing according to behavioral state. *Nat Neurosci,* 5**,** 517-23.

NICOLL, R. A., ECCLES, J. C., OSHIMA, T. & RUBIA, F. 1975. Prolongation of hippocampal inhibitory postsynaptic potentials by barbiturates. *Nature,* 258**,** 625-7.

NIELL, C. M. & STRYKER, M. P. 2008. Highly selective receptive fields in mouse visual cortex. *J Neurosci,* 28**,** 7520-36.

NIELL, C. M. & STRYKER, M. P. 2010. Modulation of visual responses by behavioral state in mouse visual cortex. *Neuron,* 65**,** 472-9.

NISHIKAWA, K. & MACIVER, M. B. 2000. Membrane and synaptic actions of halothane on rat hippocampal pyramidal neurons and inhibitory interneurons. *J Neurosci,* 20**,** 5915-23.

NOBLE, D. & STEIN, R. B. 1966. The threshold conditions for initiation of action potentials by excitable cells. *J Physiol,* 187**,** 129-62.

NOBRE, A., CORREA, A. & COULL, J. 2007. The hazards of time. *Curr Opin Neurobiol,* 17**,** 465-70.

OBERLAENDER, M., DE KOCK, C. P., BRUNO, R. M., RAMIREZ, A., MEYER, H. S., DERCKSEN, V. J., HELMSTAEDTER, M. & SAKMANN, B. 2012. Cell type-specific three-dimensional structure of thalamocortical circuits in a column of rat vibrissal cortex. *Cereb Cortex,* 22**,** 2375-91.

OLLERENSHAW, D. R., BARI, B. A., MILLARD, D. C., ORR, L. E., WANG, Q. & STANLEY, G. B. 2012. Detection of tactile inputs in the rat vibrissa pathway. *J Neurophysiol,* 108**,** 479-90.

OLLERENSHAW, D. R., ZHENG, H. J. V., MILLARD, D. C., WANG, Q. & STANLEY, G. B. 2014. The adaptive trade-off between detection and discrimination in cortical representations and behavior. *Neuron,* 81**,** 1152-1164.

OLSEN, S. R., BORTONE, D. S., ADESNIK, H. & SCANZIANI, M. 2012. Gain control by layer six in cortical circuits of vision. *Nature,* 483**,** 47-52.

PANZERI, S. & DIAMOND, M. E. 2010. Information Carried by Population Spike Times in the Whisker Sensory Cortex can be Decoded Without Knowledge of Stimulus Time. *Front Synaptic Neurosci,* 2**,** 17.

PASTERNAK, J. R. & WOOLSEY, T. A. 1975. The number, size and spatial distribution of neurons in lamina IV of the mouse SmI neocortex. *J Comp Neurol,* 160**,** 291-306.

PAUZIN, F. P. & KRIEGER, P. 2018. A Corticothalamic Circuit for Refining Tactile Encoding. *Cell Rep,* 23**,** 1314-1325.

PERL, E. R. 1963. Somatosensory mechanisms. *Annu Rev Physiol,* 25**,** 459-92.

PETERS, A. & WALSH, T. M. 1972. A study of the organization of apical dendrites in the somatic sensory cortex of the rat. *J Comp Neurol,* 144**,** 253-68.

PETERSEN, C. C. & SAKMANN, B. 2000. The excitatory neuronal network of rat layer 4 barrel cortex. *J Neurosci,* 20**,** 7579-86.

PETERSEN, C. C., HAHN, T. T., MEHTA, M., GRINVALD, A. & SAKMANN, B. 2003. Interaction of sensory responses with spontaneous depolarization in layer 2/3 barrel cortex. *Proc Natl Acad Sci U S A,* 100**,** 13638-43.

PETERSEN, C. C. 2007. The functional organization of the barrel cortex. *Neuron,* 56**,** 339-55.

PETILLA INTERNEURON NOMENCLATURE, G., ASCOLI, G. A., ALONSO-NANCLARES, L., ANDERSON, S. A., BARRIONUEVO, G., BENAVIDES-PICCIONE, R., BURKHALTER, A., BUZSAKI, G., CAULI, B., DEFELIPE, J., FAIREN, A., FELDMEYER, D., FISHELL, G., FREGNAC, Y., FREUND, T. F., GARDNER, D., GARDNER, E. P., GOLDBERG, J. H., HELMSTAEDTER, M., HESTRIN, S., KARUBE, F., KISVARDAY, Z. F., LAMBOLEZ, B., LEWIS, D. A., MARIN, O., MARKRAM, H., MUNOZ, A., PACKER, A., PETERSEN, C. C., ROCKLAND, K. S., ROSSIER, J., RUDY, B., SOMOGYI, P., STAIGER, J. F., TAMAS, G., THOMSON, A. M., TOLEDO-RODRIGUEZ, M., WANG, Y., WEST, D. C. & YUSTE, R. 2008. Petilla terminology: nomenclature of features of GABAergic interneurons of the cerebral cortex. *Nat Rev Neurosci,* 9**,** 557-68.

PIERRET, T., LAVALLEE, P. & DESCHENES, M. 2000. Parallel streams for the relay of vibrissal information through thalamic barreloids. *J Neurosci,* 20**,** 7455-62.

PITAS, A., ALBARRACIN, A. L., MOLANO-MAZON, M. & MARAVALL, M. 2017. Variable Temporal Integration of Stimulus Patterns in the Mouse Barrel Cortex. *Cereb Cortex,* 27**,** 1758-1764.

PITTSON, S., HIMMEL, A. M. & MACIVER, M. B. 2004. Multiple synaptic and membrane sites of anesthetic action in the CA1 region of rat hippocampal slices. *BMC Neurosci,* 5**,** 52.

POUILLE, F. & SCANZIANI, M. 2001. Enforcement of temporal fidelity in pyramidal cells by somatic feed-forward inhibition. *Science,* 293**,** 1159-63.

POULET, J. F., FERNANDEZ, L. M., CROCHET, S. & PETERSEN, C. C. 2012. Thalamic control of cortical states. *Nat Neurosci,* 15**,** 370-2.

PUCCINI, G. D., COMPTE, A. & MARAVALL, M. 2006. Stimulus dependence of barrel cortex directional selectivity. *PLoS One,* 1**,** e137.

QI, G., RADNIKOW, G. & FELDMEYER, D. 2015. Electrophysiological and morphological characterization of neuronal microcircuits in acute brain slices using paired patch-clamp recordings. *J Vis Exp***,** 52358.

QI, G. & FELDMEYER, D. 2016. Dendritic Target Region-Specific Formation of Synapses Between Excitatory Layer 4 Neurons and Layer 6 Pyramidal Cells. *Cereb Cortex,* 26**,** 1569-1579.

RAMCHARAN, E. J., GNADT, J. W. & SHERMAN, S. M. 2000. Burst and tonic firing in thalamic cells of unanesthetized, behaving monkeys. *Vis Neurosci,* 17**,** 55-62.

REICHOVA, I. & SHERMAN, S. M. 2004. Somatosensory corticothalamic projections: distinguishing drivers from modulators. *J Neurophysiol,* 92**,** 2185-97.

REINHOLD, K., LIEN, A. D. & SCANZIANI, M. 2015. Distinct recurrent versus afferent dynamics in cortical visual processing. *Nat Neurosci,* 18**,** 1789-97.

RITT, J. T., ANDERMANN, M. L. & MOORE, C. I. 2008. Embodied information processing: vibrissa mechanics and texture features shape micromotions in actively sensing rats. *Neuron,* 57**,** 599-613.

ROUILLER, E. M. & WELKER, E. 2000. A comparative analysis of the morphology of corticothalamic projections in mammals. *Brain Res Bull,* 53**,** 727-41.

SACHDEV, R. N., EBNER, F. F. & WILSON, C. J. 2004. Effect of subthreshold up and down states on the whisker-evoked response in somatosensory cortex. *J Neurophysiol,* 92**,** 3511-21.

SADOVSKY, A. J. & MACLEAN, J. N. 2013. Scaling of topologically similar functional modules defines mouse primary auditory and somatosensory microcircuitry. *J Neurosci,* 33**,** 14048-60, 14060a.

SCENIAK, M. P. & MACIVER, M. B. 2006. Cellular actions of urethane on rat visual cortical neurons in vitro. *J Neurophysiol,* 95**,** 3865-74.

SCHNEIDER, D. M., NELSON, A. & MOONEY, R. 2014. A synaptic and circuit basis for corollary discharge in the auditory cortex. *Nature,* 513**,** 189-94.

SCHOLFIELD, C. N. 1980. Potentiation of inhibition by general anaesthetics in neurones of the olfactory cortex in vitro. *Pflugers Arch,* 383**,** 249-55.

SCHROEDER, C. E. & LAKATOS, P. 2009. Low-frequency neuronal oscillations as instruments of sensory selection. *Trends Neurosci,* 32**,** 9-18.

SCHUBERT, D., KOTTER, R., LUHMANN, H. J. & STAIGER, J. F. 2006. Morphology, electrophysiology and functional input connectivity of pyramidal neurons characterizes a genuine layer va in the primary somatosensory cortex. *Cereb Cortex,* 16**,** 223-36.

SCHUBERT, D., KOTTER, R. & STAIGER, J. F. 2007. Mapping functional connectivity in barrel-related columns reveals layer- and cell type-specific microcircuits. *Brain Struct Funct,* 212**,** 107-19.

SCHUMMERS, J., MARINO, J. & SUR, M. 2002. Synaptic integration by V1 neurons depends on location within the orientation map. *Neuron,* 36**,** 969-78.

SHERMAN, S. M. & GUILLERY, R. W. 1996. Functional organization of thalamocortical relays. *J Neurophysiol,* 76**,** 1367-95.

SHERMAN, S. M. 2001. Tonic and burst firing: dual modes of thalamocortical relay. *Trends Neurosci,* 24**,** 122-6.

SHERMAN, S. M. 2005. Thalamic relays and cortical functioning. *Prog Brain Res,* 149**,** 107-26.

SHERMAN, S. M. 2016. Thalamus plays a central role in ongoing cortical functioning. *Nat Neurosci,* 19**,** 533-41.

SHETH, B. R., MOORE, C. I. & SUR, M. 1998. Temporal modulation of spatial borders in rat barrel cortex. *J Neurophysiol,* 79**,** 464-70.

SHOYKHET, M., DOHERTY, D. & SIMONS, D. J. 2000. Coding of deflection velocity and amplitude by whisker primary afferent neurons: implications for higher level processing. *Somatosens Mot Res,* 17**,** 171-80.

SILLITO, A. M. 1975. The contribution of inhibitory mechanisms to the receptive field properties of neurones in the striate cortex of the cat. *J Physiol,* 250**,** 305-29.

SILLITO, A. M. & JONES, H. E. 2002. Corticothalamic interactions in the transfer of visual information. *Philos Trans R Soc Lond B Biol Sci,* 357**,** 1739-52.

SILLITO, A. M., CUDEIRO, J. & JONES, H. E. 2006. Always returning: feedback and sensory processing in visual cortex and thalamus. *Trends Neurosci,* 29**,** 307-16.

SIMONS, D. J. 1978. Response properties of vibrissa units in rat SI somatosensory neocortex. *J Neurophysiol,* 41**,** 798-820.

SIMONS, D. J. & WOOLSEY, T. A. 1979. Functional organization in mouse barrel cortex. *Brain Res,* 165**,** 327-32.

SIMONS, D. J. 1983. Multi-whisker stimulation and its effects on vibrissa units in rat SmI barrel cortex. *Brain Res,* 276**,** 178-82.

SIMONS, D. J. & CARVELL, G. E. 1989. Thalamocortical response transformation in the rat vibrissa/barrel system. *J Neurophysiol,* 61**,** 311-30.

SIMONS, S. B., TANNAN, V., CHIU, J., FAVOROV, O. V., WHITSEL, B. L. & TOMMERDAHL, M. 2005. Amplitude-dependency of response of SI cortex to flutter stimulation. *BMC Neurosci,* 6**,** 43.

SOSNIK, R., HAIDARLIU, S. & AHISSAR, E. 2001. Temporal frequency of whisker movement. I. Representations in brain stem and thalamus. *J Neurophysiol,* 86**,** 339-53.

STAIGER, J. F., ZILLES, K. & FREUND, T. F. 1996. Distribution of GABAergic elements postsynaptic to ventroposteromedial thalamic projections in layer IV of rat barrel cortex. *Eur J Neurosci,* 8**,** 2273-85.

STERIADE, M., MCCORMICK, D. A. & SEJNOWSKI, T. J. 1993. Thalamocortical oscillations in the sleeping and aroused brain. *Science,* 262**,** 679-85.

STERIADE, M., JONES, E. G. & MCCORMICK, D. A. 1997. *Thalamus,* Amsterdam ; New York, Elsevier.

STRATFORD, K. J., TARCZY-HORNOCH, K., MARTIN, K. A., BANNISTER, N. J. & JACK, J. J. 1996. Excitatory synaptic inputs to spiny stellate cells in cat visual cortex. *Nature,* 382**,** 258-61.

SUN, Q. Q., HUGUENARD, J. R. & PRINCE, D. A. 2006. Barrel cortex microcircuits: thalamocortical feedforward inhibition in spiny stellate cells is mediated by a small number of fast-spiking interneurons. *J Neurosci,* 26**,** 1219-30.

SWADLOW, H. A. 1989. Efferent neurons and suspected interneurons in S-1 vibrissa cortex of the awake rabbit: receptive fields and axonal properties. *J Neurophysiol,* 62**,** 288-308.

SWIFT, J. A. 1991. Fine details on the surface of human hair. *Int J Cosmet Sci,* 13**,** 143-59.

SZWED, M., BAGDASARIAN, K. & AHISSAR, E. 2003. Encoding of vibrissal active touch. *Neuron,* 40**,** 621-30.

TANIGUCHI, H., HE, M., WU, P., KIM, S., PAIK, R., SUGINO, K., KVITSIANI, D., FU, Y., LU, J., LIN, Y., MIYOSHI, G., SHIMA, Y., FISHELL, G., NELSON, S. B. & HUANG, Z. J. 2011. A resource of Cre driver lines for genetic targeting of GABAergic neurons in cerebral cortex. *Neuron,* 71**,** 995-1013.

TANNAN, V., WHITSEL, B. L. & TOMMERDAHL, M. A. 2006. Vibrotactile adaptation enhances spatial localization. *Brain Res,* 1102**,** 109-16.

TEMEREANCA, S. & SIMONS, D. J. 2003. Local field potentials and the encoding of whisker deflections by population firing synchrony in thalamic barreloids. *J Neurophysiol,* 89**,** 2137-45.

TEMEREANCA, S. & SIMONS, D. J. 2004. Functional topography of corticothalamic feedback enhances thalamic spatial response tuning in the somatosensory whisker/barrel system. *Neuron,* 41**,** 639-51.

THOMSON, A. M. & BANNISTER, A. P. 2003. Interlaminar connections in the neocortex. *Cereb Cortex,* 13**,** 5-14.

THOMSON, A. M. 2010. Neocortical layer 6, a review. *Front Neuroanat,* 4**,** 13.

TIMOFEEVA, E., MERETTE, C., EMOND, C., LAVALLEE, P. & DESCHENES, M. 2003. A map of angular tuning preference in thalamic barreloids. *J Neurosci,* 23**,** 10717-23.

TOMMERDAHL, M., FAVOROV, O., WHITSEL, B. L., NAKHLE, B. & GONCHAR, Y. A. 1993. Minicolumnar activation patterns in cat and monkey SI cortex. *Cereb Cortex,* 3**,** 399-411.

TOMMERDAHL, M., FAVOROV, O. & WHITSEL, B. L. 2002. Optical imaging of intrinsic signals in somatosensory cortex. *Behav Brain Res,* 135**,** 83-91.

TRAGESER, J. C. & KELLER, A. 2004. Reducing the uncertainty: gating of peripheral inputs by zona incerta. *J Neurosci,* 24**,** 8911-5.

TRAGESER, J. C., BURKE, K. A., MASRI, R., LI, Y., SELLERS, L. & KELLER, A. 2006. State-dependent gating of sensory inputs by zona incerta. *J Neurophysiol,* 96**,** 1456-63.

TRAUB, R. D. & MILES, R. 1991. Multiple modes of neuronal population activity emerge after modifying specific synapses in a model of the CA3 region of the hippocampus. *Ann N Y Acad Sci,* 627**,** 277-90.

TSYTSAREV, V., PUMBO, E., TANG, Q., CHEN, C. W., KALCHENKO, V. & CHEN, Y. 2016. Study of the cortical representation of whisker frequency selectivity using voltage-sensitive dye optical imaging. *Intravital,* 5**,** e1142637.

URBAIN, N. & DESCHENES, M. 2007. Motor cortex gates vibrissal responses in a thalamocortical projection pathway. *Neuron,* 56**,** 714-25.

URBAIN, N., SALIN, P. A., LIBOUREL, P. A., COMTE, J. C., GENTET, L. J. & PETERSEN, C. C. H. 2015. Whisking-Related Changes in Neuronal Firing and Membrane Potential Dynamics in the Somatosensory Thalamus of Awake Mice. *Cell Rep,* 13**,** 647-656.

VEINANTE, P. & DESCHENES, M. 1999. Single- and multi-whisker channels in the ascending projections from the principal trigeminal nucleus in the rat. *J Neurosci,* 19**,** 5085-95.

VELEZ-FORT, M., ROUSSEAU, C. V., NIEDWOROK, C. J., WICKERSHAM, I. R., RANCZ, E. A., BROWN, A. P. Y., STROM, M. & MARGRIE, T. W. 2014. The Stimulus Selectivity and Connectivity of Layer Six Principal Cells Reveals Cortical Microcircuits Underlying Visual Processing. *Neuron,* 84**,** 238.

VIERCK, C. J., JR. & JONES, M. B. 1970. Influences of low and high frequency oscillation upon spatio-tactile resolution. *Physiol Behav,* 5**,** 1431-5.

VILARCHAO, M. E., ESTEBANEZ, L., SHULZ, D. E. & FEREZOU, I. 2018. Supra-barrel Distribution of Directional Tuning for Global Motion in the Mouse Somatosensory Cortex. *Cell Rep,* 22**,** 3534-3547.

WARK, B., LUNDSTROM, B. N. & FAIRHALL, A. 2007. Sensory adaptation. *Curr Opin Neurobiol,* 17**,** 423-9.

WARREN, R. A., AGMON, A. & JONES, E. G. 1994. Oscillatory synaptic interactions between ventroposterior and reticular neurons in mouse thalamus in vitro. *J Neurophysiol,* 72**,** 1993-2003.

WEHR, M. & ZADOR, A. M. 2003. Balanced inhibition underlies tuning and sharpens spike timing in auditory cortex. *Nature,* 426**,** 442-6.

WELKER, C. & WOOLSEY, T. A. 1974. Structure of layer IV in the somatosensory neocortex of the rat: description and comparison with the mouse. *J Comp Neurol,* 158**,** 437-53.

WELKER, E. & VAN DER LOOS, H. 1986. Quantitative correlation between barrel-field size and the sensory innervation of the whiskerpad: a comparative study in six strains of mice bred for different patterns of mystacial vibrissae. *J Neurosci,* 6**,** 3355-73.

WELKER, E., HOOGLAND, P. V. & VAN DER LOOS, H. 1988. Organization of feedback and feedforward projections of the barrel cortex: a PHA-L study in the mouse. *Exp Brain Res,* 73**,** 411-35.

WEST, D. C., MERCER, A., KIRCHHECKER, S., MORRIS, O. T. & THOMSON, A. M. 2006. Layer 6 cortico-thalamic pyramidal cells preferentially innervate interneurons and generate facilitating EPSPs. *Cereb Cortex,* 16**,** 200-11.

WHITE, E. L. & DEAMICIS, R. A. 1977. Afferent and efferent projections of the region in mouse SmL cortex which contains the posteromedial barrel subfield. *J Comp Neurol,* 175**,** 455-82.

WHITE, E. L. & KELLER, A. 1987. Intrinsic circuitry involving the local axon collaterals of corticothalamic projection cells in mouse SmI cortex. *J Comp Neurol,* 262**,** 13-26.

WHITE, E. L. & PETERS, A. 1993. Cortical modules in the posteromedial barrel subfield (Sml) of the mouse. *J Comp Neurol,* 334**,** 86-96.

WHITELEY, S. J., KNUTSEN, P. M., MATTHEWS, D. W. & KLEINFELD, D. 2015. Deflection of a vibrissa leads to a gradient of strain across mechanoreceptors in a mystacial follicle. *J Neurophysiol,* 114**,** 138-45.

WHITMIRE, C. J. & STANLEY, G. B. 2016. Rapid Sensory Adaptation Redux: A Circuit Perspective. *Neuron,* 92**,** 298-315.

WHITMIRE, C. J., WAIBLINGER, C., SCHWARZ, C. & STANLEY, G. B. 2016. Information Coding through Adaptive Gating of Synchronized Thalamic Bursting. *Cell Rep,* 14**,** 795-807.

WILENT, W. B. & CONTRERAS, D. 2004. Synaptic responses to whisker deflections in rat barrel cortex as a function of cortical layer and stimulus intensity. *J Neurosci,* 24**,** 3985-98.

WILENT, W. B. & CONTRERAS, D. 2005a. Stimulus-dependent changes in spike threshold enhance feature selectivity in rat barrel cortex neurons. *J Neurosci,* 25**,** 2983-91.

WILENT, W. B. & CONTRERAS, D. 2005b. Dynamics of excitation and inhibition underlying stimulus selectivity in rat somatosensory cortex. *Nat Neurosci,* 8**,** 1364-70.

WIMMER, V. C., BRUNO, R. M., DE KOCK, C. P., KUNER, T. & SAKMANN, B. 2010. Dimensions of a projection column and architecture of VPM and POm axons in rat vibrissal cortex. *Cereb Cortex,* 20**,** 2265-76.

WINER, J. A., DIEHL, J. J. & LARUE, D. T. 2001. Projections of auditory cortex to the medial geniculate body of the cat. *J Comp Neurol,* 430**,** 27-55.

WOOLSEY, T. A. & VAN DER LOOS, H. 1970. The structural organization of layer IV in the somatosensory region (SI) of mouse cerebral cortex. The description of a cortical field composed of discrete cytoarchitectonic units. *Brain Res,* 17**,** 205-42.

WOOLSEY, T. A., DIERKER, M. L. & WANN, D. F. 1975. Mouse SmI cortex: qualitative and quantitative classification of golgi-impregnated barrel neurons. *Proc Natl Acad Sci U S A,* 72**,** 2165-9.

WÖRGÖTTER, F., EYDING, D., MACKLIS, J. D. & FUNKE, K. 2002. The influence of the corticothalamic projection on responses in thalamus and cortex. *Philos Trans R Soc Lond B Biol Sci,* 357**,** 1823-34.

WRIGHT, B. A. & FITZGERALD, M. B. 2004. The time course of attention in a simple auditory detection task. *Percept Psychophys,* 66**,** 508-16.

YAMAWAKI, N. & SHEPHERD, G. M. 2015. Synaptic circuit organization of motor corticothalamic neurons. *J Neurosci,* 35**,** 2293-307.

YAN, W., KAN, Q., KERGRENE, K., KANG, G., FENG, X. Q. & RAJAN, R. 2013. A truncated conical beam model for analysis of the vibration of rat whiskers. *J Biomech,* 46**,** 1987-95.

YANG, Q., CHEN, C. C., RAMOS, R. L., KATZ, E., KELLER, A. & BRUMBERG, J. C. 2014. Intrinsic properties of and thalamocortical inputs onto identified corticothalamic-VPM neurons. *Somatosens Mot Res,* 31**,** 78-93.

YU, C., DERDIKMAN, D., HAIDARLIU, S. & AHISSAR, E. 2006. Parallel thalamic pathways for whisking and touch signals in the rat. *PLoS Biol,* 4**,** e124.

YU, C., HOREV, G., RUBIN, N., DERDIKMAN, D., HAIDARLIU, S. & AHISSAR, E. 2015. Coding of object location in the vibrissal thalamocortical system. *Cereb Cortex,* 25**,** 563-77.

ZEHENDNER, C. M., LUHMANN, H. J. & YANG, J. W. 2013. A simple and novel method to monitor breathing and heart rate in awake and urethane-anesthetized newborn rodents. *PLoS One,* 8**,** e62628.

ZHANG, Z. W. & DESCHENES, M. 1997. Intracortical axonal projections of lamina VI cells of the primary somatosensory cortex in the rat: a single-cell labeling study. *J Neurosci,* 17**,** 6365-79.

ZHANG, Z. W. & DESCHENES, M. 1998. Projections to layer VI of the posteromedial barrel field in the rat: a reappraisal of the role of corticothalamic pathways. *Cereb Cortex,* 8**,** 428-36.

ZHOU, M., LIANG, F., XIONG, X. R., LI, L., LI, H., XIAO, Z., TAO, H. W. & ZHANG, L. I. 2014. Scaling down of balanced excitation and inhibition by active behavioral states in auditory cortex. *Nat Neurosci,* 17**,** 841-50.

ZHU, J. J. & CONNORS, B. W. 1999. Intrinsic firing patterns and whisker-evoked synaptic responses of neurons in the rat barrel cortex. *J Neurophysiol,* 81**,** 1171-83.

ZHU, Y., STORNETTA, R. L. & ZHU, J. J. 2004. Chandelier cells control excessive cortical excitation: characteristics of whisker-evoked synaptic responses of layer 2/3 nonpyramidal and pyramidal neurons. *J Neurosci,* 24**,** 5101-8.

ZHU, Y. & ZHU, J. J. 2004. Rapid arrival and integration of ascending sensory information in layer 1 nonpyramidal neurons and tuft dendrites of layer 5 pyramidal neurons of the neocortex. *J Neurosci,* 24**,** 1272-9.

ZUCKER, E. & WELKER, W. I. 1969. Coding of somatic sensory input by vibrissae neurons in the rat's trigeminal ganglion. *Brain Res,* 12**,** 138-56.

6 Appendix:

6.1 Supplemental figures

Figure S1. L6-Ntsr1 spiking scaled with light intensity

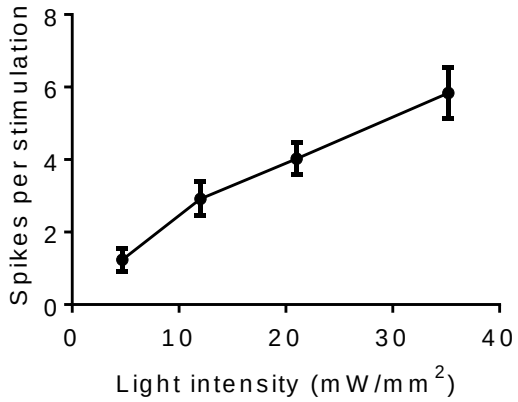

Spiking in L6-Ntsr1 cells (n=8) evoked with a 50 ms blue (470 nm) light pulse.

Figure S2. The decreased spontaneous activity induced by L6-Ntsr1 photo-activation was dependent on the light (470 nm) intensity.

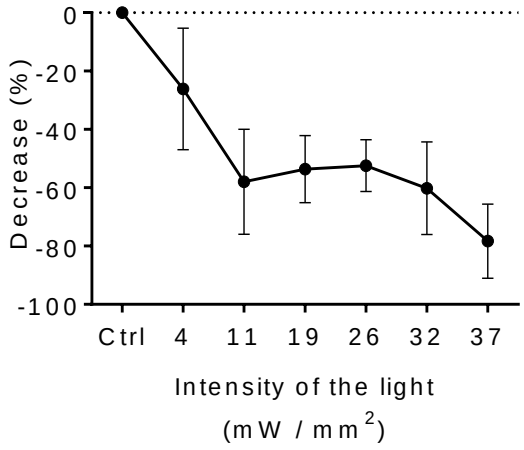

Graph shows the average decrease from 6 excitatory cells.

Figure S3. Spontaneous spiking in cortical cells modulated by L6-Ntsr1 photoactivation

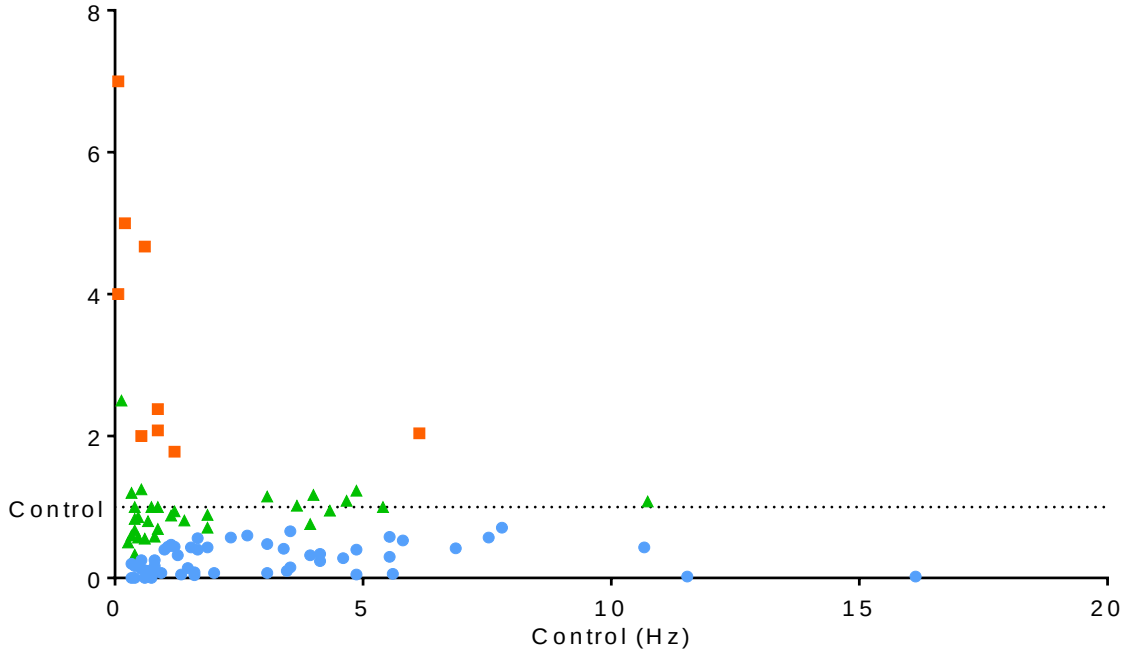

L6-photoactivation decreased spontaneous spiking over a broad range of control activities. The few cells where photoactivation increased spontaneous spiking, were cells with a relatively low spiking activity in control. (X-axis) is the number of spikes in control condition counted in a 15 second time window reported in Hz. Y-axis is the relative change triggered by L6-Ntsr1 activation (number of spikes with L6-activation / number of spikes in control).

Red = cells showing a significant increase in spontaneous activity with L6-Ntsr1 activation

Blue = cells showing a significant decrease in spontaneous activity with L6-Ntsr1 activation

Green = cells with a non-significant effect of L6-Ntsr1 activation

Figure S4. L6-Ntsr1 spontaneous spiking as a function of time after blue light onset

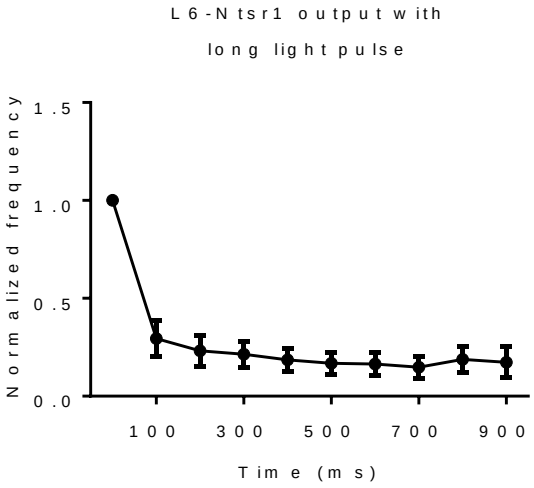

Normalized spiking frequency as a function of time after onset of blue light. The light pulse was 1000 ms long. Spiking decreases after the first 100 ms and then remains constant. Whisker evoked responses were evoked 100 ms after light onset. (n = 8, L6-Ntsr1 pyramidal cells).

Figure S5: Infragranular FS interneurons activated by direct projections from Ntsr1

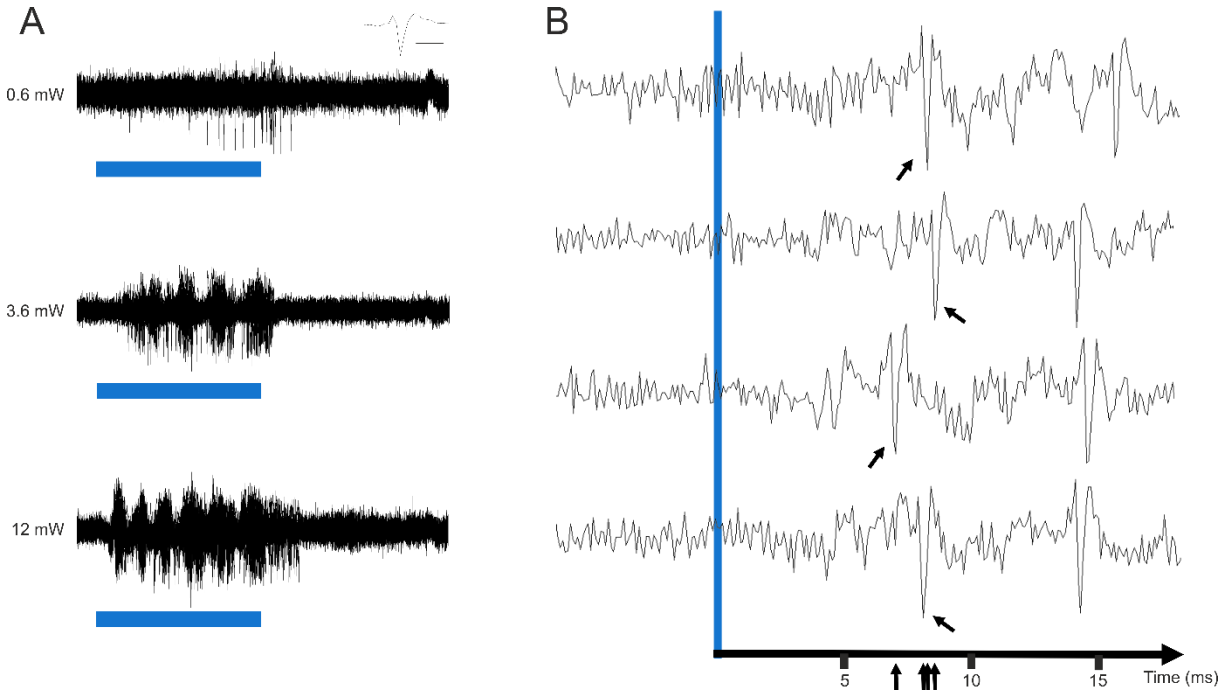

A. *In vivo* juxtacellular recording of an infragranular interneuron (depth: 880 µm) activated by Ntsr1 cells in response to the 470-nm light stimulation at varying intensities (blue bar, 50 ms). Recordings show the overlay of 50 sweeps for each light intensity.
B. Appearance of 1st spike after the onset of the 470nm light (12 mW) is of short latency (average = 6.9 ms) and the variation of this latency is low (standard deviation = 3.5 ms). Furthermore, the 1st spike of short latency is present in all sweeps. These features are characteristic of a direct activation via L6 CT cells.

Figure S6. The whisker-evoked response as a function of time between blue light onset and whisker deflection

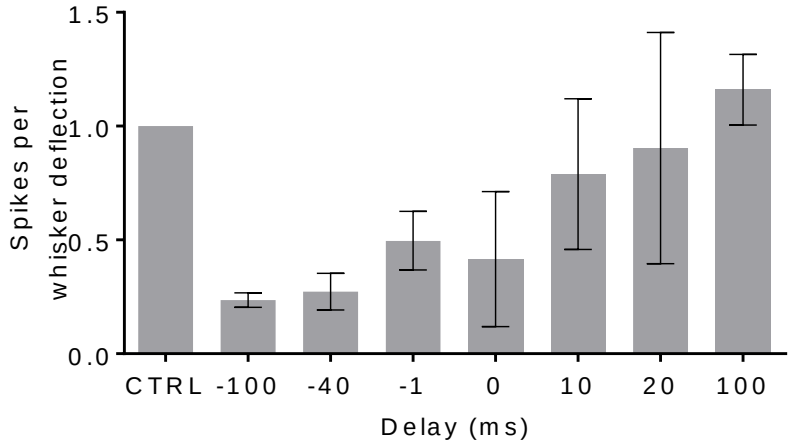

The whisker-evoked response can be progressively retrieved by increasing the delay between the whisker stimulation onset and the blue light pulse. "-100" = light started 100 ms before the whisker deflection; this was the standard delay used. "100" = light started 100 ms after the whisker deflection. The number of spikes is normalized to control condition, i.e., without photo-activation of L6-Ntsr1 cell. (n = 11, (one L2/3 cell; six L4 cells and four L5 cells)).

Figure S7. Position of the in vivo electrode when recording from VPM thalamus

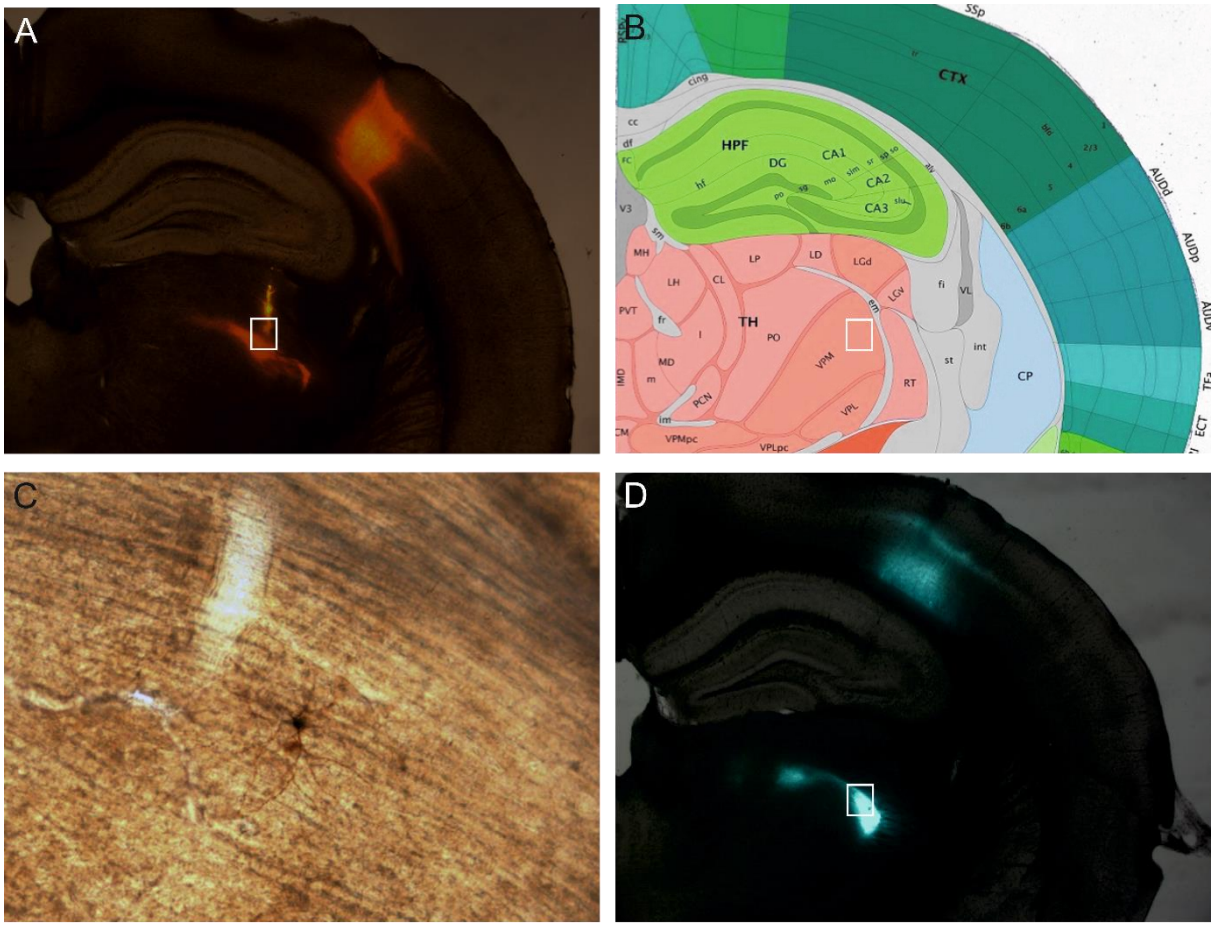

A. Brain slice showing that the anatomical position of the in vivo tungsten recordings in VPM thalamus was verified after each experiment by the DiI staining of the electrode. Note that the DiI labelling (red vertical trace) overlaps with the ChR2-mCherry labelling in VPM thalamus.
B. A coronal brain section from a mouse brain atlas (Allen Brain Atlas). Aligning the experimental brain section with the atlas shows that the recording site (white rectangle) was in VPM.
C. In vivo recording using a glass pipette from a thalamic cell. The cell was filled with biocytin during the recordings, and brain slices were subsequently stained with DAB.

The labelled cell was in the area marked with a white rectangle. The area has dense L6 corticothalamic innervation (ArchT-GFP) and corresponds to the VPM are in the atlas Area where the cell has been filled.

Figure S8. Effect of L6-activation on VPM thalamus. The results of Mease et al., 2014 could be retrieved

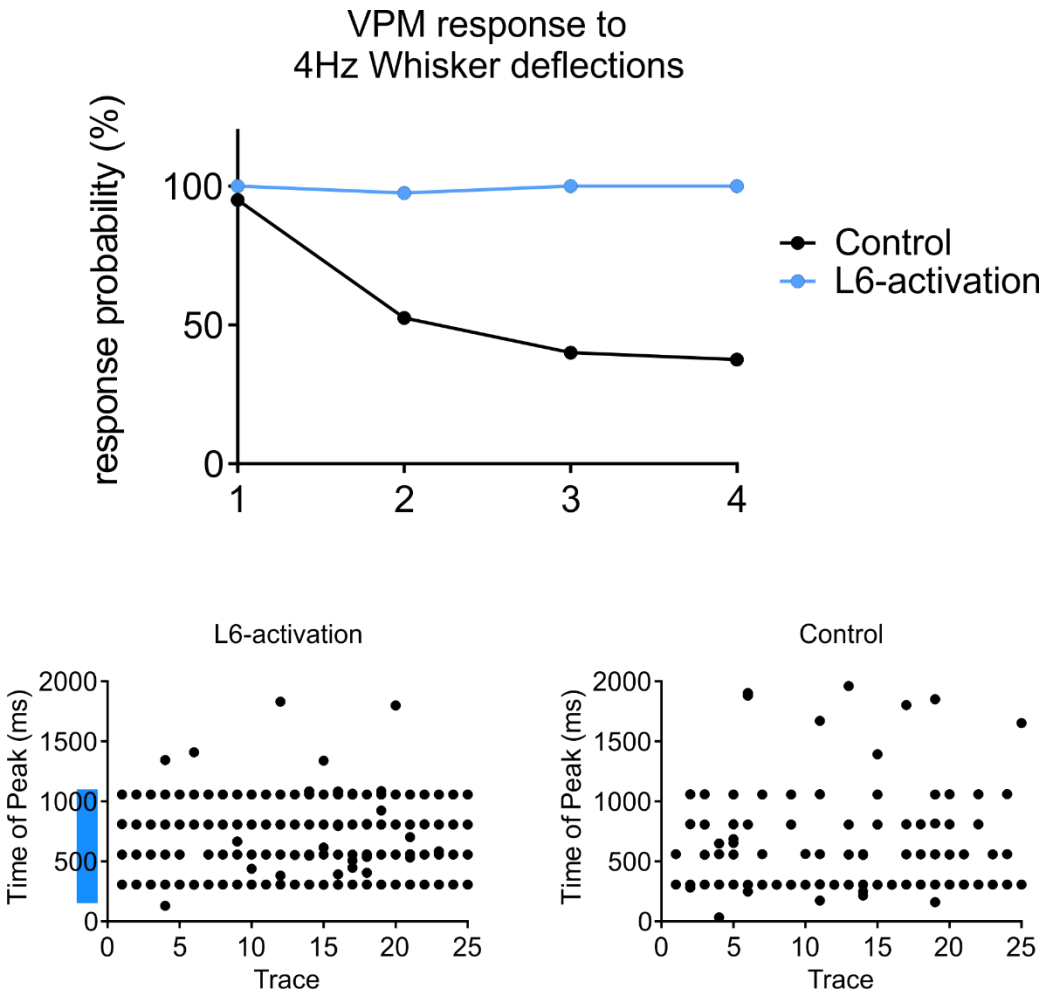

Top: Activation of L6 alters the relay of high-frequency sensory stimuli. Here an example of a VPM neuron stimulated with four whisker deflections delivered at 4Hz (x-axis) with and without L6 photoactivation (40 sweeps).

Bottom: Illustration of the phenomenon seen in A. Four whisker deflections at 4Hz (time: 300, 550, 800 and 1050 ms on the y-axis) displayed for 25 traces (x-axis). The reduce adaptation in L6-activation condition can be clearly seen.

Figure S9. Gad-2 cre expression from pia to white matter

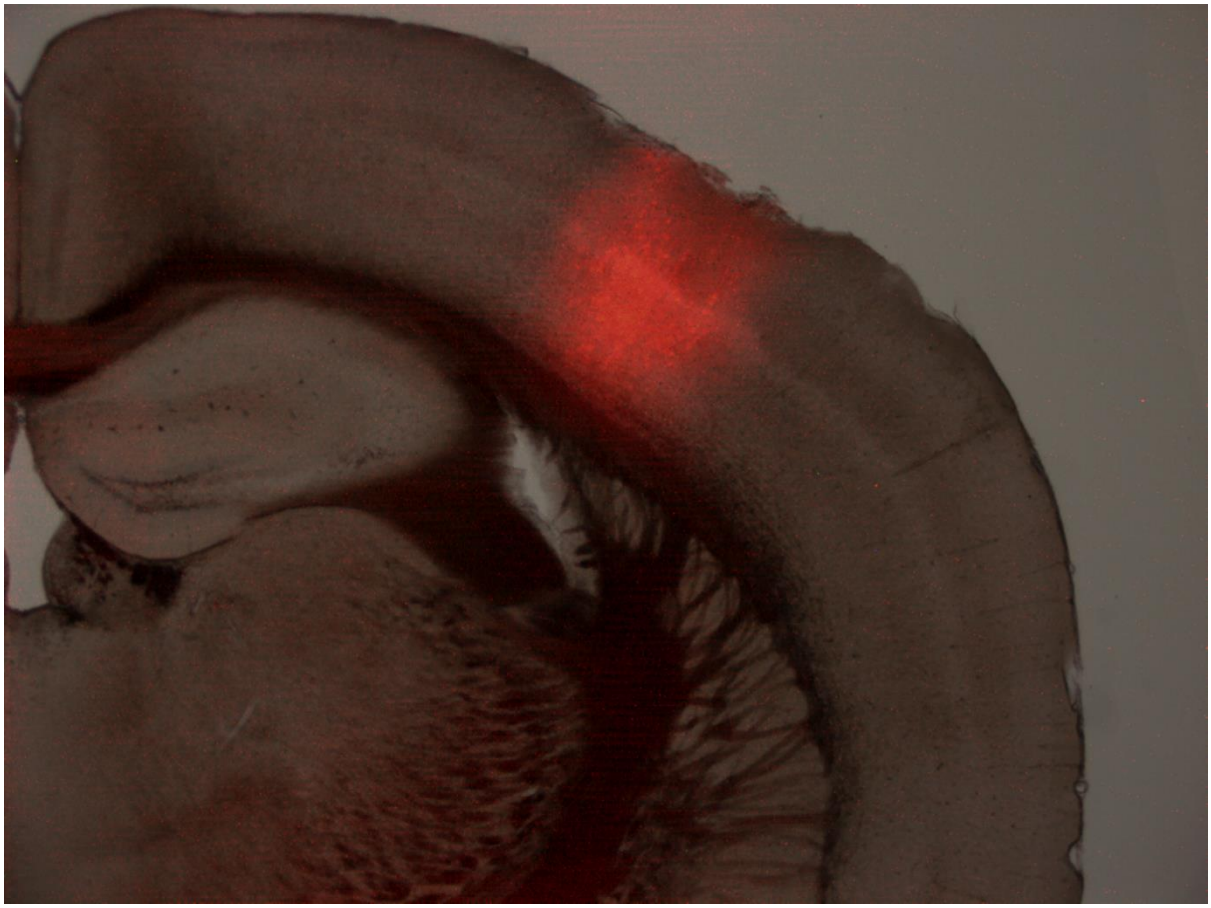

All layers Gad2-postive interneurons are expressing ChR2-mCherry (in red) in the barrel cortex.

Figure S10. Infragranular FS interneuron activated by L6-Ntsr1 cells features.

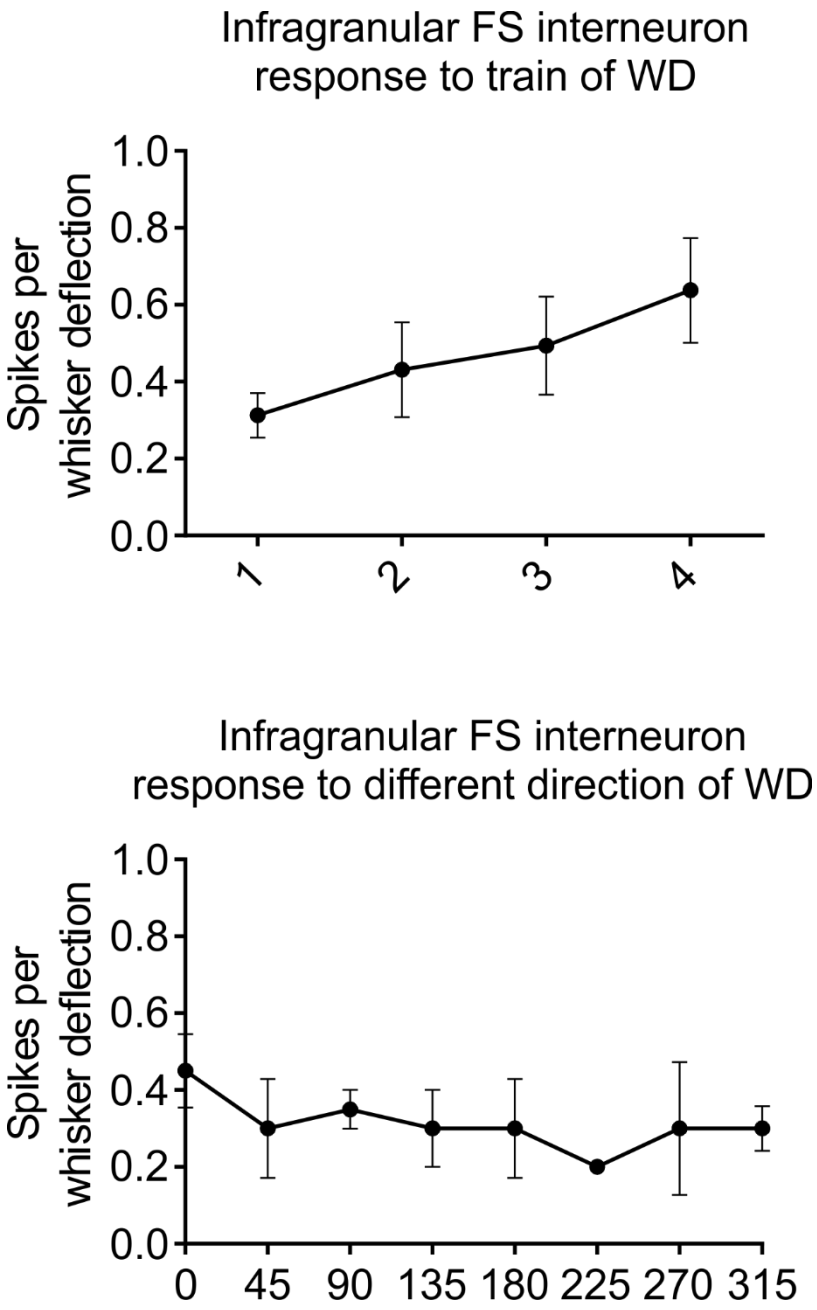

Top: Average response of an infragranular interneuron activated by Ntsr1 cells in response to 4 whisker deflections delivered at 4Hz in control condition and in eight different direction (160 repeats in total; 20 repeats per direction). Paired t-test between the 1st and 4th stimulation showed a significant difference ($p = 0.0396$).

Bottom: Average response of the same cell (interneuron activated by Ntsr1 cells) for each direction (20 repeats per direction). Here only the reponse of the 1st stimulation of the 4Hz train is plotted. One way ANOVA showed no significant difference between the responses ($p = 0.6418$). Meaning that this GABAergic interneuron display no direction selectivity.

Figure S11. Distribution of the principal direction.

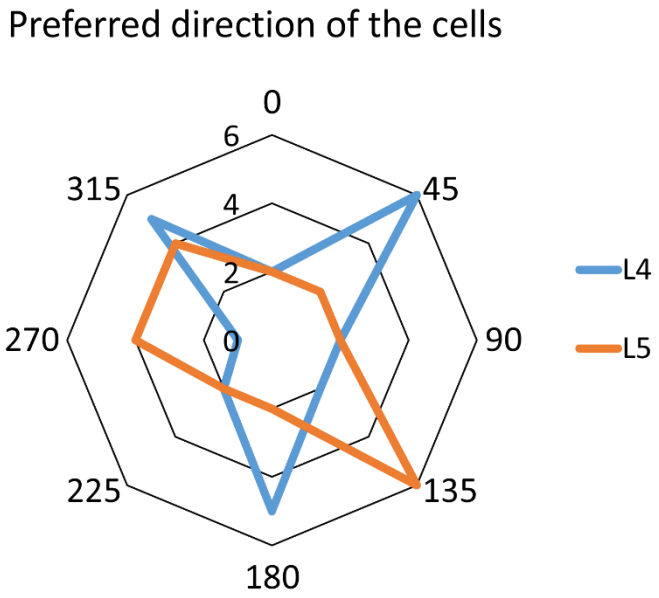

For each angle, the number of cells displaying this direction as PD is plotted.

L4: n = 25 (Ntsr1 = 13, Gad2 = 12) / L5: n = 24 (Ntsr1 = 12, Gad2 = 12)

One way ANOVA between the number of cell in each direction showed no significance, p = 0.6798. Calculated for both layers together.

6.2 Curriculum Vitae

François PAUZIN

31 years

GENERAL INFORMATION:
Birth: 04/06/1987 **Nationality**: French
Address: 596, montée de la vieille église 38200 JARDIN FRANCE
Phone: 0049-160.56.25.174
Email: francois.pauzin@rub.de
Language: French: native English: fluently Dutch, Italian, and German: basics
Driving license: yes

Education:

October 2014 until June 2018: PhD student under the supervision of Prof. Dr. Patrik Krieger, in the department of Systems Neuroscience, Faculty of Medicine, Ruhr-Universität Bochum, Germany. My main work consisted *in vivo* electrophysiology combined with optogenetics to study the importance of corticothalamic feedback for sensory processing of tactile information in the mouse whisker system. First name publication in Cell Report. See next page. Four more paper in preparation. The results on directional selectivity presented in the thesis are in preparation. Not discussed in the present thesis are two more studies where I am co-author. In these two studies the behavioral effect of acute reversible and chronic silencing of L6 Ntsr1 cells are studied. In addition, anatomical work using trans-synaptic tracing techniques are included in a manuscript under preparation.

Skills: I consider myself as an electrophysiologist specialized on using genetic tools, including optogenetics, to study brain circuits. In particular, I have gained expertise in accurate stereotaxic injections of cortical and deep brain structures.

July 2013: Graduation of my Research Master in Neurosciences in Rouen University.

January to June 2013: Master 2 internship in Radboud University Nijmegen in the department of Neurosciences. Establishment of a scanning probe microscopy technique (Scanning Ion Conductance Microscopy) to electrically image whisker topology in a nanometer resolution.

February to July 2012: Internship in Radboud University Nijmegen (Netherlands) in the department of Animal Physiology. Establishment of a combination of scanning probe microscopy technique (Scanning Ion Conductance microscopy) and fluorescence microscopy to electrically image living cells in order to follow the morphology of active synapses in time with nanometer resolution to elucidate mechanisms that control neuroplasticity.

September to January 2011: First year of Research Master in Neurosciences in Rouen University (France).

2011: Graduation of my bachelor in Biology and Biochemistry in Rouen University

2010: Obtaining of my nutritionist diploma in Rouen University.

6.3 List of Publications

PAUZIN, F.P. & KRIEGER, P. 2018. A Corticothalamic Circuit for Refining Tactile Encoding. *Cell Rep*, 22, 23, 1314-1325

6.4 Acknowledgements

I would like to acknowledge my supervisor Patrik Krieger, without whom my career in neuroscience wouldn't have started on the same way. Your professionalism inspired me daily, your critical sense in science brought my extra strength, your passion for science and the trust you gave on my experimental and theoretical work will always be inked in my mind. Your knowledge let me realize which kind of man I would like to be. And the icing on the cake, the man you are and the atmosphere you can bring at work contributed a lot to define myself as what I can call a happy man! Merci beaucoup Patrik!

I would like to thank my working colleagues, Desire Humanes-Valera, Tobias Breuer and Josephine Eckardt for technical help and for all the constructive scientific discussions we had throughout my PhD. Special thanks for your daily enthusiasm Josephine, you are awesome!

Thank you to Nadja Schwarz, a bachelor student at RUB. Your motivation in getting electrophysiology data was a great help in enlarging the direction selectivity data!

I would like to thank Ann-Christin Ammann and Fatima Arakrak for the technical assistance, scientist beginner like me wouldn't be able to work properly and efficiently without you.

I would like to sincerely thank member of neighboring labs, especially Maximillian Hauser, Abdelrahman Rayan and Ute Neubacher for their kindness and helpful advices throughout my PhD. Ute, the abundance of the useful advices you gave me are unforgettable! Max and Abdel, I hope to keep contact with you, I love speaking sciences with you!

Finally, I would like to thank new friends I meet in Germany without whom life would be less enjoyable, Tim Hartl, Tim Jaeger, I am really glad I meet you!